The impact of the CRISPR/Cas system on the interaction of *Neisseria meningitidis* with human host cells

---

Der Einfluss des CRISPR/Cas-Systems auf die Interaktion von *Neisseria meningitidis* mit menschlichen Wirtszellen

Doctoral thesis for a medical doctoral degree at the
Graduate School of Life Sciences,
Julius-Maximilians-Universität Würzburg,
Section Infection and Immunity

submitted by

Hanns Antony Hagmann
from
Berlin

Würzburg, 2019

Submitted on: …….
office stamp

Members of the Thesis Committee:

Chairperson:

Prof. Dr. med. Oliver Kurzai

Primary Supervisor:

Prof. Dr. rer. nat. Dr. med. Christoph U. Schoen

Supervisor (second):

Prof. Dr. rer. nat. Jörg Vogel

Supervisor (third):

Prof. Dr. rer. nat. Roy Gross

Supervisor (fourth):

Prof. Dr. med. Johannes G. Liese

Date of Public Defence: .....……..

Date of Receipt of Certificates: .....……..

AFFIDAVIT

I hereby confirm that my thesis entitled ‘The impact of the CRISPR/Cas system on the interaction of *Neisseria meningitidis* with human host cells‘ is the result of my own work. I did not receive any help or support from commercial consultants. All sources and/or materials applied are listed and specified in the thesis.

Furthermore, I confirm that this thesis has not yet been submitted as part of another examination process neither in identical nor in similar form.

…… ……

Place, Date Signature

EIDESSTATTLICHE ERKLÄRUNG

Hiermit erkläre ich an Eides statt, die Dissertation „The impact of the CRISPR/Cas system on the interaction of *Neisseria meningitidis* with human host cells“ eigenständig, das heißt insbesondere selbständig und ohne Hilfe eines kommerziellen Promotionsberaters, angefertigt und keine anderen als die von mir angegebenen Quellen und Hilfsmittel verwendet zu haben.

Ich erkläre außerdem, dass die Dissertation weder in gleicher noch in ähnlicher Form bereits in einem anderen Prüfungsverfahren vorgelegen hat.

……. …….

Ort, Datum Unterschrift

Table of Content

Table of Content

1 Summary

Neisseria meningitidis, a commensal β-proteobacterium residing exclusively in the human nasopharynx, is a leading cause of sepsis and epidemic meningitis worldwide. While comparative genome analysis was able to define hyperinvasive lineages that are responsible for most of the cases of invasive meningococcal disease (IMD), the genetic basis of their virulence remains unclear. Recent studies demonstrate that the type II-C CRISPR/Cas system of meningococci is associated with carriage and less invasive lineages. CRISPR/Cas, an adaptive defence system against foreign DNA, was shown to be involved in gene regulation in *Francisella novicida*. This study shows that knockout strains of *N. meningitidis* lacking the Cas9 protein are impaired in the adhesion to human nasopharyngeal cells in a strain-dependant manner, which constitutes a central step in the pathogenesis of IMD. Consequently, this study indicates that the meningococcal CRISPR/Cas system fulfils functions beyond the defence of foreign DNA and is involved in the regulation of meningococcal virulence.

2 Zusammenfassung

Neisseria meningitidis, ein ß-Proteobakterium, welches als Kommensale ausschließlich den humanen Nasopharynx besiedelt, ist ein weltweit führender Verursacher von Sepsis und epidemischer Meningitis. Auch wenn mittels vergleichender Genomanalysen hyperinvasive Stämme definiert werden konnten, welche für die meisten Fälle von invasiven Meningokokkenerkrankungen verantwortlich sind, bleibt die genetische Grundlage ihrer Virulenz ungeklärt. In vorangegangenen Studien konnte gezeigt werden, dass das Typ II-C CRISPR/Cas-System der Meningokokken assoziiert ist mit Trägerstämmen. CRISPR/Cas ist ein adaptives Verteidigungssystem der Bakterien gegen fremde DNA, das darüber hinaus Aufgaben in der Genregulation von *Francisella novicida* erfüllt. Diese Arbeit zeigt, dass knockout Stämme von *N. meningitidis*, denen das Cas9-Protein fehlt, in Abhängigkeit von ihrem genetischen Hintergrund die Fähigkeit verlieren an Zellen des menschlichen Nasopharynx zu adhärieren. Die Adhäsion an den Wirtszellen stellt einen zentralen Schritt in der Pathogenese der invasiven Meningokokkenerkrankungen dar. Die Ergebnisse dieser

Arbeit deuten darauf hin, dass das CRISPR/Cas-System in Meningokokken neben seiner Funktion als bakterielles Immunsystem an der Regulation der bakteriellen Virulenz beteiligt sein könnte.

3 Introduction

3.1 *Neisseria meningitidis* - an accidental pathogen

N. meningitidis is an encapsulated, aerobic, gram-negative diplococcus that resides predominantly on mucosal surfaces of the upper respiratory tract in humans [1]. This genetically highly diverse β-proteobacterium is part of the family of *Neisseriaceae* and shares about 90% nucleotide identity with *N. lactamica* and *N. gonorrhoeae* [1]. While *N. meningitidis* can be found in the nasopharynx of up to 10% of the healthy population as a commensal bacterium [2], it sometimes leads to severe infections such as sepsis, purulent meningitis, or Waterhouse-Friderichsen-syndrome, which are lethal in 10% of the cases and occur as sporadic cases and as global epidemics [3, 4].

The only natural habitat of *N. meningitidis* is the human nasopharynx and therefore the colonisation without sequelae is eminently important for the transmission via inhalation of airborne droplets or close contact [5, 6]. Crucial for colonization is the adhesion of the bacteria to the epithelial cell layer in the human nasopharynx [7].

Meningococci can sometimes, probably by accident, cross the mucosal surface of the nasopharynx and enter the bloodstream [8]. In this nutrient rich environment, the bacteria multiply rapidly, evade the immune system of the host, and cause life-threatening sepsis [9]. Once they reach the endothelial cell layer of brain vessels, they may cross the blood-brain barrier and replicate in the human cerebrospinal fluid of the subarachnoidal space, which causes acute bacterial meningitis [1, 7]. The mechanisms that drive these commensal bacteria to cause invasive disease remain enigmatic [10]. Invasive meningococcal disease (IMD) regularly fails to promote the spread of bacteria between patients and frequently kills the host, and this therefore signifies an evolutionary dead end for the invasive bacteria [8].

3.2 Pathogenomics of *N. meningitidis*

In contrast to pathogenic *Escherichia coli,* a defined set of virulence genes remains untraceable in *N. meningitidis* [11]. With regard to the genetic equipment, meningococcal strains isolated from healthy carriers and patients suffering from IMD are almost indistinguishable [12]. Numerous factors have been described that are involved in the bacteria-host interaction and thus might coincidentally contribute to

meningococcal virulence: the polysaccharide capsule [13], various adhesins [14], endotoxins such as lipopolysaccharides [15], and its natural competence for the uptake of DNA that leads to a high genome flexibility [16]. However, many of the so-called meningococcal virulence genes have also been found in commensal strains [17]. Nevertheless, analysis of meningococcal isolates by multilocus sequence typing revealed the presence of hyperinvasive lineages responsible for most IMD cases [18]. The genetic basis of virulence in these strains remains unclear. It has been shown that clustered, regularly interspaced, short palindromic repeats (CRISPR), and CRISPR-associated (*cas*) genes are more frequently found in non-hyperinvasive strains [19] and thus might constitute an 'anti-virulence' factor in meningococci.

3.3 CRISPR/Cas

The CRISPR/Cas system is a sequence based, adaptive bacterial defence system against viruses and invading DNA [20]. It is characterized by the CRISPR array, a sequence of noncoding DNA that contains palindromic repeats which are almost always identical within a particular array [21]. Those repeats are separated by unique parts of DNA, called spacers, which were found

to match frequently to phages and other extrachromosomal elements [22-26]. The CRISPR/Cas system additionally contains a set of two to six *cas* genes with functional domains, including endo- and exonuclease domains, helicases, RNA-DNA binding domains, and domains involved in transcription regulation [21, 22, 27, 28]. The CRISPR/Cas system may be found in various prokaryotic organisms and is therefore manifold. Between species, the repeat and the spacer sequences may differ in number, length, and structure [21, 29, 30] as well as the total number of CRISPR/Cas loci in the genome [31] or the number and sequence of the Cas genes [22]. The CRISPR/Cas systems may be divided into six main types distinguished by their Cas genes [32]. One of these, the type II CRSIPR/Cas systems is associated with pathogenic bacteria such as *F. novicida*, *Campylobacter jejuni*, and *N. meningitidis* [33]. This type of CRISPR/Cas system, which is only found in a bacteria [33], yields *cas* genes encoding for Cas1, Cas2, and, demarcating from other groups, Cas9 [34]. The group is further divided into three subgroups according to the presence or absence of a fourth protein. Type II-A

obtains additionally a gene called *csn2*, type II-B *cas4,* whereas type II-C lacks a fourth *cas* gene [35].

The role of the Type II CRISPR/Cas systems in host protection is well established [36]. CRISPR RNA (crRNA), processed by the endogenous endonuclease RNase III (encoded by *rnc*) [37] and a *trans* activating CRISPR RNA (tracrRNA), build a ribonucleoprotein complex with Cas9 to recognize target DNA by sequence and degrade it by cleavage [38, 39].

However, far less is known about the potential contribution of the CRISPR/Cas system to gene regulation and virulence [40, 41]. A recent study revealed that Cas9 is critical for the interaction of *C. jejuni* with host cells [42]. Furthermore, it has been demonstrated that Cas9 in combination with tracrRNA and a small CRISPR/Cas-associated RNA (scaRNA) is involved in gene regulation in *F. novicida*. The ribonucleoprotein complex degrades the mRNA of a bacterial lipoprotein (blp) called FTN_1102 and therefore downregulates the respective gene. Furthermore, it has been shown that in *F. novicida,* the crRNA, Cas1, Cas2, Cas4, and the endogenous RNase III are not involved in this pathway [35]. Nevertheless, the authors of the study

analysed virulence traits of *cas9* deletion mutants in *N. meningitidis* strain 92045. Since the mutants were unable to adhere to, invade, and replicate in human adenocarcinoma alveolar basal epithelial cells, a contribution of Cas9 to pathogenicity and virulence of meningococci has been assumed. However, pneumonia is rarely a part of IMD [43] and the CRISPR/Cas systems of *F. novicida* and *N. meningitidis* are similar but not identical, and therefore the results are not necessarily applicable.

Cas4 is present in *F. novicida* but absent in *N. meningitidis,* which is why the meningococcal CRISPR/Cas system is classified as type II-C whereas *F. novicida* harbours a type II-B CRISPR/Cas system [34, 44]. Nevertheless, the meningococcal CRISPR/Cas system, which has recently been described as the most streamlined CRISPR/Cas system characterized to date, uses a unique *rnc*-independent crRNA maturation pathway with promoters within each CRISPR repeat. Furthermore, it is in possession of two forms of tracrRNA differing in length processed by RNase III [32, 45].

An obvious explanation for the association of CRISPR/Cas to non-hyperinvasive strains is the

restriction of lysogenization with the meningococcal disease-associated prophage MDAΦ, which was shown to increase host cell colonization [46]. While there was a highly significant inverse association between the presence of a CRISPR/Cas locus and MDAΦ [19], isolates such as the *N. meningitidis* serogroup C strain 8013 and the serogroup A strain WUE2594 belong to hyperinvasive lineages, which contain a CRISPR/Cas system but lack MDAΦ [47, 48]. Therefore, these strains are particularly suitable to examine the putative regulatory function of the CRISPR/Cas system on genes mediating meningococcal virulence.

Table 3.1 *Comparison of the two meningococcal strains used in this study*

	8013	**WUE2594**
Genome characteristics		
GenBank accession number	FM999788	FR774048
Genome size (Mb)	2.28	2.23
GC content	51.4%	51.8%
Predicted number of coding sequences	1912	1941
Molecular epidemiology		
Lineage	Invasive	Invasive
Source	IMD	IMD
Country	France	Germany
Year of isolation	1989	1991
Clonal complex (CC)	ST-18	ST-5
Serogroup	C	A
Reference	[47]	[48]

3.4 The genetic basis for the interaction of *N. meningitidis* with human host cells

The adhesion of meningococci to host cells is a process actively promoted by the bacteria, and their capacity to adhere depends on their genetic equipment. It is mainly affected by the type IV pilus (tfp), the so-called major adhesins Opa and Opc, minor adhesins such as NhhA, App or NadA and the polysaccharide capsule [14, 49, 50].

In almost all aspects of meningococcal colonization and infection, tfp plays a central role. [51] They are homopolymeric filaments composed of the major subunit pilin (*pilE*) but many more genes are required for tfp biogenesis and/or function [47, 52].

Neisserial tfp is divided into two classes based on the binding of the monoclonal antibody SM1 to pilin [53]. Class I pilin contains the conserved amino acid motif EYYLN recognized by SM1 and is encoded by a *pilE* gene that is located in the genome between the genes *fkbP* and *lpxC* [54, 55]. In close proximity to the PilE gene, the class I locus contains *pilS* (silent) cassettes. These are not expressed but occasionally recombine with *pilE*, hence promoting variety of possible pilin

versions. This process is called antigenic variation and requires a conserved motif called guanine quartets (G4) adjacent to *pilE* [56]. It is furthermore enhanced by a 66 bp long sequence named Sma/Cla element [57]. However, in meningococci expressing class II pili, *pilE* and *pilS* are found in distinct loci. In addition, the *pilS* cassettes are less numerous and the G4 and Sma/Cla elements are absent in the *pilE* locus. There is evidence that class II tfp do not undergo antigenic variation. Strain 8013 is known to harbour a class I tfp whereas WUE2594 possesses a class II pilin [55]. The *pilE* loci of 8013 and WUE2594 are depicted in Figure 3.1.

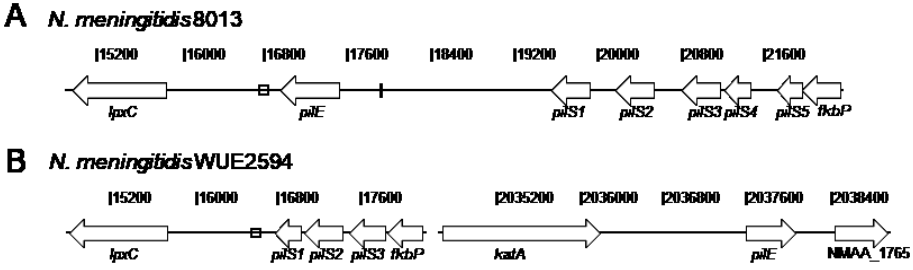

Figure 3.1 *pilE and pilS loci in 8013 and WUE2594*

Depicted are the *pilE* and *pilS* loci of *N. meningitidis* 8013 (A) and WUE2594 (B). The scalebar in each panel in bp above the genes denotes the place in the genome according to the published genome sequence. Black vertical lines indicate guanine quartets (G4, 5′-GGGTGGGTTGGGTGGG-3′) and black boxes Sma/Cla sequences [55]. Drawn to scale.

In general, pilin is synthesized as prepilin and subsequently cleaved by the prepilin peptidase *pilD* [58]. After processing, the mature pilin is approximately 145-160 aa long with 25 conserved hydrophobic N-terminal residues that are embedded in the core of the pilus and a C-terminal disulphide bond, which is partially exposed at the surface. The posttranslational modifications of pilin include the glycosylation of serine residues, controlled by the *pgl* gene cluster [59-62]. Several other proteins are necessary for tfp function.

PilG is known to be required for piliation [63]. PilF promotes the elongation [64] whereas PilT is antagonistically involved in retraction of the pilus [65]. PilT is furthermore required for twitching motility [66] and intimate adhesion on host cells [67]. PilQ, another protein involved in pilus retraction, requires PilW to anchor in the outer cell membrane. The genes *pilQ* and *pilW* are located in one gene cluster together with *pilP*, *pilM*, *pilN,* and *pilO*, whose exact role in the tfp biogenesis are not entirely understood [68]. Likewise, the role of PilC is not fully understood even though it is shown that *pilC* null mutants are impaired in pilus expression, and it has been assumed that PilC acts antagonistically to PilT [66, 69]. PilC1 has been demonstrated to be involved in the adhesion to host cells [70, 71]. Several other proteins, such as PilH, PilI, PilJ, PilK, PilV, PilX, and ComP, are also targets of the prepilin peptidase and are, in the case of ComP, PilV, and PilX, also involved in host-cell interaction and adhesion [72, 73].

The outer membrane proteins known as Opa and Opc are another class of major adhesins. Opc interacts with cytoskeletal *α*-actinin of host cells and is therefore also an effective invasin [74]. *N. meningitidis* possesses four

Opa genes (*opaA*, *opaB*, *opaC,* and *opaD*) [47]. Encoding identical or different Opa proteins, they express up to four different Opa variants simultaneously [75]. Opa proteins play a central role in developing IMD, since they are known to mediate bacterial adherence and to modulate human cellular immunity [76, 77].

In addition to those major adhesins, there is a class of so-called minor adhesins including the *Neisseria hia* homolog A (NhhA), the adhesion and penetration protein (App), and the neisserial adhesin A (NadA) [50]. NhhA and App are homologous to the autotransporterproteins Hia/Hsf and Hap of *Haemophilus influenzae* [78-80]. NhhA is predominantly present in invasive strains, whereas App is found in carrier and invasive strains [79, 80]. Nevertheless, both are reported to mediate adhesion to host cells [79, 80]. Also frequently found in hyperinvasive lineages is NadA, an oligomeric coiled-coil adhesin (Oca) that directly interacts with protein receptors on epithelial cells [81].

Thirteen capsular polysaccharides have been described but only six (A, B, C, W135, X, Y) are significantly associated to systemic infections [13]. The polysaccharide capsule is the main virulence

determinant in *N. meningitidis* [82]. The capsules differ in the polysaccharides they are composed of. While the serogroup A strain WUE2594 expresses homopolymeric (α1→6) N-acetylmannosamine 1-phosphate polysaccharide, the serogroup C strain 8013 expresses homopolymers of N-acetylneuraminic acid with (α2→9)-linkages, which are partially O-acetylated [13]. The capsule sterically inhibits the interaction of most adhesins with host cells but it does not prohibit the adhesion mediated by NhhA, App, NadA [50], or the tfp-mediated adhesion. In fact, the tfp appears to be required for adhesion in the presence of a capsule [14].

3.5 Aims of the study

To reveal the impact of the CRISPR/Cas system of *N. meningitidis* on the interaction to host cells, this study examines the adhesion and invasion of *cas9*, *rnc*, tracrRNA, and CRISPR array deletion mutants in the strains 8013 and WUE2594 on Detroit562 human nasopharyngeal cells.

4 Materials

4.1 Laboratory equipment

The following Table 4.1 enlists the laboratory equipment used in this study in alphabetical order. The states of registered business addresses are abbreviated by ISO-3166-1 alpha-2 country codes.

Table 4.1 *Laboratory equipment*

Device	Type	Manufacturer
Agarose gel electrophoresis chamber	MINI-BASIC	*Cti*, Idstein DE
Agarose gel electrophoresis chamber	Electrophoresis chamber 'Maxi'	*Von Keutz*, Reiskirchen DE
Agarose gel electrophoresis chamber	SubCell® GT	*Bio-Rad*, Dreireich DE
Analytical balance	ABT 120-5DM	*Kern & Sohn,* Balingen DE
Analytical balance	P-1200	*Mettler-Toledo*, Greifensee CH
Bunsen burner	Fireboy (electric)	*Tecnomara*, Zürich CH
Bio Hazard bag	Ref. 86.1203	*Sarstedt,* Nümbrecht DE
Centrifuge (4 °C)	Megafuge 1.0 R	*Haraeus*, Hanau DE

Device	Type	Manufacturer
Centrifuge for cell culture	Megafuge 1.0 R	*Haraeus*, Hanau DE
Centrifuge (benchtop, 4 °C)	Mikro Rapid	*Hettich*, Tuttlingen DE
Centrifuge (benchtop)	Biofuge pico	*Haraeus*, Hanau DE
Centrifuge (-Mini)	SproutTM	*Biozym*, Hessisch Oldendorf DE
Centrifuge tube 15 ml	Cellstar® Tubes 15 ml	*Greiner bio-one* Frickenhausen DE
Centrifuge tube 50 ml	Cellstar® Tubes 50 ml	*Greiner bio-one* Frickenhausen DE
Chronograph	Ref. 38.2021	*TFA Dostmann,* Wertheim DE
Cryo tubes	KV12	*Hartenstein,* Würzburg DE
Cuvettes for photometer	Nr. 67.742	*Sarstedt,* Nümbrecht DE
Colony counter	ProtoCOL	*Meintrup DWS*, Lähden DE
Cotton swabs	Ref. 1030128	*Heinz Herenz,* Hamburg DE
Disposal bag	Ref. 86.1197	*Sarstedt,* Nümbrecht DE
OD_{600} photometer	WPA biowave	*Biochrom*, Berlin DE

Device	Type	Manufacturer
Heating block	VLM Q1	*VLM*, Bielefeld DE
Hemocytometer	ZK-03	*Hartenstein,* Würzburg DE
Imaging system	ChemiDoc MP	*Bio-Rad*, Dreieich DE
Incubator (37 °C)	Haraeus Kelvitron® t	*Haraeus*, Hanau DE
Incubator (37 °C/ 5% CO_2)	Haraeus 6000	*Haraeus*, Hanau DE
Incubator (37 °C/ 5% CO_2) for cell culture	MCO-20AIC	*SANYO*, Oizumi-Machi JP
Incubation hood	CERTOMAT® H	*B. Braun*, Melsungen DE
Inoculation loop	Ref. 86.1562.010	*Sarstedt,* Nümbrecht DE
Laboratory film	Parafilm M	*Bemis,* Neenah US
Magnetic stirrer	IKAMAG® RCT	*IKA*®, Staufen DE
Membrane pump	Typ 400057	*ILMVAC,* Ilmenau DE
Microscope	Wilovert®	*WILL*, Wetzlar DE
Microcentrifuge tubes 0.5 ml	Ref. 72.704	*Sarstedt,* Nümbrecht DE
Microcentrifuge tubes 1 ml	Ref. 72.706	*Sarstedt,* Nümbrecht DE
Microcentrifuge	Ref. 72.695.500	*Sarstedt,* Nümbrecht DE

Device	Type	Manufacturer
tubes 2 ml		
Microwave	R-941STW	*Sharp,* Osaka JP
Nitrocellulose Transfer Membrane	Ref. 10401196	*GE Healthcare,* Freiburg DE
Oven	OV 5	*Biometra*, Göttingen DE
PCR thermocycler	T3 Thermocycler	*Biometra*, Göttingen DE
pH indicator strips	PH33	*Hartenstein,* Würzburg DE
Pipette 10 µl	Research plus, 0.5-10 µl	*Eppendorf*, Hamburg DE
Pipette 100 µl	Research plus, 10-100 µl	*Eppendorf*, Hamburg DE
Pipette 1000 µl	Research plus, 100-1000 µl	*Eppendorf*, Hamburg DE
Pipette controller	Accu-jet®	*BRAND,* Wertheim DE
Pipette controller	Accu-jet® pro	*BRAND*; Wertheim DE
Pipette tip 10 µl	Ref. 70.1115	*Sarstedt,* Nümbrecht DE
Pipette tip 200 µl	Ref. 70.760.002	*Sarstedt,* Nümbrecht DE
Pipette tip 1000 µl	Ref. 70.762	*Sarstedt,* Nümbrecht DE
Power supply	EV243 Consort Power Supply	*Consort*, Turnhout BE

Device	Type	Manufacturer
Power supply	Standard Power Pack P25	*Biometra*, Göttingen DE
Protective gloves	Peha-soft nitrile Fino L	*Hartmann,* Heidenheim DE
Protein gel electrophoresis	Mini-Protean	*Bio-Rad*, Dreieich DE
Safety cabinet	Safe 2020 1.8	*Thermo Scientific*, Frankfurt DE
Safety cabinet for cell culture	NUAIRE	*Thermo Scientific*, Frankfurt DE
Serological pipette 5 ml	Ref. 86.1253.001	*Sarstedt,* Nümbrecht DE
Serological pipette 5 ml	Ref. 86.1254.001	*Sarstedt,* Nümbrecht DE
Serological pipette 5 ml	Ref. 86.1685.001	*Sarstedt,* Nümbrecht DE
Semi-dry blotter	PEGASUS S	*PHASE*, Lübeck DE
Shaker	CERTOMAT® U	*B. Braun*, Melsungen DE
Shaker	Phero Shaker	*Biotec-Fischer*, Reiskirchen DE
Spectrophotometer	PEQLAB, ND-1000	*VWR*, Erlangen DE
Spectrophotometer	Multiskan EX	*Thermo Scientific*, Frankfurt DE

Device	Type	Manufacturer
Surgical face mask	Foliodress mask loop	*Hartmann,* Heidenheim DE
Thermoshaker	Thermomixer 5436	*Eppendorf*, Hamburg DE
UV crosslinker	18000	*Life Technologies*, Darmstadt DE
Vortex mixer	REAX 2000	*Heidolph*, Schwabach DE
Waterbath for cell culture	WB 10	*Memmert*, Schwabingen DE
Waterbath	WB 7	*Memmert*, Schwabingen DE

4.2 Chemicals and consumables

Standard laboratory chemicals were purchased from *AppliChem* (Darmstadt DE), *Merck* (Darmstadt DE), *Carl Roth* (Karlsruhe DE), *Roche* (Mannheim DE) or *Sigma-Aldrich* (Schnelldorf DE). All specific reagents are listed alphabetically in Table 4.2.

Table 4.2 *Specific reagents*

Reagent	Source
3-propanesulfonic acid (MOPS)	*AppliChem*, Darmstadt DE
Ammonium persulfate (APS)	*Roth*, Karlsruhe DE
Anti-Digoxidenin-AP Fab fragments (Anti-DIG-ATP)	*Roche*, Mannheim DE
Bromphenol blue	*Merck*, Darmstadt
β-mercaptoethanol (β-ME)	*Roth*, Karlsruhe DE
Chloroform ultra pure	*AppliChem*, Darmstadt DE
Crystal violet	*BD,* Heidelberg DE
ddH_2O	*B.Braun,* Melsungen DE
DIG DNA labelling mix	*Roche*, Mannheim DE
Dithiothreitol (DTT)	*AppliChem*, Darmstadt DE
Ethylenediaminetetraacetic acid (EDTA)	*AppliChem*, Darmstadt DE
Ethanol absolute	*AppliChem*, Darmstadt DE
Formaldehyde solution, 36.5-38%	*Sigma-Aldrich*, Schnelldorf DE
Formamide, deionized	*AppliChem*, Darmstadt DE
GelRed™	*Biotium*, Fremont US

Reagent	Source
Hexanucleotide mix (10x)	*Roche*, Mannheim DE
Nonfat dried milk powder	*AppliChem*, Darmstadt DE
Nuclease-free water	*Ambion*, Austin US
Polyacrylamide (PAA): Rotiphorese Gel 30	*Roth*, Karlsruhe DE
Polyacrylamide (PAA): Rotiphorese Gel 40	*Roth*, Karlsruhe DE
Sodium dodecyl sulfate (SDS) pellets	*Roth*, Karlsruhe DE
Tetramethylethylendiamine (TEMED)	*Roth*, Karlsruhe DE
Trishydroxymethylaminomethane (TRIS)	*Sigma-Aldrich*, Schnelldorf DE
Triton-X 100%	*Roth*, Karlsruhe DE
Xylene cyanole	*Sigma-Aldrich*, Schnelldorf DE

Standard consumables were purchased from *Ambion* (Austin US), *Biozym* (Hessisch Oldendorf DE), *Eppendorf* (Wesseling-Berzdorf DE), *Greiner bio-one* (Frickenhausen DE), *Hartenstein* (Würzburg DE) and *Sarstedt* (Nümbrecht DE). All specific consumables are listed alphabetically in Table 4.3.

Table 4.3 *Special consumables*

Application	Product	Source
Agarose-gels	UltraPure™ agarose	*Life Technologies*, Darmstadt DE
dNTPs		
PCR amplification	100mM dNTP set (dATP, dCTP, dGTP, dTTP)	*Sigma-Aldrich*, Schnelldorf DE
Reaction buffers		
for *Taq* polymerase	ThermoPol reaction buffer	*New England Biolabs,* Frankfurt DE
for Q5® polymerase	Q5 reaction buffer	*New England Biolabs,* Frankfurt DE
for restriction enzymes	CutSmart® Buffer, NEBuffer 3.1	*New England Biolabs,* Frankfurt DE
for T4 DNA Ligase	T4 DNA Ligase Buffer	*New England Biolabs,* Frankfurt DE
Oligos		
PCR amplification	DNA oligonucleotides	*Sigma-Aldrich*, Schnelldorf DE
Ladders		
	DNA HyperLadder™ 1kb	*Bioline,* Luckenwalde DE

Application	Product	Source
	DNA Molecular Weight Marker VII, DIG-labeled	*Roche,* Mannheim DE
	PageRuler™ Prestained Protein Ladder, 10 to 180 kDa	*Life Technologies,* Darmstadt DE
Blotting		
Southern blot	Amersham Hybond™-N$^+$	*GE Healthcare,* Freiburg DE
Antibodies		
First antibody	Monoclonal Anti-polyhistidine antibody produced in mouse	*Sigma-Aldrich,* Schnelldorf DE
Second antibody	Anti-Mouse IgG-Peroxidase antibody produced in rabbit	*Sigma-Aldrich,* Schnelldorf DE
Varying Applications		
Static biofilm formation	96 Well microtiter plate	*Sarstedt,* Nümbrecht DE
Cell culturing	TC Flask T75 standard	*Sarstedt,* Nümbrecht DE
Cell invasion/adhesion	24-well cell culture plates	*Sarstedt,* Nümbrecht DE

4.3 Kits

All kits are listed in Table 4.4 ordered by purpose.

Table 4.4 *Kits*

Application	Product	Source
DNA extraction	Invisorb Spin DNA Extraction Kit	*STRATEC Biomedical AG,* Birkenfeld DE
gDNA isolation	QIAamp DNA Mini Kit	*Qiagen,* Hilden DE
PCR purification	MSB Spin PCRapace	*STRATEC Biomedical AG*, Birkenfeld DE
Plasmid isolation	QIAprep Spin Miniprep Kit	*Qiagen,* Hilden DE

4.4 Enzymes

The following Table 4.5 lists all enzymes used in this study.

Table 4.5 *Enzymes*

Enzyme	Source
DNase I, RNase-free	*Thermo Scientific,* Schwerte DE
Klenow enzyme	*Roche*, Mannheim DE
Lysozyme	*Roth*, Karlsruhe DE
Restriction endonucleases	*New England Biolabs,* Frankfurt DE
T4 DNA ligase	*New England Biolabs,* Frankfurt DE
Taq DNA polymerase	*New England Biolabs,* Frankfurt DE
Q5® High-Fidelity DNA polymerase	*New England Biolabs,* Frankfurt DE

4.5 Buffers and Solutions

If not indicated otherwise, utilized reagents were purchased from *Carl Roth* (Karlsruhe DE), *Difco* (Heidelberg DE), *Merck* (Darmstadt DE), or *Sigma-Aldrich* (Steinheim DE).

Unless stated otherwise, all solutions and buffers were sterilized by autoclaving at 121 °C, 1 bar for 20 minutes.

For various microbiological and cell culture methods 1x Phosphate-buffered saline (PBS, Table 4.6) was used. It has final concentrations of 2.6 mM potassium chloride (KCl), 1.4 mM potassium phosphate monobasic (KH_2PO_4), 137.9 mM sodium chloride (NaCl) and 8.0 mM sodium phosphate dibasic (Na_2HPO_4). The following Table 4.6 lists the instructions for preparation.

Table 4.6 *Phosphate-buffered saline*

Content	Preparation
10x PBS	
GIBCO® DPBS	1 pellet
ddH_2O	ad 1000 ml
1x PBS	
10x PBS	100 ml
ddH_2O	ad 1000 ml

For long term storage of bacteria, a glycerol based freezing medium was used. The following Table 4.7 lists the instructions for preparation.

Table 4.7 *Freezing medium*

Content	Preparation
Glycerol, 86%	233 ml
Caso-Bouillon (*BD*, Heidelberg DE)	15 g
ddH_2O	ad 500 ml

For electrophoretic separation of DNA in agarose gels 1x TAE (Table 4.8) was used as running buffer. The 6x DNA loading buffer (Table 4.8) was stored at 4 °C in a 1.5 ml microcentrifuge tube until usage. For DNA staining loaded agarose gels were bathed in GelRed™ solution (Table 4.8) for 30-45 minutes.

Table 4.8 *Buffers and solutions used for electrophoretic separation of DNA*

Content	Preparation
50x TAE (TRIS-acetate EDTA)	
TRIS	242 g
100% acetic acid	57.1 ml
0.5 M EDTA (pH 8.0)	100 ml
ddH_2O	ad 1000 ml, adjust pH to 8.3

Content	Preparation
1x TAE	
50x TAE	40 ml
ddH_2O	ad 2000 ml
6x DNA loading buffer	
Saccharose	40 g
Glycine	30 ml
Bromphenolblue	100 mg
Xylencyanol	100 mg
ddH_2O	ad 100 ml
GelRed™ solution	
ddH2O	150 ml
GelRed™	15 µl

The composition of all buffers and solutions used for Southern blots is given in Table 4.9.

Table 4.9 *Buffers and solutions used for Southern blots*

Content	Preparation
10x Blocking reagent	
Blocking reagent (*Roche*, Mannheim DE)	10 g
1x Maleic acid buffer	ad 100 ml, storage at -10 °C
1x Blocking solution	
10x blocking reagent	10 ml
1x Maleic acid buffer	90 ml
Antibody solution	
Anti-DIG-AP (*Roche*, Mannheim DE) 1:10000 in 1x Blocking solution	
Storage at 4 °C	
CSPD working solution	
CSPD (*Roche*, Mannheim DE) 1:100 in detection buffer	
Storage at 4 °C	
Coomassie staining solution	
10 % acetic acid	
60 mg/l Coomassie Blue R-250	

Content	Preparation
Gel fixing solution	
25% isopropanolol	
10% acetic acid	
in ddH_2O	
Detection buffer	
1 M TRIS/HCl, pH 9.6	100 ml (0.1M)
5M NaCl	20 ml (0.1M)
ddH_2O	ad 1000 ml
High SDS hybridisation buffer	
20x SSC	125 ml
10x Blocking reagent	100 ml
SDS	35 g
10% N-Lauroylsarcosine	0.5 ml
5x Sodium phosphate buffer, pH 7.0	25 ml
ddH_2O	ad 500 ml, storage at -20 °C

Content	Preparation
1x Maleic acid buffer	
Maleic acid	23.2 g
NaCl	17.53 g
ddH_2O	ad 2000 ml, adjust pH to 7,5
20x Saline-Sodium-Citrate (SSC)	
NaCl	175.5 g
Sodium citrate	88.2 g
ddH_2O	ad 1000 ml, adjust pH to 7.0
Stringent washing buffer I	
20x SSC	100 ml
10x SDS	10 ml
ddH_2O	ad 1000 ml
Stringent washing buffer II	
20x SSC	5 ml
10x SDS	10 ml
ddH_2O	ad 1000 ml

Content	Preparation
Washing buffer	
1x Maleic acid buffer	1000 ml
Tween 20	3 ml
ddH_2O	ad 2000ml

Table 4.10 lists all buffers, gels and solutions used for electrophoretic separation of denatured proteins using SDS polyacrylamide gels (SDS PAGE).

Table 4.10 *SDS PAGE*

Content	Preparation
1x Electrophoresis buffer	
10x Lämmli	200 ml
10% SDS	10 ml
ddH_2O	ad 2000 ml
10x Lämmli	
TRIS	30 g
Glycine	144 g
ddH_2O	ad 1000 ml, adjust pH to 8.3

Content	Preparation
Lower TRIS	
TRIS	90.85 g
10% SDS	20 ml
ddH_2O	ad 500 ml, storage at 4 °C
Upper TRIS	
TRIS	30.3 g
10% SDS	20 ml
ddH_2O	ad 500 ml, storage at 4 °C
Sample buffer	
B-mercaptoethanol	5 ml
20% SDS	10 ml
Glycerol	25 ml
Bromphenol blue	a spatula tip
0.5 M TRIS/HCl pH 6.8	ad 100 ml, storage at -20 °C

Content	Preparation
Separation gel 12.5%	
Lower TRIS	3 ml
PAA 30	5 ml
10% APS	60 µl
TEMED	20 µl
ddH_2O	4 ml, yielding 2 gels
Loading gel	
Upper TRIS	1.25 ml
PAA 30	0.75 ml
10% APS	35 µl
TEMED	20 µl, yielding 2 gels

4.6 Culture media

Unless stated otherwise, culture media were sterilized by autoclaving at 121 °C with 1 bar for 20 minutes or filtrated through 0.2 µm membrane filters (*Sarstedt*, Nümbrecht DE).

4.6.1 Liquid media for *N. meningitidis* cultivation

In this study proteose peptone medium (PPM) was used as rich medium for *N. meningitidis*. The following Table 4.11 lists its preparation. To obtain PPM$^+$ (Table 4.13) the supplements (Table 4.12) were added right before use.

Table 4.11 *Composition of PPM*

Content	Preparation
Bacto™ proteose peptone (*BD,* Heidelberg DE)	15 g
NaCl	5 g
Potato starch (*Honeywell*, Offenbach DE)	0.5 g
KH_4PO_4	4 g
K_2HPO_4 (dipotassium phosphate)	1 g
ddH_2O	ad 1000 ml, adjust to pH 7.8

Table 4.12 *Supplements of PPM$^+$ medium*

Content	Preparation
8.4% $NaHCO_3$	
$NaHCO_3$	21 g
ddH_2O	ad 250 ml
2 M $MgCl_2$	
$MgCl_2$ x 6 H_2O	101.7 g
ddH_2O	ad 250 ml
PolyViteX (*bioMèrieux*, Nürtingen DE)	
Cobalamin	0.1 mg/l
L-glutamine	100 mg/l
Adenine	10 mg/l
Guaninchlorhydrate	0.3 mg/l
4-Aminobenzoic acid (PABA)	0.13 mg/l
L-cystine	11 mg/l
Diphosphopyridinnucleotid, oxidized	2.5 mg/l
Cocarboxylase	1.04 mg/l
Iron(III)nitrate	0.2 mg/l
Thiamine chlorhydrate	0.03 mg/l

Content	Preparation
Cysteine chlorhydrate	259 mg/l

Table 4.13 *Composition of PPM$^+$*

Content	Preparation
PPM	98 ml
8.4% $NaHCO_3$	500 µl
2 M $MgCl_2$	500 µl
PolyViteX	1 ml

The gonococcus base liquid (GCBL) medium was used for transformation of *N. meningitidis*. The following Table 4.14 lists its composition. To obtain GCBL$^+$ (Table 4.16) the supplements (Table 4.15) were added right before use.

Table 4.14 *Composition of GCBL medium*

Content	Preparation
Bacto™ proteose peptone (*BD,* Heidelberg DE)	15 g
K_2HPO_4	4 g
KH_2PO_4	1 g
NaCl	1g
ddH_2O	ad 1000 ml

Table 4.15 *Supplements of GCBL^{++} medium*

Content	Preparation
Kellogg's supplement I	
Glucose	40 g
L-glutamine	1 g
Thiamine pyrophosphate	2 mg
ddH_2O	ad 100 ml, storage at -20 °C
Kellogg's supplement II	
Iron(III) nitrate	50 mg
ddH_2O	ad 100 ml, storage at -20 °C

Content	Preparation
Sodium bicarbonate ($NaHCO_3$)	
$NaHCO_3$	0.42 g
ddH_2O	ad 100 ml

Table 4.16 *Composition of GCBL^{++} medium*

Content	Preparation
GCBL	97.9 ml
Kellogg's I	1 ml
Kellogg's II	100 µl
$NaHCO_3$	1 ml

4.6.2 Solid media for *N. meningitidis* cultivation

For cultivation of *N. meningitidis* strains on solid media, supplemented gonococcus base (GCB^{++}) agar plates or Columbia agar plates with 5% sheep blood (COS plates; *BD*, Heidelberg DE) were used. The following Table 4.17 lists the composition of GCB^{++} agar plates.

Table 4.17 *Composition of GCB^{++} agar*

Content	Preparation
Difco™ GC Medium Base (*BD*, Heidelberg DE)	36.25 g
Agar	1.25 g
ddH_2O	ad 1000 ml
Kellogg's I	10 ml, added after autoclavation
Kellogg's II	1 ml, added after autoclavation

4.6.3 *E. coli* cultivation

For cultivation of *E. coli* in liquid medium *Luria-Bertani* (LB) medium was used. Table 4.18 lists its composition. For cultivation on solid media 1.5% agar was added to the liquid medium before autoclaving. For chemical transformations of *E. coli* Super Optimal broth with Catabolic repression (SOC; Table 4.20) was used. To obtain SOC the supplements were added to Super Optimal Broth (SOB; Table 4.19) right before use.

Table 4.18 *Composition of LB medium*

Content	Preparation
Peptone	10 g
Yeast extract	5 g
NaCl	10 g
ddH_2O	ad 1000 ml

Table 4.19 *Composition of Super Optimal Broth (SOB) medium*

Content	Concentration
Bacto™ tryptone 2% Bacto™ yeast extract (*BD*, Heidelberg DE)	0.5%
NaCl	10 mM
KCl	2.5 mM

Table 4.20 *Composition of Super Optimal broth with Catabolic repression (SOC) medium*

Content	Preparation
SOB	5 ml
2 M $MgCl_2$	25 µl
1 M $MgSO_4$	50 µl
1 M glucose	100 µl

4.6.4 Cell culture media and solutions

Table 4.21 lists solutions and media used for cell culturing with their intended usage and the source of purchase

Table 4.21 *Solutions and media used for cell culture*

Product	Application	Source
MEM Eagle (EMEM)	Cell culture medium	*LONZA,* Basel CH
Fetal calf serum (FCS)	Medium supplement	*Thermo Fisher*, Frankfurt DE
Nonessential amino acids (NEAA)	Medium supplement	*LONZA,* Basel CH
Sodium pyruvate (NaPyr 100 mM)	Medium supplement	*LONZA,* Basel CH

Product	Application	Source
Trypsin-EDTA (0.05%)	Dissociation of cells	*Thermo Fisher*, Frankfurt DE
Gentamicin (10 mg/ml)	Antibacterial agent	*Biochrom,* Berlin DE
Saponin (20%)	Permeabilization of cells	*SERVA,* Heidelberg DE
RPMI 1640 + Glutamax™ -I	Cell culture medium	*Thermo Fisher*, Frankfurt DE
Dimethyl sulfoxide (DMSO)	Cell cryopreservation	*Roth*, Mannheim DE

As standard cell culture medium EMEM^{+++} was used. Table 4.22 lists its composition.

Table 4.22 *Composition of EMEM*$^{+++}$

Content	Preparation
EMEM	500 ml
FCS	50 ml
NEAA	5 ml
NaPyr	5 ml

Given in Table 4.23 are the concentrations of components of EMEM supplemented with 1% NEAA and 1% sodium pyruvate (100 mM) calculated using the manufacturers' published formulation. Due to the addition of 10% FCS the concentrations of amino acids are likely higher in EMEM^{+++} (see Table 4.22) but because of its natural origin the exact formulation of FCS underlies fluctuations and cannot be assessed exactly.

Table 4.23 *Formulation of EMEM supplemented with 1% NEAA and 1% sodium pyruvate (100mM)*

Component	Concentration (g/l)
Inorganic Salts	
$CaCl_2$	0.196
$MgSO_4$	0.096
KCl	0.392
$NaHCO_3$	1.471
NaCl	6.667
$NaH_2PO_4\,H_2O$	0.137
Amino acids	
L-Alanine	0.017
L-Arginine HCl	0.124

Component	Concentration (g/l)
L-Asparagine H_2O	0.028
L-Aspartic Acid	0.026
L-Cystine 2HCl	0.031
L-Glutamic Acid	0.029
L-Glutamine	0.286
Glycine	0.007
L-Histidine HCl H_2O	0.041
L-Isoleucine	0.051
L-Leucine	0.051
L-Lysine HCl	0.071
L-Methionine	0.015
L-Phenylalanine	0.032
L-Proline	0.023
L-Serine	0.021
L-Threonine	0.047
L-Tryptophan	0.01
L-Tyrosine 2Na $2H_2O$	0.051
L-Valine	0.046

Component	Concentration (g/l)
Vitamins	
Choline Chloride	0.001
Folic Acid	0.001
myo-Inositol	0.002
Nicotinamide	0.001
D-Pantothenic Acid (hemicalcium)	0.001
Pyridoxine HCl	0.001
Riboflavin	0.001
Thiamine HCl	0.001
Other	
D-Glucose	0.98
Phenol Red, Sodium Salt	0.01
Sodium Pyruvate	0.216

For long-term storage, 1x 10^6 cells were resuspended in freezing medium (Table 4.24) and stored in liquid nitrogen at -196 °C.

Table 4.24 *Composition of cell freezing medium*

Content	Preparation
RPMI 1640 + Glutamax™-I	50 ml
FCS	30 ml
DMSO	20 ml

In some experiments the cell culture medium RPMI$^+$ was used. Table 4.25 lists its composition.

Table 4.25 *Composition of RPMI$^+$*

Content	Preparation
RPMI 1640 + Glutamax™-I	500 ml
FCS	50 ml

4.7 Antibiotic supplements

Table 4.26 lists the antibiotics and the concentrations used in this study.

Table 4.26 *Antibiotics*

Antibiotic	**Final concentration (µg/ml)**		**Stock concentration (µg/ml)**		**Solvent**
	E.c.[a]	*N.m.*[b]	*E.c.*[a]	*N.m.*[b]	
Ampicillin	100	-	100	-	ddH_2O
Kanamycin	30	100	30	100	ddH_2O
Erythromycin	250	7	100	7	100% Ethanol
Chloramphenicol	30	7	30	7	70% Ethanol

[a]for *E. coli*

[b]for *N. meningitidis*

4.8 Oligonucleotides

The oligonucleotides used in this study are listed in Table 4.27.

Table 4.27 *Sequences of oligonucleotides*

ID[a]	Sequence (5'-3')[b]	Target site
242	AATACGAC TCACTATA GGGC	pBluescript-SK
243	ACCATGAT TACGCCAA GC	pBluescript-SK
328	GGTATTGA TAATCCTG ATATGAA	Tn*903* Kanamycin resistance cassette
329	GATGGTCG GAAGAGGC ATAAATT	Tn*903* Kanamycin resistance cassette
550	gcgcgcGG ATCC$_{BamHI}$T CCAACAGG TTGGCAAT CCGCAAT	WUE2594/ 8013 downstream *rnc*
551	gcgcgcGA ATTC$_{EcoRI}$G GCGGCGCG TGAATATG CCGTCTGA	WUE2594/ 8013 downstream *rnc*

ID[a]	Sequence (5'-3')[b]	Target site
552	gcgcgcGA ATTC$_{EcoRI}$T ACCGTCTT CCGCAAAA AACAGCC	WUE2594/ 8013 upstream *rnc*
554	gcgcgcAA GCTT$_{HindIII}$ TTCGCTGC CGATTTCG TTGGTGA	WUE2594/ 8013 upstream *rnc*
617	ATTCGTTG GAAACCAG CTCGAA	WUE2594/ 8013 *rnc* locus
618	ATATCTTC GGGATACA TCGGCACG	WUE2594/ 8013 *rnc* locus
729	gcgcgcGG ATCC$_{BamHI}$A AATCGCCT GTCTGTAA GGCATG	WUE2594/ 8013 upstream tracrRNA
730	gcgcgcGA ATTC$_{EcoRI}$G TATATAAA TAAGACAA TAAGATAT ATTATCA	WUE2594 upstream tracrRNA
732	gcgcgcGA ATTC$_{EcoRI}$T GCCGTCTG AAACCGAT TTTGGGCT T	WUE2594 downstream tracrRNA

ID[a]	Sequence (5'-3')[b]	Target site
733	gcgcgcAA GCTT$_{HindIII}$ AACTGTCG AAACTCAA ACCGCAA	WUE2594 downstream tracrRNA
739	AATCTTTG CGGCTGAA CGTATG	WUE2594 tracrRNA locus
740	ATCGAACC GGTGCGGC TCATTGA	WUE2594 tracrRNA locus
833	gcgcgcGA ATTC$_{EcoRI}$G TATATAAA TAAGACAA TCAGATAT	8013 upstream tracrRNA
834	gcgcgcAA GCTT$_{HindIII}$ AAGTCCGCC AAATCGCAC CGACCA	8013 downstream tracrRNA
835	gcgcgcGA ATTC$_{EcoRI}$T GCCGTCTG AAACCGGT TTTTGGGC T	8013 downstream tracrRNA
903	GCCGTCTG AAGCCGCA AGACAGCG	8013 *cas9* locus

ID[a]	Sequence (5'-3')[b]	Target site
904	TATGAAAC AAGCCTAA TGCAGGCA	8013 *cas9* locus
905	TCGAAACT CAAACCGC AAGACAGC	WUE2594 *cas9* locus
906	TATGAAAC AAGCCTAA TGCAGGTA	WUE2594 *cas9* locus
935	CGGGAAGA TGCGTGAT CTGA	Kanamycin probe
936	CCTCTTCC GACCATCA AGCA	Kanamycin probe
970	TTCGCCCA AATCGCAG GAAATGA	WUE2594/ 8013 *rnc*
971	TGTTTTGA AACAGCAG GCACACG	WUE2594/ 8013 *rnc*
972	GCAAATGC GGTTGTAG CTCCCTT	WUE2594 CRISPR
973	CCCGACAC ATCCGTCA TCAACG	WUE2594 CRISPR
974	AATCTTCC GCACTTCC AGGGGTT	8013 CRISPR

ID[a]	Sequence (5'-3')[b]	Target site
975	CAAGTGCG AGGCGCGT ATATTGT	8013 CRISPR
976	TGCCGAAG CCTCAACA TTGATGG	WUE2594/ 8013 *cas9*
977	TTGGCGTT TCTCAATT TCTTTGC	WUE2594/ 8013 *cas9*
988	CCGAACCG CTGGCGCG TTAA	8013 NMV0959 locus
989	ATTAATGC CGCCTCCG TCGG	8013 *porA* locus
1031	GAAGCGAA CTCAATCC ATTCA	8013 CRISPR locus
1032	CAATGGAA AGCTAATG TATTA	8013 CRISPR locus
1035	gtttGGAT CC_{BamHI}AGC CACGTTGT GTCTCAAA	Tn*903* Kanamycin resistance cassette
1043	gttttATG CAT_{NsiI}GG AATACGTT GGGGGAAA AC	8013 *rnc*

ID[a]	Sequence (5'-3')[b]	Target site
1044	gttttGGA TCC$_{BamHI}$AA AGGCTCCA AAAGGAGC CTTTTCAT TTCTTTTT CCTCTTCA GC	8013 *rnc*
1045	gttttATG CAT$_{NsiI}$TTC TTATTTCA AATCTGTG ACAC	8013 CRISPR
1046	gttttGGA TCC$_{BamHI}$AA AGGCTCCA AAAGGAGC CTTTAATA AGGATTTC CCGTCGAA GT	8013 CRISPR
1047	gttttATG CAT$_{NsiI}$CC GTAAACAA CGTTGCAA ATAA	8013 tracrRNA
1048	gttttGGA TCC$_{BamHI}$AA AGGCTCCA AAAGGAGC CTTTTAAA CGATGCCC CTTAAAGC AG	8013 tracrRNA

ID[a]	Sequence (5'-3')[b]	Target site
1049	CACTTTCC CTGTTTCT ATG	*cat* Chloramphenicol resistance cassette
1054	GCCGTCTG AACGGGGC GGTGAAGC GGATAG	pCompInd
1055	GCCGTCTG AACGAACC GCTGGCGC GTTAAACA	pCompInd
1110	gtttttCA TATG$_{NdeI}$AC GCGTCTTA AGGCGGCC	*cat* Chloramphenicol resistance cassette
1111	gtttttTC TAGA$_{XbaI}$GT CAACCGTG ATATAGAT TGAA	*cat* Chloramphenicol resistance cassette
1117	gttttCAT ATG$_{NdeI}$CGC TGAGGTCT GCCTCGTG	Tn*903* Kanamycin resistance cassette
1118	gttttTCT AGA$_{XbaI}$AGC CACGTTGT GTCTCAAA	Tn*903* Kanamycin resistance cassette
1122	CGAGCAAT ACAGCGGC AGATTTTC C	8013 NMV1884

ID[a]	Sequence (5'-3')[b]	Target site
1123	CTAAACCT AAAGTGAA TAGCTCAC TTATCAG	*ermC*
1227	CGCCAAGA AGAAAACC GCAA	8013 *cas9* probe
1228	TTTCGCTG CCCAATAC CAGT	8013 *cas9* probe
1229	ATTGGCGC GAAAAATC GGAC	8013 NMV0031 probe
1230	CCGCACTT TTTCTGAT GGGC	8013 NMV0031 probe
10509	gcgcgcGG ATCC$_{BamHI}$G TCAGCCGC GACGACTA CGGCGGC	WUE2594/ 8013 upstream *cas9*
10510	gcgcgcGA ATTC$_{EcoRI}$T TATTACTC CGTAAACA ACGTTGC	WUE2594/ 8013 upstream *cas9*
10511	gcgcgcGA ATTC$_{EcoRI}$A TTAATCTA TCCCTGTT TCAGACT	8013 downstream *cas9*

ID[a]	Sequence (5'-3')[b]	Target site
10512	gcgcgcCT CGAG$_{XhoI}$TA GTTCAATG CGGCATTG ACGGCA	8013 downstream *cas9*
10515	gcgcgcGA ATTC$_{EcoRI}$A TTAATCTA TCCCTGTT TCAGGCG	WUE2594 downstream *cas9*
10516	gcgcgcCT CGAG$_{XhoI}$TA GTTCAATG CGGCATTG ACGGCG	WUE2594 downstream *cas9*
11114	gcgcgcGG ATCC$_{BamHI}$C GGCAACAT TTCAGCAC CTTG	WUE2594 downstream CRISPR
11115	gcgcgcGA ATTC$_{EcoRI}$A CTTCGACG GGAAATCC TTAT	WUE2594/ 8013 downstream CRISPR
11116	gcgcgcGA ATTC$_{EcoRI}$C AGCCGTTG CGATAAGC GAAC	WUE2594/ 8013 upstream CRISPR
11306	gcgcgcAA GCTT$_{HindIII}$ CTGGTCCA ACTTCAAT AGCGG	WUE2594 upstream CRISPR

ID[a]	Sequence (5'-3')[b]	Target site
11443	GGATCC$_{BamHI}$ CGTGATAC ATTTGTAC GAACA	8013 downstream CRISPR
11444	AAGCTT$_{HindIII}$ CAGTTTGA GAGTAAAG CAGGG	8013 upstream CRISPR
11604	TGCCGTCC AGTAACTG ATGTTCTT	WUE2594 downstream CRISPR
11605	GCATCAAA CAACACCT CATCAAAA	WUE2594 upstream CRISPR
12662	tattGACG TC$_{AatII}$TTC TAGCCGTT GTGAGATG ATAAG	8013 *cas9*
12663	tcgcTTAA TTAA$_{PacI}$C GGACAGGC GGGCGTTT TTTC	8013 *cas9*

[a]ID-number 0-9999 according to the AG SCHOEN oligonucleotide collection, 10000-99999 according to the common IMIB oligonucleotide collection
[b]Restriction sites are underlined, small letters indicate nonsense-nucleotides

4.9 Plasmids

The plasmids used for cloning are listed in Table 4.28.

Table 4.28 *Utilized plasmids*

ID[a]	Plasmid	Description and Usage	Res.[b]	Reference
315	pBluescript-SK	standard cloning vector	Amp^r	*Stratagene,* La Jolla US
	pBluescript II - SK (+)	standard cloning vector	Amp^r	*Stratagene,* La Jolla US
	pGCC2	standard vector for complementation	Ery^r	[83]
	pCompInd	standard vector for complementation	Cm^r	[84]
58	pUC4K	Delivery plasmid harbouring kanamycin resistance cassette	Km^r	*GE Healthcare*, Freiburg DE
5101	pBJ104	Kanamycin resistance cassette with *EcoRI* sites from pUC4K cloned between PCR product 10509/10510 comprising 8013 *cas9* UP fragment and PCR product 10511/10512 comprising 8013 *cas9* DOWN fragment into *XhoI* and *BamHI* sites of pBS-SK; used for **8013 *cas9* knockouts**	Amp^r/ Km^r	[45]

ID[a]	Plasmid	Description and Usage	Res.[b]	Reference
5117	pBJ102	Kanamycin resistance cassette with *EcoRI* sites from pUC4K cloned between PCR product 550/551 comprising 8013 *rnc* UP fragment and PCR product 552/554 comprising 8013 *rnc* DOWN fragment into *HindIII* and *BamHI* sites of pBS-SK; used for **8013 *rnc* knockouts**	Amp^r/ Km^r	[45]
5124	pBJ107	Kanamycin resistance cassette with *EcoRI* sites from pUC4K cloned between PCR product 834/835 comprising 8013 tracrRNA UP fragment and PCR product 833/729 comprising 8013 tracrRNA DOWN fragment into *HindIII* and *BamHI* sites of pBS-SK; used for **8013 tracrRNA knockouts**	Amp^r/ Km^r	[45]
5105	pBJ106	Kanamycin resistance cassette with *EcoRI* sites from pUC4K cloned between PCR product 11443/11115 comprising 8013	Amp^r/ Km^r	this study

ID[a]	Plasmid	Description and Usage	Res.[b]	Reference
		CRISPR array UP fragment and PCR product 11116/11444 comprising CRISPR array DOWN fragment into *HindIII* and *BamHI* sites of pBS-SK; used for **8013 CRISPR knockouts**		
5238	pAH-1	PCR product 1043/1044 comprising *rnc* (NMV-1713) of *N. meningitidis* 8013 cloned between the *NsiI* and the *BamHI* sites of pCompInd; used for **8013 *rnc* complementation**	Amp^r/ Cm^r	this study
5239	pAH-2	PCR product 1047/1048 comprising tracrRNA (genomic region 1916964 to 1916858) of *N. meningitidis* 8013 cloned between the *NsiI* and the *BamHI* sites of pCompInd; used for **8013 tracrRNA complementation**	Amp^r/ Cm^r	this study
	pGCC2	PCR product 12662/12663	Amp^r/	[45]

ID[a]	Plasmid	Description and Usage	Res.[b]	Reference
	cas9-comp	comprising *cas9* (NMV-1993) of *N. meningitidis* 8013 cloned between the *AatII* And the *PacI* sites of pGCC2; used for **8013 *cas9* complementation**	Ery^r	
5100	pBJ103	Kanamycin resistance cassette with *EcoRI* sites from pUC4K cloned between PCR product 10509/10510 comprising WUE2594 *cas9* UP fragment and PCR product 10515/10516 comprising WUE2594 *cas9* DOWN fragment into *XhoI* and *BamHI* sites of pBS-SK; used for **WUE2594 *cas9* knockouts**	Amp^r/ Km^r	this study
5116	pBJ101	Kanamycin resistance cassette with *EcoRI* sites from pUC4K cloned between PCR product 550/551 comprising WUE2594 *rnc* UP fragment and PCR product 552/554 WUE2594 *rnc* DOWN fragment into *HindIII* and *BamHI* sites of	Amp^r/ Km^r	this study

ID[a]	Plasmid	Description and Usage	Res.[b]	Reference
		pBS-SK; used for **WUE2594 *rnc* knockouts**		
5125	pBJ108	Kanamycin resistance cassette with *EcoRI* sites from pUC4K cloned between PCR product 729/730 comprising WUE2594 tracrRNA UP fragment and PCR product 732/733 comprising WUE2594 tracrRNA DOWN fragment into *XhoI* and *BamHI* sites of pBS-SK; used for **WUE2594 tracrRNA knockouts**	Amp^r/ Km^r	this study
5104	pBJ105	Kanamycin resistance cassette with *EcoRI* sites from pUC4K cloned between PCR product 11114/11115 comprising WUE2594 CRISPR UP fragment and PCR product 11116/11306 comprising WUE2594 CRISPR DOWN fragment into *HindIII* and *BamHI* sites of pBS-SK; used for **WUE2594 CRISPR knockouts**	Amp^r/ Km^r	this study

ID[a]	Plasmid	Description and Usage	Res.[b]	Reference
5243	pAH-4	PCR product of 1117/1118 comprising the Tn*903* kanamycin resistance determinant of pUC4K cloned between the *NdeI* and *XbaI* sites of pCompInd	Amp^r/ Km^r	this study
5244	pAH-5	PCR product of 1117/1035 comprising the Tn*903* kanamycin resistance determinant of pUC4K cloned between the *NdeI* and *BamHI* sites of pCompInd	Amp^r/ Km^r/ Cm^r	this study
5242	pAH-3	PCR product 1110/1111 comprising the *cat* chloramphenicol resistance determinant cloned between the *NdeI* and *XbaI* sites of pCompInd	Amp^r/ Cm^r	this study

[a]ID-number according to the strain collection of the Institute for Hygiene and Microbiology (IHM), Würzburg
[b]antibiotic resistance cassettes obtained by the strain; Km^r, kanamycin; Amp^r, ampicillin; Ery^r, erythromycin; Cm^r, chloramphenicol

4.10 Microorganisms

The strains used in this study are listed in Table 4.29. Figure 6.1 on page 117 depicts the genealogy of 8013 strains used in this study.

Table 4.29 *Strains used in this study*

ID[a]	MO[b]	Strain	relevant characteristics	b.r.[c]	Source/ Reference
286	*E.c.*	XL1-Blue MRF'	*Δ((mcrA)183Δ(mcrCB-hsdSMR-mrr)173 recA1 endA1 gyrA96 thi-1 hsdR17 supE44 relA1 lac F´ proAB lacIqZΔM15 Tn10 Tetr*	-	*Stratagene*, La Jolla US
19	*E.c.*	DH5α	*fhuA2 lac(del)U169 phoA glnV44 Φ80' lacZ(del)M15 gyrA96 recA1 relA1 endA1 thi-1 hsdR17*	-	*Thermo Fisher*, Frankfurt DE
29	*N.m.*	WUE2594	wild type	-	Accession-No: FR774048.1 [48]
5098	*N.m.*	WUE2594	Δ*cas9*::Km^r	1	this study
5122	*N.m.*	WUE2594	ΔtracrRNA::Km^r	1	this study

ID[a]	MO[b]	Strain	relevant characteristics	b.r.[c]	Source/ Reference
5114	*N.m.*	WUE2594	Δ*rnc*::Km^r	1	this study
5102	*N.m.*	WUE2594	ΔCRISPR::Km^r	1	this study
31	*N.m.*	8013	wild type	-	Accession-No: FM999788.1
5099	*N.m.*	8013	Δ*cas9*::Km^r	3	[45]
	N.m.	8013	Δ*cas9*::Km^r Ery^r	2	[45]
5123	*N.m.*	8013	ΔtracrRNA::Km^r	2	[45]
5245	*N.m.*	8013	ΔtracrRNA::Km^r Cm^r	2	this study
5115	*N.m.*	8013	Δ*rnc*::Km^r	2	[45]
5246	*N.m.*	8013	Δ*rnc*::Km^r Cm^r	2	this study
5103	*N.m.*	8013	ΔCRISPR::Km^r	2	this study
5247	*N.m.*	8013	Cm^r	1	this study
	N.m.	8013	Δ*cas9*::Km^r C*cas9* Ery^r	3	[45]
5240	*N.m.*	8013	ΔtracrRNA::Km^r C*tracrRNA* Cm^r	2	this study
5249	*N.m.*	8013	ΔtracrRNA::Km^r C*cas9* Ery^r	1	this study
5248	*N.m.*	8013	ΔtracrRNA::Km^r CtracrRNA Cm^r	2	this study

ID[a]	MO[b]	Strain	relevant characteristics	b.r.[c]	Source/ Reference
			C*cas9* Ery^r		
5241	*N.m.*	8013	Δ*rnc*::Km^r C*rnc* Cm^r	2	this study

[a]ID-number according to the strain collection of the Institute for Hygiene and Microbiology (IHM), Würzburg
[b]microorganism
[c]Number of biological replicates used for experiments
Abbreviations: *N.m.*, *N. meningitidis*; *E.c.*, *E. coli*

4.11 Cell lines

Cell adhesion and invasion assays were performed with a nasopharyngeal epithelial cell line called Detroit562 (ATCC® number CCL-138™) [85, 86].

5 Methods

5.1 Cultivation of bacteria

E. coli were cultivated overnight at 37 °C on LB agar plates in an incubator or in LB media (Table 4.18) at 200 rpm in an incubator shaker. To select recombinant clones, the medium was supplemented with the appropriate antibiotic before usage. The antibiotic substances and their suitable concentrations are listed in Table 4.26.

N. meningitidis were cultivated overnight at 37 °C with 5% CO_2 on COS or GCB^{++} agar plates (Table 4.17) in an incubator. The selection of recombinant clones occurred similar to *E. coli* by adding antibiotics (Table 4.26) to the GCB^{++} agar plates. For cultivation in liquid culture, the bacteria were inoculated into PPM^{+} (Table 4.13) and incubated at 37 °C for the requested period shaking at 200 rpm in an incubator shaker.

5.2 Estimating the bacterial cell number by determining the optical density at 600nm

To estimate the number of bacterial cells in a liquid culture the optical density at 600 nm (OD_{600}) was measured. The bacteria from an agar plate ware

inoculated into liquid medium and pre-incubated for 60 minutes at 37 °C in an incubation shaker. The photometer was calibrated with 1 ml of blank medium. Afterwards 1 ml of the bacterial suspension was pipetted into a cuvette and the absorption at 600 nm was measured. An OD_{600} of 1.0 is equivalent to approximately 1x 10^9 cells/ml of *N. meningitidis* and approximately 2x 10^8 cells/ml of *E. coli.* Based on this, the number of bacterial cells in the liquid medium was calculated or the suspension was adjusted to the requested OD_{600}.

5.3 Preparation of chemically competent *E.coli* cells

The chemically competent *E. coli* cells used in this study are XL-1 Blue MRF' and DH5α (Table 4.29). The frozen glycerol stocks were streaked on LB agar plates and incubated overnight at 37 °C in an incubator. The next day one single colony was inoculated into 15 ml of LB medium and incubated overnight at 37 °C and 200 rpm in an incubator shaker. After incubation 1 ml of starter culture was transferred into 25 ml LB medium and incubated at 37 °C in a thermoshaker for 1 to 2 h. The cells were chilled on ice when the OD_{600} reached 0.5 to

0.7. After 10 to 20 minutes the tubes were centrifuged at 4 °C for 5 minutes at 4000 rpm, the supernatant was decanted, and the pellet was chilled on ice for 1 minute. Then the cells were resuspended and washed with 10 ml of ice cold 80 mM $MgCl_2$/ 20 mM $CaCl_2$. The suspension was centrifuged again at 4 °C for 5 minutes at 4000 rpm, the supernatant was decanted and the pellet was resuspended in 10 ml of ice cold 80 mM $MgCl_2$/ 20 mM $CaCl_2$ and chilled on ice for another 30 minutes. The cells suspension was centrifuged at 4 °C for 5 minutes at 4000 rpm and the supernatant was decanted. The remaining pellet was resuspended in 800 µl of 100 mM $CaCl_2$/ 20% glycerol and 100 µl aliquots were frozen in liquid nitrogen. The aliquots were stored at -80 °C until transformation.

5.4 Transformation of *E. coli*

Chemically competent *E. coli* strains DH5a and XL-1 Blue MRF' were stored in 100 µl aliquots at -80 °C. For transformation the aliquots were slowly thawed on ice. After the addition of 10 µl plasmid or ligation product the bacteria were chilled on ice for another 30 minutes. Afterwards the cells were heat shocked at 42 °C for 90 seconds and immediately cooled down on ice for 2 minutes. Afterwards 800 µl of SOC medium

(Table 4.20) were added and the bacteria were incubated at 37 °C for 1 h at 200 rpm in an incubation shaker. Finally, the bacteria were streaked on LB agar plates and incubated overnight at 37 °C. To ease single colony picking 100 µl, 200 µl, and 500 µl of each charge were plated separately. If the selection of transformants was requested, the LB agar plates were supplemented with the appropriate antibiotics (Table 4.26).

5.5 Transformation of *N. meningitidis*

Strains of *N. meningitidis* were stored at -80 °C in freezing medium (Table 4.24). The strain of interest was streaked on COS agar plates the day before transformation and incubated overnight at 37 °C with 5% CO_2. After incubation the bacteria were inoculated in PPM^+ for 1 h at 37 °C at 200 rpm in an incubation shaker. After pre-culture, the suspensions were adjusted to $OD_{600} = 0.1$ in a final volume of 1 ml PPM^+. For transformation 600 ng to 1 µg of plasmid DNA (Chapter 5.7) were added to the suspension and incubated for 5 to 6 hours at 37 °C and 200 rpm in an incubation shaker. Subsequently, 100 µl of the culture were streaked directly on GCB^{++} agar plates. The remaining suspension was centrifuged at 5000 rpm for 5 minutes at room temperature. The supernatant was

discarded, the pellet was resuspended in 100 µl PPM^{+} and the suspension was plated on GCB^{++} agar plates. The plates were incubated overnight at 37 °C with 5% CO_2. For selection of transformants, the GCB^{++} agar plates were supplemented with the appropriate antibiotics (Table 4.26).

5.6 Preparation of meningococcal genomic DNA

Meningococcal genomic DNA was isolated using the QIAamp DNA Mini Kit (Table 4.4) according to the manufacturer's protocol with some modifications. Meningococci were streaked on GCB^{++} agar plates and incubated overnight by 37 °C and 5% CO_2. The next day, colonies were harvested with a cotton swab and resuspended in 1.25 ml PBS (Table 4.6). The bacterial suspension was centrifuged for 5 minutes at 8000 rpm, the supernatant was discarded, and the pellet was resuspended in 180 µl ATL buffer (QIAamp DNA Mini Kit) with 20 µl Proteinase K (20 mg/ml). Subsequently, the suspension was incubated at 56 °C and vortexed every 30 minutes for 3 hours. Afterwards, the tube was briefly centrifuged and 80 µl RNase A (5 mg/ml) were added. After vortexing 10 times, 200 µl AL buffer

(QIAamp DNA Mini Kit) were added. Then the tubes were vortexed another 10 times and incubated for 10 minutes at 70 °C. After the addition of 200 µl ethanol the tubes were vortexed 10 times and briefly centrifuged. The fluid was pipetted onto a QIAamp spin column and centrifuged for 1 minute at 8000 rpm. Next, the column was transferred into a fresh tube, 500 µl AW1 buffer (QIAamp DNA mini kit) were applied and centrifuged for 1 minute at 8000 rpm. The flow-through was discarded and the column was washed with 500 µl AW2 buffer for 3 minutes at 13000 rpm. Once again, the flow-through was discarded. Afterwards, the column was dried via 1 minute centrifugation at 13000 rpm. Then the column was transferred into a fresh 2 ml microcentrifugation tube. To elute the DNA, 100 µl 1x TE buffer (QIAamp DNA mini kit) was applied to the column and incubated at room temperature for 5 minutes. Finally the tube was centrifuged for 1 minute at 8000 rpm. The concentration and purity of the DNA was measured spectrophotometrically.

5.7 Isolation of plasmid DNA

Plasmid DNA was isolated using the QIAprep Spin Miniprep Kit (Table 4.4). The *E. coli* strain carrying the plasmid of interest was streaked on a selective LB agar

plate and incubated overnight at 37 °C. After incubation a single colony was picked and inoculated into 5 ml LB medium containing the appropriate antibiotic. This suspension was incubated overnight at 37 °C and 200 rpm in an incubation shaker. The next day, the culture was centrifuged at 8000 rpm for 5 minutes, the supernatant discarded, and the pellet resuspended in 250 µl P1 buffer (QIAprep Spin Miniprep Kit). The suspension was transferred into a 1.5 ml microcentrifuge tube, 250 µl P2 buffer (QIAprep Spin Miniprep Kit) were added and mixed thoroughly by inverting the tube 4 to 6 times. After the addition of 350 µl N3 buffer, the fluids were mixed immediately by inverting 4 to 6 times. Then the tube was centrifuged for 10 minutes at 13000 rpm in a microcentrifuge at room temperature. The supernatant was transferred into aa QIAprep spin column and centrifuged for 30 to 60 seconds at 13000 rpm. After discarding the flow-through, the column was washed by adding 500 µl PB Buffer (QIAprep Spin Miniprep Kit) and centrifuging 30 to 60 seconds at 13000 rpm. The flow-through was discarded again and the column was washed with 750 µl PE buffer (QIAprep Spin Miniprep Kit). To remove residual ethanol, the spin column was transferred into a fresh tube and centrifuged at full speed

for 3 minutes. Finally, the spin column was transferred into a fresh microcentrifugation tube and 30 to 50 µl ddH_2O were added. After incubating for 5 minutes at room temperature, the tube was centrifuged for 2 minutes at 13000 rpm. The concentration and purity of the DNA was measured spectrophotometrically.

5.8 Preparation of bacterial lysates for colony PCR

To obtain bacterial lysates, a single colony was inoculated into 20 to 30 µl 1x PBS (Table 4.6). The suspension was incubated for 5 (*E. coli*) or 15 (*N. meningitidis*) minutes at 100 °C in a heating block and then immediately cooled down on ice for 5 minutes. After centrifuging 1 minute at 13000 rpm, the supernatant was discarded, and the pellet was resuspended in 30 µl 1x PBS. Bacterial lysates were used for quick PCR checks in transformation procedures. One µl per 25 µl PCR formulation was used.

5.9 Polymerase chain reaction (PCR)

Polymerase chain reactions were used to amplify specific DNA fragments. For cloning purposes Q5® High-Fidelity DNA polymerase was used because of its proof-reading activity. To screen colonies in

transformation procedures or to verify genomic alterations, *Taq* DNA polymerase was utilized. Generally, 100 ng of template DNA was used. To screen for transformants, 1 µl bacterial lysate or a colony was used as template. PCRs were generally prepared on ice and quickly transferred into a preheated thermocycler. To recognize DNA contamination, each PCR was done with a negative control without DNA template. The expected size of the PCR product was calculated by *in silico* genome analyses using Artemis (Table 5.10).

PCRs using *Taq* polymerase were performed in modification of the manufacturer's protocol as given in Table 5.1.

Table 5.1 *PCR protocol for Taq DNA polymerase*

Ingredient	**25 µl reaction**	**Final Concentration**
10x ThermoPol reaction buffer	2.5 µl	1x
20 mM dNTPs	0.25 µl	200 µM
25 µM forward primer	0.5 µl	0.5 µM
25 µM reverse primer	0.5 µl	0.5 µM
Template DNA	Variable	<1 µg

Ingredient	25 µl reaction	Final Concentration
Taq DNA polymerase	0.25 µl	0.05 U/µl
ddH_2O	ad 25 µl	

The standard PCR program for PCRs using *Taq* polymerase is given in Table 5.2.

Table 5.2 *Thermocycling program for Taq DNA polymerase*

Step	Temperature	Time
1. Initial denaturation	95 °C	30 seconds (5 minutes for lysates)
2. Denaturation	95 °C	30 seconds
3. Annealing	(T_a) 50-65 °C	30 seconds
4. Extension	68 °C	1 minute/kb
5. Step 2 to 4 repeated 25 to 35 times		
6. Final extension	68 °C	5 minutes
7. Hold	4 °C	∞

The melting temperatures (T_m) of each primer were estimated with the following formula.

$$Tm = 2 * (A + T) + 4 * (G + C)$$

Using *Taq* polymerase, the annealing temperature (T_a) was obtained by subtracting 5 °C from the melting temperatures (T_m). The following Table 5.3 shows the standard protocol for PCRs utilizing the Q5® High-Fidelity DNA polymerase.

Table 5.3 *PCR protocol for Q5® High-Fidelity DNA polymerase*

Ingredient	**50 µl reaction**	**Final Concentration**
5x Q5 reaction buffer	10 µl	1x
20 mM dNTPs	0.5 µl	200 µM
25 µM forward primer	1 µl	0.5 µM
25 µM reverse primer	1 µl	0.5 µM
Template DNA	variable	<1 µg
Q5® High-Fidelity DNA polymerase	0.5 µl	0.02 U/µl
ddH_2O	ad 50 µl	

The standard PCR program for PCRs using the Q5® High-Fidelity DNA polymerase is given in Table 5.4.

Table 5.4 *Thermocycling program for Q5® High-Fidelity DNA polymerase*

Step	Temperature	Time
1. Initial denaturation	98 °C	30 seconds
2. Denaturation	98 °C	10 seconds
3. Annealing	(T_a) 50-72 °C	30 seconds
4. Extension	72 °C	20-30 seconds/kb
5. Step 2 to 4 repeated 25 to 35 times		
6. Final extension	72 °C	2 minutes
7. Hold	4 °C	∞

Applying the Q5® High-Fidelity DNA polymerase the annealing temperature (T_a) was calculated using the NEB T_m Calculator (http://tmcalculator.neb.com/#!/).

5.10 Major PCRs

The following Table 5.5 lists major PCRs performed in this study. The primers (see Table 4.27) are listed next to a short description, elongation time, annealing temperature and the used polymerase.

Table 5.5 *Major PCRs performed in this study*

Primer 1[a]	Primer 2[a]	Description and Usage	ET[b] (s)	AT[c]	PM[d]
1110	1111	8013 *cas9* complementation	30	55 °C	Q5
1122	1123	8013 *cas9* complementation verification	120	56 °C	*Taq*
976	1122	8013 *cas9* complementation verification	300	56 °C	*Taq*
977	1123	8013 *cas9* complementation verification	300	56°C	*Taq*
10511	10512	8013 *cas9* knockout	20	50 °C	Q5
903	904	8013 *cas9* knockout verification	300	60 °C	*Taq*
328	904	8013 *cas9* knockout verification	40	55 °C	*Taq*

Primer 1[a]	Primer 2[a]	Description and Usage	ET[b] (s)	AT[c]	PM[d]
329	903	8013 *cas9* knockout verification	40	55 °C	*Taq*
1045	1046	8013 CRISPR complementation	40	59 °C	Q5
974	975	8013 CRISPR knock-in verification/ knockout exclusion	40	64 °C	*Taq*
11443	11115	8013 CRISPR knockout	10	63 °C	Q5
11444	11116	8013 CRISPR knockout	10	63 °C	Q5
1031	1032	8013 CRISPR knockout verification	210	60 °C	*Taq*
328	1031	8013 CRISPR knockout verification	40	55 °C	*Taq*
329	1032	8013 CRISPR knockout verification	40	55 °C	*Taq*
329	11444	8013 CRISPR knockout verification/ knockout vector check	40	50 °C	*Taq*
328	11443	8013 CRISPR knockout verification/ knockout vector check	40	50 °C	*Taq*
1043	1044	8013 *rnc* complementation	20	53 °C	Q5

Primer 1[a]	Primer 2[a]	Description and Usage	ET[b] (s)	AT[c]	PM[d]
971	1049	8013 *rnc* complementation verification	180	65 °C	*Taq*
971	988	8013 *rnc* complementation verification	180	65 °C	*Taq*
970	989	8013 *rnc* complementation verification	180	65 °C	*Taq*
1047	1048	8013 tracrRNA complementation	20	53 °C	Q5
1049	989	8013 tracrRNA complementation verification	180	65 °C	*Taq*
1048	988	8013 tracrRNA complementation verification	180	65 °C	*Taq*
1047	989	8013 tracrRNA complementation verification	180	65 °C	*Taq*
833	729	8013 tracrRNA knockout	20	56 °C	Q5
834	835	8013 tracrRNA knockout	20	56 °C	Q5
903	328	8013 tracrRNA knockout verification	60	50 °C	*Taq*

Primer 1[a]	Primer 2[a]	Description and Usage	ET[b] (s)	AT[c]	PM[d]
988	989	8013 tracrRNA/ *rnc* knockout verification	240	60 °C	*Taq*
903	739	8013 tracrRNA knockout verification	210	60 °C	*Taq*
976	977	8013/ WUE2594 *cas9* knock-in verification/ knockout exclusion	40	60 °C	*Taq*
970	971	8013/ WUE2594 *rnc* knock-in verification/ knockout exclusion	40	64 °C	*Taq*
10509	10510	8013/ WUE2594 *cas9* knockout	20	50 °C	Q5
552	554	8013/ WUE2594 *rnc* knockout	20	55 °C	Q5
550	551	8013/ WUE2594 *rnc* knockout	20	55 °C	Q5
617	618	8013/ WUE2594 *rnc* knockout verification	210	60 °C	*Taq*
317	329	8013/ WUE2594 *rnc* knockout verification	60	50 °C	*Taq*
618	328	8013/ WUE2594 *rnc* knockout verification	60	50 °C	*Taq*
739	329	8013/ WUE2594 tracrRNA knockout verification	60	50 °C	*Taq*

Primer 1[a]	Primer 2[a]	Description and Usage	ET[b] (s)	AT[c]	PM[d]
723	733	WUE2594 tracrRNA knockout	20	55 °C	Q5
729	730	WUE2594 tracrRNA knockout	20	55 °C	Q5
740	328	WUE2594 tracrRNA knockout verification	60	50 °C	*Taq*
739	740	WUE2594 tracrRNA knockout verification	210	60 °C	*Taq*
10515	10516	WUE2594 *cas9* knockout	20	50 °C	Q5
905	906	WUE2594 *cas9* knockout verification	300	60 °C	*Taq*
328	906	WUE2594 *cas9* knockout verification	40	50 °C	*Taq*
329	905	WUE2594 *cas9* knockout verification	40	50 °C	*Taq*
11116	11306	WUE2594 CRISPR knockout	20	60 °C	Q5
11114	11115	WUE2594 CRISPR knockout	20	60 °C	Q5
11604	11605	WUE2594 CRISPR knockout verification	210	60 °C	*Taq*
328	11605	WUE2594 CRISPR knockout verification	40	55 °C	*Taq*

Primer 1[a]	Primer 2[a]	Description and Usage	ET[b] (s)	AT[c]	PM[d]
329	11604	WUE2594 CRISPR knockout verification/ knockout vector check	40	55 °C	*Taq*
972	973	WUE2594 CRISPR knock-in verification/ knockout exclusion	40	64 °C	*Taq*
243	1049	pCompInd integration control	150	50 °C	*Taq*
1035	1118	pAH-5 construction	60	55 °C	Q5
1117	1118	pAH-4 construction	60	55 °C	Q5
1054	1055	pAH-4/ pAH-5 control	210	58 °C	*Taq*
12662	12663	pGCC2 *cas9*-comp	100	52°C	Q5
1227	1228	8013 *cas9* probe	8	55°C	Q5
1229	1230	8013 NMV0031 probe	8	55°C	Q5
243	242	pBluescript II –SK integration control	180	58°C	*Taq*

[a]ID-number 0-9999 according to the AG SCHOEN oligonucleotide collection, 10000-99999 according to the common IMIB oligonucleotide collection
[b] elongation time
[c] annealing temperature (T_a)
[d] utilized polymerase: ‘Q5’ for Q5® High-Fidelity DNA polymerase, ‘*Taq*’ for *Taq* polymerase

PCR analysis of mutant strains were always performed according to the same principle. Primers located outside of the region used for recombination and outward facing primers located on the resistance gene were combined as depicted in Figure 5.1.

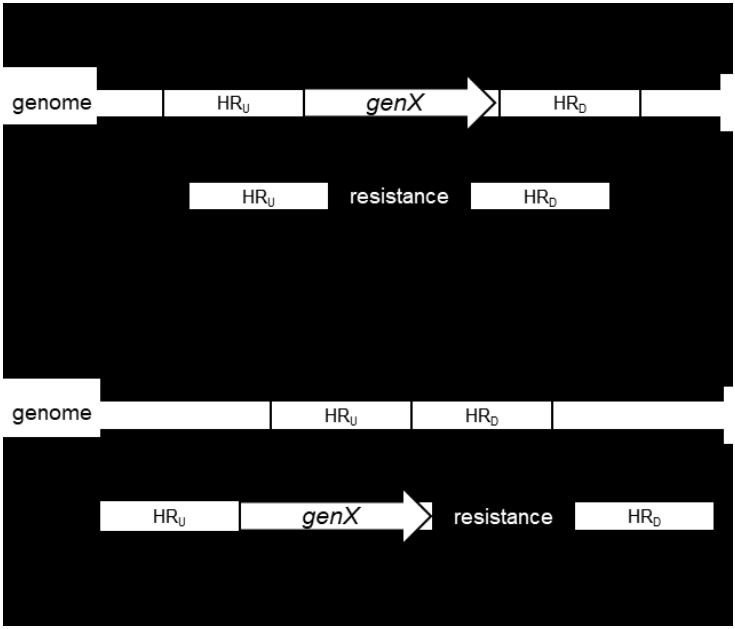

Figure 5.1 *Schematic representation of PCRs used for mutant verification*

Schematic representation of the replacement (A) and complementation (B) of a fictional gene called *genX* via homologous recombination. The homologous regions upstream (HR_U) and downstream (HR_D) of *genX* are identical in the genome and on the knockout vector. To

verify recombinant strains by PCR primers located outside of the region used for recombination (Out1 and Out2) and outward facing primers located on the resistance gene respectively the gene to be complemented (In1 and In2) were combined. The combination of Out1 and Out2 amplifies the whole region of recombination and this way detects double cross-over mutants. The combinations Out1 x In1 and Out2 x In2 additionally allow to determine the orientation of the resistance cassette.

5.11 Sequencing PCR products and plasmids

Sequencing was done by *GATC* (Köln DE). Therefore, sequencing reactions were prepared with 1 µl of the respective primer (25 µM) and 20 – 80 ng of PCR fragments or 200 – 400 ng of plasmid DNA in a 1.5 ml tube with a final volume of 10 µl in ddH_2O.

5.12 DNA digestion

The digestion of DNA fragments, plasmid DNA or genomic DNA was performed by using restriction endonucleases. Table 5.6 lists the protocol for general restriction digests. The suitable buffer was chosen according to the 'NEBuffer Activity/Performance Chart with Restriction Enzymes' provided by New England Biolabs (https://www.neb.com/tools-and-resources/usage-guidelines/nebuffer-performance-chart-with-restriction-enzymes). If two restriction enzymes

were used simultaneously, the buffer was chosen with New England Biolabs' 'Double Digest Finder' (https://www.neb.com/tools-and-resources/interactive-tools/double-digest-finder).

Table 5.6 *Standard restriction digest protocol*

Ingredient	**50 µl reaction**
Restriction enzyme	10 U
DNA	1 µg
10x NEB Buffer	5 µl
ddH_2O	ad 50 µl
Incubation time	1-2 h
Incubation temperature	37 °C

Digested DNA fragments were purified using the MSB Spin PCRapace Kit (Table 4.4). Digested plasmid DNA was separated electrophoretically and the fragments of requested size were extracted from the gel using the Invisorb Spin DNA Extraction Kit.

5.13 Agarose gel electrophoresis of DNA

To visualise PCR products, agarose gel electrophoreses were performed. The PCR products were separated electrophoretically by size in an agarose gel with TAE buffer. This way it was possible to estimate the length of PCR products.

Depending on the size of the expected PCR product, agarose was added to 1x TAE buffer at a concentration of 1% or 2% (w/v). The agarose suspension was heated in a microwave and cooled down while permanently stirred. The hand-warm agarose solution was poured into a gel tray with the well comb in place. As standard molecular weight marker 5 µl 'Hyper Ladder I' (*New England Biolabs,* Frankfurt) was used. To each PCR product sample 6x DNA loading buffer (Table 4.8) was added to a 1x concentration and pipetted into a gel pocket. DNA samples were separated for approximately 1 h at 170 V in 1x TAE buffer. The gels were stained in GelRed™ (*Biotium*, Fremont US) bath for 45 minutes afterwards. To visualize the bands of the DNA fragments via UV light at 302 nm or 312 nm the Chemi Doc MP System was used. Depending on the intended use, the PCR products were either purified or extracted from the gel. For sequencing or cloning purposes, only 3 µl of

each PCR reaction were used for electrophoretic separation. The remaining quantity was purified using the MSB Spin PCRapace Kit (Table 4.4). To separate fragments after digestion, the DNA of requested size was extracted from the gel using the Invisorb Spin DNA Extraction Kit (Table 4.4).

5.14 Purification of DNA fragments

To purify DNA fragments, the MSB Spin PCRapace Kit (Table 4.4) was used following the manufacturers description. First, 50 µl PCR-mixture were very well mixed with 250 µl Binding Buffer to ease the binding of DNA fragments to the silica membrane of the spin filter. Afterwards the sample was transferred onto the spin filter, incubated for 1 minute at room temperature and centrifuged for 4 minutes at maximum speed to remove contaminants. Impurities and detergents do not bind to the silica membrane and are therefore drawn through the column. Then, the spin filter was transferred into a new 1.5 ml receiver tube and 10 µl Elution Buffer were added. Subsequently, the sample was incubated for 1 minute at room temperature and centrifuged for 1 minute at 11000 rpm. The gathered samples were stored at 4°C.

5.15 Gel Extraction

To extract electrophoretically separated DNA from a agarose gel, the Invisorb Spin DNA Extraction Kit (Table 4.4) following the manufacturer's protocol. The bands of interest were cut and the gel slices were transferred into a 1.5 ml microcentrifugation tube. To gel slices up to 150 mg 500 µl Gel Solubilizer was added and 1 ml to gel slices up to 300 mg. The kit was not suitable for slices heavier than 300 mg. The tubes were incubated at 50 °C for 10 minutes until the gel was completely solubilized. Afterwards, 250 µl Binding Enhancer were added to 500 µl reaction volume, and 500 µl to 1 ml reaction volume respectively, and mixed thoroughly by pipetting up and down. Then 800 µl of the sample were transferred onto the spin filter and centrifuged at 11000 rpm for 2 minutes. After discarding the filtrate the residual sample volume was loaded and centrifuged the same way. To purify the extracted DNA the spin filter was washed twice by adding 500 µl Washing buffer and centrifuging for 1 minute at 11000 rpm. Subsequently, the residual ethanol was removed by centrifuging for 4 minutes at 13000 rpm. The spin filter was transferred into a new 1.5 ml receiver tube and 15 µl Elution Buffer were added directly onto the

centre of the spin filter. After incubating at room temperature for 1 minute, the tubes were centrifuged for 1 minute at 11000 rpm. The purity and concentration of the extracted DNA was measured spectrophotometrically.

5.16 DNA ligation

A ligation of purified digested DNA fragments and the linearized vector was performed by using the T4 DNA ligase. Generally, a molar ratio of 1:3 vector to insert was used in standard ligation reaction. The proportion of insert to the vector was calculated with the following formula.

$$m\ (insert)[ng] = \frac{n\ (insert)}{n\ (vector)} * m\ (vector)\ [ng] * \frac{l\ (insert)\ [bp]}{l\ (vector)[bp]}$$

Ligations were generally prepared in microcentrifuge tubes on ice and quickly transferred in a thermocycler precooled to 16 °C. The following Table 5.7 shows the standard ligation protocol using the T4 DNA ligase.

Table 5.7 *Standard ligation protocol using T4 DNA ligase*

Ingredient	20 µl reaction
10x T4 DNA Ligase buffer	2 µl
Vector DNA	50 ng
Insert DNA	Variable
T4 DNA Ligase	1 µl
ddH_2O	ad 20 µl

The ligation buffer was thawed and resuspended at room temperature. After incubating overnight at 16 °C the ligation was heat inactivated at 65 °C for 10 minutes and chilled on ice. Afterwards the ligation product was used for chemical transformation or stored at -20 °C.

5.17 Mutant construction

In general deletion mutants were generated replacing the respective gene with a kanamycin resistance cassette. Approximately 600 bp upstream and downstream of the target gene were amplified with oligonucleotides modified to introduce different enzyme restriction sites (Table 4.27). The fragments were digested, purified and cloned into the pBluescript II -SK

vector along with the digested kanamycin resistance cassette. The obtained knockout plasmids contained a kanamycin resistance cassette flanked by the upstream and downstream region of the respective gene. The meningococcal strains 8013 and WUE2594 were transformed with the linearized plasmids and thus homologous recombination resulted in a replacement of the target gene. Using linear fragments reduces the amount of transformed cells but increases the chance of double crossover mutants [87]. The correct insertion of the resistance gene was confirmed by PCR, sequencing and Southern blot analysis. In this study, knockout mutants of *cas9*, *rnc*, CRISPR and tracrRNA in 8013 as well as WUE2594 were generated. To verify the obtained results the transformation was repeated to obtain multiple biological replicates (see Table 4.29 and Figure 6.1 for detailed information).

Table 5.8 lists the gene loci of the CRISPR/Cas system genes.

Table 5.8 CRISPR/Cas system gene loci

Gene	**Protein**	**8013**		**WUE2594**	
		Locus	St.[a]	Locus	St.[a]
cas1	Cas1	1920388 to 1921302	+	376943 to 376020	-
cas2	Cas2	1921295 to 1921621	+	374160 to 375646	-
cas9	Cas9	1917073 to 1920321	+	377010 to 380258	-
rnc	RNase III	1660804 to 1661523	-	631217 to 632149	+
tracrRNA		1916858 to 1916964	-	380367 to 380473	+
CRISPR		1921685 to 1923370	-	374160 to 375646	+
scaRNA		1923335 to 1923358	+	374172 to 374195	-

[a] Strand: + leading strand / - lagging strand

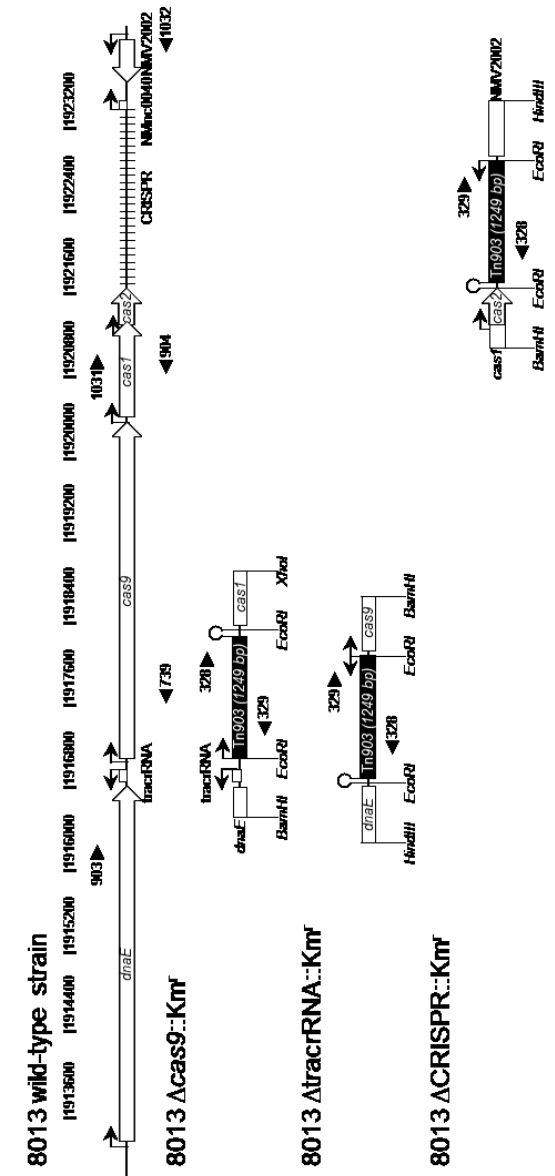
A
8013 wild-type strain
1913600
1914400
1915200
1916000
1916800
1917600
1918400
1919200
1920000
1920800
1921600
1922400
1923200
dnaE
903
tracrRNA
cas9
739
cas1
1031
cas2
904
CRISPR
NMmc0040
NMV2002
1032
8013 Δcas9::Kmr
tracrRNA
328
Tn903 (1249 bp)
cas1
dnaE
329
BamHI
EcoRI
XhoI
8013 ΔtracrRNA::Kmr
329
Tn903 (1249 bp)
cas9
dnaE
328
HindIII
EcoRI
BamHI
8013 ΔCRISPR::Kmr
329
cas1
cas2
Tn903 (1249 bp)
NMV2002
328
BamHI
EcoRI
EcoRI
HindIII

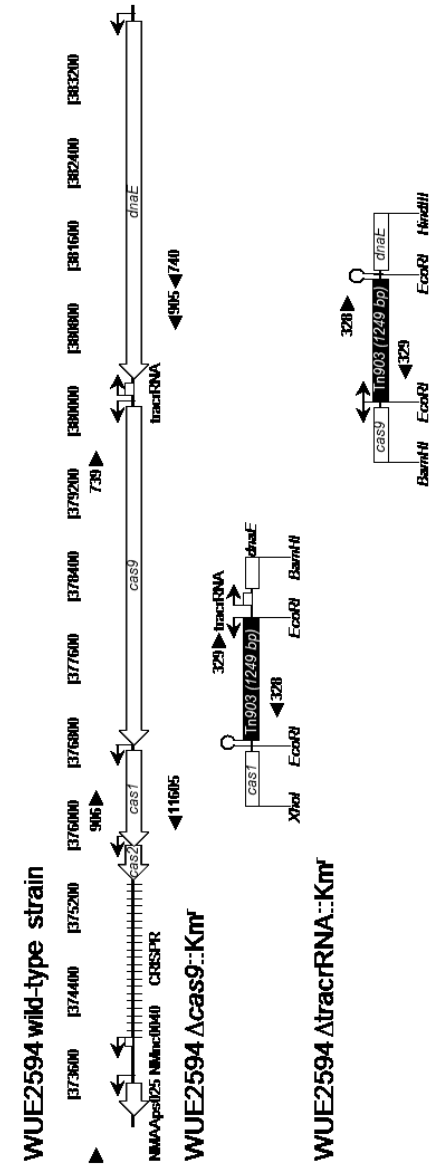
B WUE2594 wild-type strain
11604
[373600
[374400
[375200
[376000
[376800
[377600
[378400
[379200
[380000
[380800
[381600
[382400
[383200
906
739
905
740
11605
cas2
cas1
cas9
tracrRNA
dnaE
NMAAqsi025 NMlari0040 CRISPR
WUE2594 Δcas9::Kmr
329
tracrRNA
cas1
Tn903 (1249 bp)
328
dnaE
XhoI EcoRI EcoRI BamHI
WUE2594 ΔtracrRNA::Kmr
328
Tn903 (1249 bp)
dnaE
cas9
329
BamHI EcoRI EcoRI HindIII
WUE2594 ΔCRISPR::Kmr
328
cas1
Tn903 (1249 bp)
cas2
329
HindIII EcoRI EcoRI BamHI

C 8013 wild-type strain
i1653200
i1660000
i1666000
i1661600
i1662400
618
NMV1712
mc
nbH
nusB
NMV1714
617
8013 Δmc::Km^r
NMV1712
BamHI
EcoRI
328
Tn903 (1249 bp)
329
NMV1714
nbH
EcoRI
HindIII
D WUE2594 wild-type strain
i629600
i630400
i631200
i632000
i632800
617
nusB
nbH
mc
NMAA0522
NMAA0524
618
WUE2594 Δmc::Km^r
NMAA0522
328
nbH
HindIII
EcoRI
Tn903 (1249 bp)
329
EcoRI
BamHI
NMAA0524

Figure 5.2 *Mutant construction in 8013 and WUE2594*

Depicted are the CRISPR/Cas loci in 8013 (A) and WUE2594 (B) and the *rnc* loci in 8013 (C) and WUE2594 (D) as well as the linearized knockout plasmids aligned to their point of integration. The scale in bp above the genes denotes the place in the genome according to the published genome sequences. Bold white arrows indicate genes and their reading direction, gene fragments are indicated by white boxes. Promotors were predicted by BPROM (Table 5.10) and are depicted as small angled arrows. Terminators were predicted by FindTerm (Table 5.10) and are depicted as loops. Loci of non-coding RNAs are indicated by white boxes with angled arrows. Black boxes indicate non-neisserial DNA, in particular kanamycin-resistance cassettes. Vertical lines indicate CRISPR Spacer. Arrows below and above indicate the binding sites of primers used for mutant verification, primer numbers are given next to the arrows. Drawn to scale.

5.18 Complementant construction

To complement the knockout mutants, copies of the knocked-out genes were inserted into the chromosomal DNA. The requested gene was amplified from wild type DNA with oligonucleotides modified to introduce enzyme restriction sites. The complementation plasmids were digested, and the amplified gene fragment was integrated into the multiple cloning sites. Subsequently the gene was integrated by homologous recombination.

Copies of *cas9* were inserted in a locus between *lctP* and *aspC*, copies of tracrRNA and *rnc* in a locus between *porA* and NMV0959. Figure 5.3 shows the integration sites. The strains 8013Δ*cas9*::Km^r, 8013Δ*rnc*::Km^r and 8013ΔtracrRNA::Km^r were complemented with their respective knocked-out gene. In addition, 8013ΔtracrRNA::Km^r was complemented with a *cas9* copy to examine possible *cis*-effects of the tracrRNA knockout on *cas9* expression. Maybe due to the high amount of repeats in the CRISPR array, it was not possible to generate an complementant for 8013ΔCRISPR::Km^r. The WUE2594 mutants were not complemented. Figure 6.1 shows relations of the mutants and complementants, as well as the utilized plasmids in detail. The correct insertion was confirmed by PCR and Southern blot analysis.

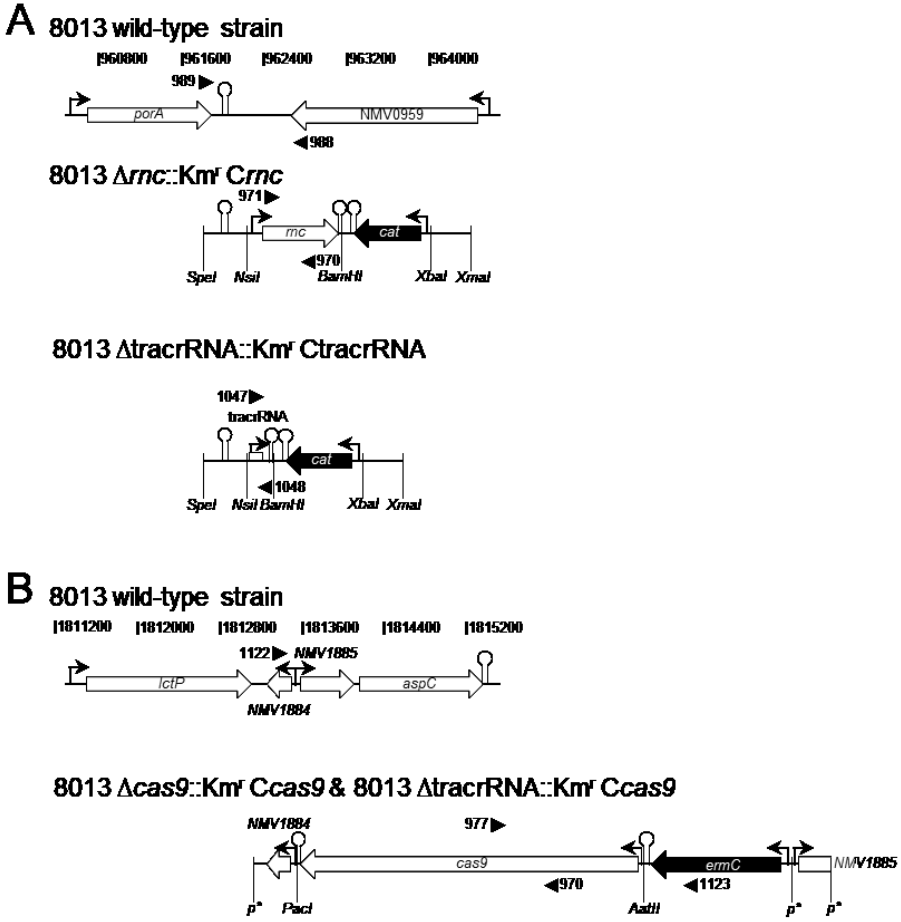

Figure 5.3 *Complementant construction in 8013*

Complementant construction using pCompInd (A) and pGCC2 (B). Schematic elements are used as described in Figure 5.1. Restriction sites of unknown sequence and estimated position are marked with *p**. Drawn to scale.

5.19 Generation of DIG-labelled DNA probes

DIG-labelled DNA probes are needed for Southern Blots. The requested DNA fragment was amplified using the Q5® High-Fidelity DNA Polymerase, purified in the prior described manner and eluted in 30 µl ddH_2O. Subsequently, 15 µl of the DNA were denatured in a heating block at 95 °C for 10 minutes and then immediately cooled down on ice. Then, 2 µl 10x hexanucleotide mix (Table 4.2), 2 µl 10x DIG DNA labelling mix (Table 4.2) and 1 µl Klenow enzyme (Table 4.5) were added. The labelling reaction was mixed thoroughly and incubated overnight at 37 °C. The reaction was stopped by adding 2 µl of 0.2 M EDTA. To precipitate the DNA 2.5 µl of 3 M sodium acetate and 75 µl ice cold 96% ethanol were added and cooled at -80 °C for 30 minutes. After centrifuging for 15 minutes at 13000 rpm and 4 °C, the supernatant was discarded and the pellet was washed with 1000 µl ice cold 70% ethanol. The ethanol was removed carefully by centrifuging for 15 minutes at 13000 rpm and 4 °C and discarding the supernatant. The pellet was dried via vacuum centrifugation for 5 minutes at medium heat. Finally, the probe was resuspended in 50 µl 1x TE buffer.

To quantify the DNA via dot blot, 1 µl of serially diluted DIG-labelled DNA and a DIG-labelled control DNA were pipetted onto a nylon membrane. The DNA was cross linked with an UV cross linker (Table 4.1) for 1 minute. Afterwards, the probes were detected by chemiluminescence with the ChemiDoc MP system and the concentration was estimated by comparison to the control DNA of known concentration.

5.20 Southern Blot

One microgram genomic DNA was digested overnight at 37 °C with a suitable restriction enzyme in a 30 µl reaction volume. The digested DNA and the DIG-labelled molecular weight marker were loaded into a 0.8% agarose gel and electrophoretically separated at 80 V for 5-6 hours. To depurinate, the gel was incubated in 0.25 M HCl for 20 minutes. Afterwards, it was denatured in 5 M NaOH/ 1.5 M NaCl for 30 minutes and neutralized in 5 M TRIS, pH 7.5/ 1.5 M NaCl for another 30 minutes. The blotting sandwich was built up and the flow of 20x SSC buffer (Table 4.9) transferred the negatively charged DNA from the agarose gel to the positively charged nylon membrane overnight. The next day, the nylon membrane was dried and cross linked in an UV crosslinker for 1 minute. The membrane was pre-

hybridized for 30 minutes in 50 ml high SDS hybridisation buffer (Table 4.9) at 48 °C. In the meantime, 500 ng of the DIG-labelled DNA probe was added to 50 ml of high SDS hybridisation buffer, boiled in a water bath for 10 minutes and immediately cooled down on ice for 10 minutes. The pre-hybridisation buffer (Table 4.9) was discarded and the membrane was incubated at 48 °C overnight in the DIG-labelled probe.

5.21 Detection of DIG-labelled DNA by chemiluminescence

For the detection of hybridized DIG-labelled DNA, the membrane was washed twice in stringent washing buffer I (Table 4.9) at room temperature for 5 minutes, and twice in stringent washing buffer II (Table 4.9) at 68 °C for 15 minutes. The following steps were performed at room temperature on a laboratory shaker. First, the membrane was incubated in 1x washing buffer (Table 4.9) for 5 minutes, then in 1x blocking solution (Table 4.9) for 30 minutes and finally in antibody solution for another 30 minutes. Afterwards the membrane was washed twice for 15 minutes in 1x washing buffer and incubated in detection buffer (Table 4.9) for 5 minutes. Finally, CSDP working solution

(Table 4.9) was pipetted onto the membrane. After 5 minutes the membrane was wrapped into a cling film and incubated at 37 °C for 15 minutes. The membrane was developed with the ChemiDoc MP System according to the manufacturer's instructions.

5.22 SDS-PAGE

For the preparation of SDS-polyacrylamide gels the 12.5% separating gel solution (Table 4.10) was mixed thoroughly and pipetted into the casting frame. To obtain horizontal separating gel, water was filled into the casting frame on top of the SDS-polyacrylamide gel. After 30 minutes the water was discarded and the loading gel (Table 4.10) was pipetted into the frame. A comb was inserted without trapping air under its teeth. After 1 hour, the gel was either used immediately or stored at 4 °C until usage. Before gel electrophoresis, protein samples were incubated at 95 °C for 10 minutes and immediately cooled on ice. The 12.5% SDS-polyacrylamide gels were loaded with 10 – 20 µl protein sample and 5 µl prestained protein marker (Table 4.3). The proteins were separated at 160 V for approximately 1.5 hours in electrophoresis buffer (Table 4.10). Subsequently, the gel was fixed in fixing solution for 30-60 minutes. Afterwards, it was transferred into

Coomassie staining solution (Table 4.10) and incubated until the desired band intensity was reached. To destain the gel it was bathed in 10% acetic acid for 2 hours or more.

5.23 *In vitro* growth experiments with *N.meningitidis*

The strains were grown overnight at 37 °C/ 5% CO_2 on COS agar plates. The next day, the mutants and the corresponding wild type were inoculated into the medium of interest. The cultures were incubated at 37 °C and 200 rpm for 1 hour. Afterwards, the meningococci were adjusted to an OD_{600} of 0.1 and further incubated at 37 °C and 200 rpm. Growth was determined by measuring the OD_{600} every hour.

5.24 Serial dilution

Serial dilutions were used to reduce the number of bacteria to a countable level when plated. One hundred millilitre of 1 ml bacterial suspension were transferred into 900 µl 1x PBS and mixed thoroughly to reduce the plated number of colony-forming units (CFU) by 10^{-1}. Subsequently, 100 µl of the 10^{-1} dilution were transferred into 900 µl sterile 1x PBS to reduce the plated CFU another time by 10^{-1}. After mixing thoroughly this step

was repeated until an estimated scale of 10^2 to 10^3 was reached. Three stages of the dilution series were plated in triplicates. The mean CFU of each dilution step was determined and multiplied by the cumulative dilution factor.

5.25 Cell adhesion and invasion assay

Cell adhesion and invasion assays were performed on Detroit562 nasopharyngeal epithelial cells (Chapter 4.11). Detroit562 cells double cell number within a day so 1x 10^5 cells per well were seeded two days in advance into a 24-well plate to obtain 4x 10^5 for experiment. The wild type strain and the respective mutant strains were streaked out on COS blood agar plates overnight at 37 °C/ 5% CO_2. The next day the bacteria were inoculated into 5 ml preculture medium (Table 5.9) and cultured for 1 hour at 37 °C and 200 rpm in an incubation shaker. In the meantime, the Detroit562 cells were washed twice with 1 ml cell culture medium (Table 5.9) to remove non-adherent cells. After that, 1 ml infection medium (Table 5.9) was added to each well and the viability and confluence was checked with a microscope. After incubating, the number of bacterial cells was estimated by measuring the OD_{600} and the Detroit562 cells were infected with a predetermined

multiplicity of bacteria (‘multiplicity of infection’ see Table 5.9). Subsequently, the 24 well plate was incubated for 4 hours at 37 °C with 5% CO_2. In the meantime, the number of seeded bacteria was determined by adding the same infection volume to 1 ml 1x PBS and plating serial dilutions in triplicates. Four hours post infection, CFU in the supernatant was determined the same way. The supernatant was removed carefully, and the cells were washed with 1 ml infection medium. Four wells per strain were used to determine the ‘invasive’ or ‘gentamicin protected’ bacteria and treated with 0.2 mg/ml gentamicin for 1 hour at 37 °C to kill the extracellular bacteria. Another 4 wells per strain were used to assess the ‘adherent’ or ‘cell associated’ bacteria and treated with 1% saponin for 15 minutes to break up the Detroit562 cells. The CFU of the ‘adherent’ bacteria were determined by plating the serial dilution in triplicates. One hour post gentamicin treatment the ‘invasive’ bacteria were determined the same way. The next day, the CFU was determined via colony counter and the ‘adherent’ bacteria were compared to the ‘seeded’ bacteria. Likewise, the ‘invasive’ bacteria were compared to the ‘adherent’ bacteria.

Table 5.9 *Specifications of the adhesion and invasion assay for 8013 and WUE2594 strains*

	WUE2594	**8013**
Preculture medium	GCBL^{++} (Table 4.16)	EMEM^{+++} (Table 4.22)
Cell culture medium	EMEM^{+++}	EMEM^{+++}
Infection medium	RPMI^{+} (Table 4.25)	EMEM^{+++}
Multiplicity of infection (MOI)	10	20

5.26 Static biofilm assay for *N. meningitides*

The requested strains were grown at 37 °C/ 5% CO_2 on COS agar plates for 8 hours. After incubation the meningococci were resuspended in the medium of interest and adjusted to an OD_{600} of 0.1. One hundred microliter bacterial suspension were seeded per well of a 96-well microtiter plate and incubated at 37 °C, 5% CO_2 overnight. After 16 hours of incubation the supernatant was removed, and the adherent bacteria were stained by adding 100 µl 0.05% crystal violet for 10 minutes at room temperature. The wells were washed twice with 200 µl PBS per well. Subsequently, the remaining crystal violet

stain of the biofilm was dissolved with 100 µl 96% ethanol per well and incubated at room temperature for 20 minutes. Finally, the optical density at 595 nm (OD_{595}) was measured for each well in a spectrometer.

5.27 Computational analyses

The following Table 5.10 lists the software and computational tools utilized for this study. The Basic Local Alignment Search Tool of the National Center of Biotechnology Information (NCBI BLAST) (http://blast.ncbi.nlm.nih.gov/Blast.cgi) was used for similarity searches against nucleotide databases.

Table 5.10 *Utilized software*

Program	Application	Developer/ Source
Excel 2016	Statistics and spreadsheet analysis	*Microsoft*
SnapGene 2.8	Plasmid construction	*GSL Biotech LLC*
Serial Cloner 2.6	DNA sequence analysis	*Serial Basic*
BioEdit 7.2.5	Sequence alignment and analysis	*Ibis Bioscience* [88]

Program	Application	Developer/ Source
Blast 2.8.1+	Sequence alignment and comparison	National Center for biotechnology Information (NCBI) [89, 90]
Gimp 2.8.20	Creating graphical figures or illustrations	S. Kimball, P. Mattis (GPLv3+)
Image Lab 5.2	Software for ChemiDoc MP Imaging System	*Bio-Rad*, Hercules US
Artemis 16.0.0	Genome browsing	*Wellcome Trust Sanger Institute* [91]
NeMeSys	Neisseria genome browsing	[47]
BPROM	Promotor prediction	*Softberry* [92]
FindTerm	Terminator prediction	*Softberry* [92]
ACT 13.0.0	Pairwise comparison of two or more DNA sequences	*Wellcome Trust Sanger Institute* [93]
PowerPoint 2016	Creating graphical figures or illustrations	*Microsoft*
Word 2016	Textwork	*Microsoft*

6 Results

6.1 Verification of 8013 and WUE2594 mutant strains

In order to analyse the influence of the CRISPR/Cas system experimentally, knockout mutants of *cas9*, *rnc*, tracrRNA, and the CRISPR-array were constructed in the genetic background of *N. meningitidis* strain 8013 and WUE2594.

The knockout mutants were generated by replacing the entire coding sequence with a kanamycin resistance cassette (see 5.17). The deletion of the tracrRNA, *rnc* and, CRISPR in 8013 was performed twice and the deletion of *cas9* in 8013 was done three times in order to gain multiple biological replicates (see Figure 6.1). The 8013 *cas9*, *rnc,* and tracrRNA knockout strains were complemented by inserting a copy of the respective wild type gene along with their promotor region into the *porA* locus using the integration plasmid pCompInd or into the *lctP-aspC* locus using pGCC2. In order to analyse potential polar effects of the tracrRNA knockout on the expression of *cas9,* a second copy of *cas9* was integrated in the genome of an 8013 tracrRNA knockout strain (see Chapter 5.18).

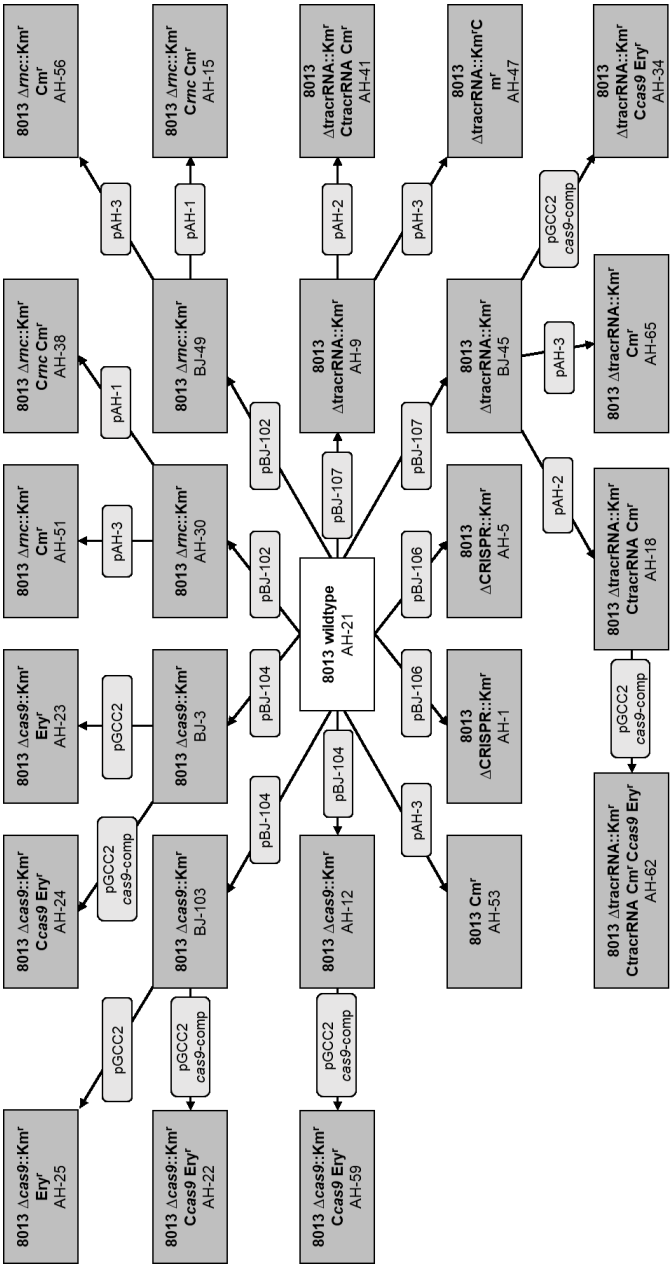
8013 wildtype
AH-21
pBJ-102
pBJ-104
pBJ-106
pBJ-107
pAH-1
pAH-2
pAH-3
pGCC2
pGCC2 cas9-comp
8013 Δcas9::Kmr Eyr AH-25
8013 Δcas9::Kmr Ccas9 Eyr AH-22
8013 Δcas9::Kmr Ccas9 Eyr AH-24
8013 Δcas9::Kmr Eyr AH-23
8013 Δcas9::Kmr BJ-103
8013 Δcas9::Kmr BJ-3
8013 Δrnc::Kmr Cmr AH-56
8013 Δrnc::Kmr Crnc Cmr AH-15
8013 Δrnc::Kmr Cmr AH-51
8013 Δrnc::Kmr Crnc Cmr AH-38
8013 Δrnc::Kmr AH-30
8013 Δrnc::Kmr BJ-49
8013 Δcas9::Kmr Ccas9 Eyr AH-59
8013 Δcas9::Kmr Ccas9 Eyr AH-12
8013 Cmr AH-53
8013 ΔCRISPR::Kmr AH-1
8013 ΔCRISPR::Kmr AH-5
8013 ΔtracrRNA::Kmr AH-9
8013 ΔtracrRNA::Kmr CtracrRNA Cmr AH-41
8013 ΔtracrRNA::Kmr BJ-45
8013 ΔtracrRNA::Kmr Cmr AH-47
8013 ΔtracrRNA::Kmr CtracrRNA Cmr AH-18
8013 ΔtracrRNA::Kmr Ccas9 Eyr AH-34
8013 ΔtracrRNA::Kmr Cmr AH-65
8013 ΔtracrRNA::Kmr CtracrRNA Cmr Ccas9 Eyr AH-62

Figure 6.1 *Genealogy of 8013 mutant strains used in this study*

This flowchart depicts the wild type strain and the respective mutants of strain 8013. Boxes in dark grey indicate biological replicates of transformed strains. The bold text provides a short description of the genotype. The names are given below according to the AG SCHOEN strain list. Arrows indicate transformations with the utilized plasmid in boxes with blunt edges.

The correct insertion of the resistance cassette in WUE2594 and 8013 mutant strains was confirmed by southern blot analysis (Figure 6.2, Figure 6.3, and Figure 6.4), RT-PCR (Figure 6.5), and PCR (Figure 6.6 A+B).

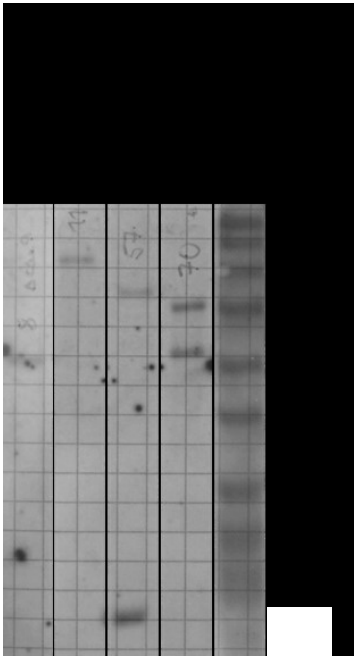

Figure 6.2 *Southern blot analysis of WUE2594 knockout mutants*

Southern blot analysis to verify the genotypes of WUE2594Δ*cas9*::Km^r, WUE2594Δ*rnc*::Km^r, WUE2594ΔtracrRNA::Km^r and WUE2594ΔCRISPR::Km^r. The genomic DNA of the mutant and the wild type strains were digested simultaneously with *ClaI* and *HindIII* and used for Southern blot hybridisation with the kanamycin resistance gene as probe. On the right side is the DNA Molecular Weight Marker VII, DIG-labelled (M), labelled with the band size in bp. The sizes of the expected fragments and the location of *ClaI* and *HindIII* restriction sites in the genome are given schematically in Figure 6.3.

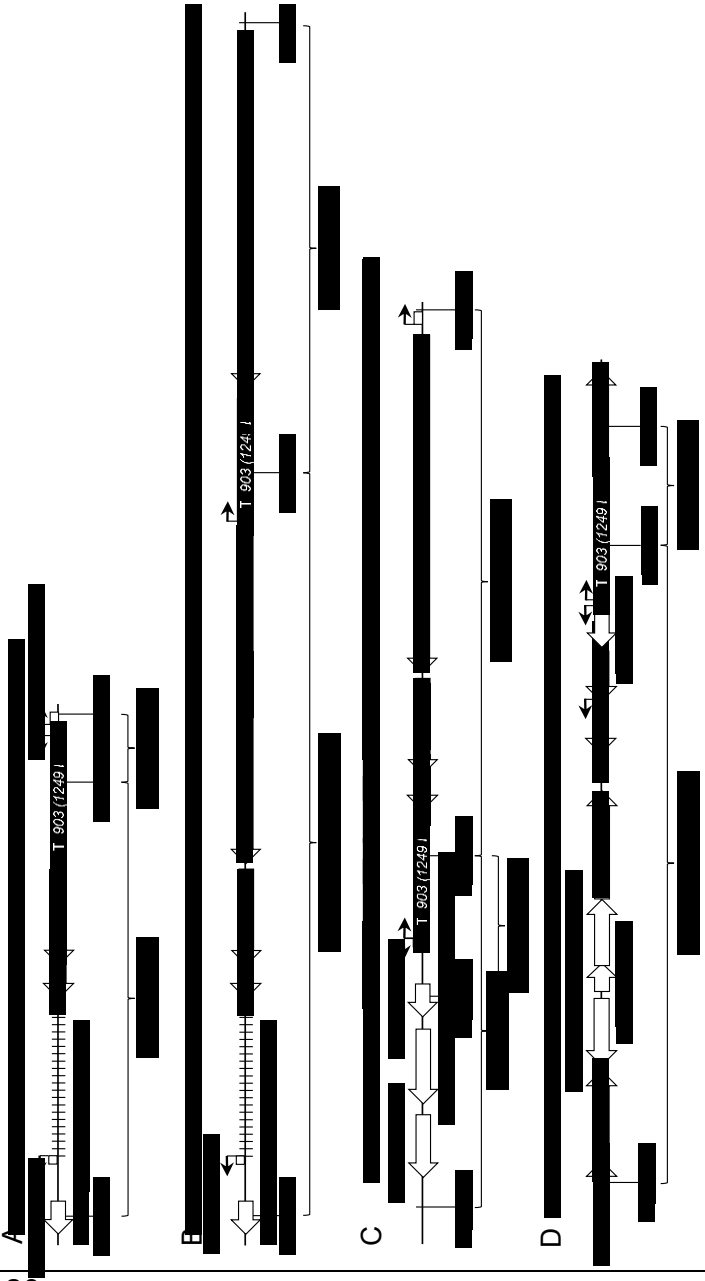
A
T 903 (1249 l
B
T 903 (124: l
C
T 903 (1249 l
D
T 903 (1249 l

Figure 6.3 *Computationally predicted fragment sizes of WUE2594 mutant strains in Southern blot with Tn903-probe after HindIII/ClaI double digest*

Depicted are the CRISPR/Cas loci of WUE2594Δ*cas9*::Km^r (A), WUE2594ΔtracrRNA::Km^r (B) and WUE2594ΔCRISPR::Km^r (C) and the WUE2594Δ*rnc*::Km^r *rnc* locus (D). The scale in bp above the genes denotes the place in the genome according to the published genome sequence of the wild type strain. Bold white arrows indicate genes and their reading direction. Loci of non-coding RNAs are indicated by white boxes with angled arrows. Black boxes indicate non-neisserial DNA, in particular, kanamycin-resistance cassettes (*Tn903)*. Vertical lines indicate CRISPR spacers. Restriction sites of *ClaI* and *HindIII* are given below the genes. The braces mark genome fragments after *HindIII/ClaI,* double digest hybridising with the *Tn903*-probe in Southern blot, and their computationally estimated size in bp. Drawn to scale.

The WUE2594 *cas9, rnc,* and tracrRNA knockout strains demonstrated fragment sizes as expected (Figure 6.3) in the Southern blot. Strain WUE2594ΔCRISPR had one fragment of the expected size (5.4 kbp) but also a fragment of approximately 3.8 kbp, which is not computationally predicted. Even if a point mutation would alter the *ClaI* restriction site upstream the kanamycin restriction site and therefore inhibit the digestion, the

next *ClaI* restriction site would lead to a fragment significantly smaller than 3.8 kbp (see Figure 6.3).

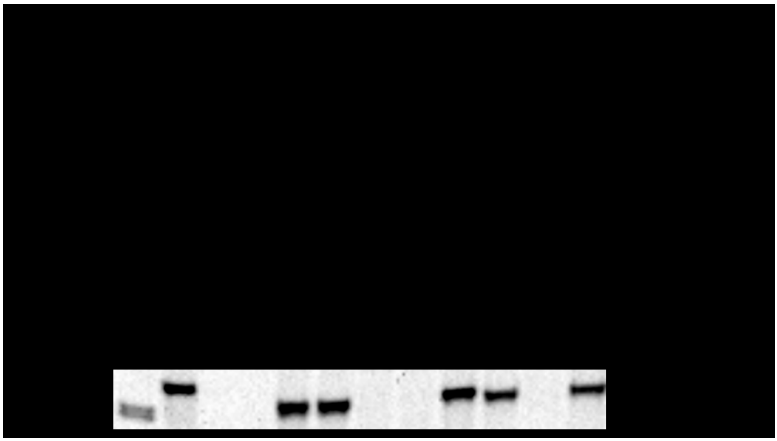

Figure 6.4 *Southern blot analysis of 8013 cas9 mutant strains*

Southern blot analysis to verify the genotypes of 8013Δ*cas9*::Km^r and 8013Δ*cas9*::Km^r C*cas9* strains. The genomic DNA of the mutant and the wild type strains were digested and used for Southern blot hybridisation with *cas9* as probe.

The Southern blot analysis of 8013 *cas9* mutant strains showed *cas9* detectable in the wild type and the complemented strains but not in the knockout-strains. Additionally, the *cas9* knockout strains and the respective complemented strains in the genetic background of 8013 were verified via RT-PCR

(Figure 6.5), which demonstrates that *cas9* is not transcribed in the knockout strains but in the complemented strains and the wild type.

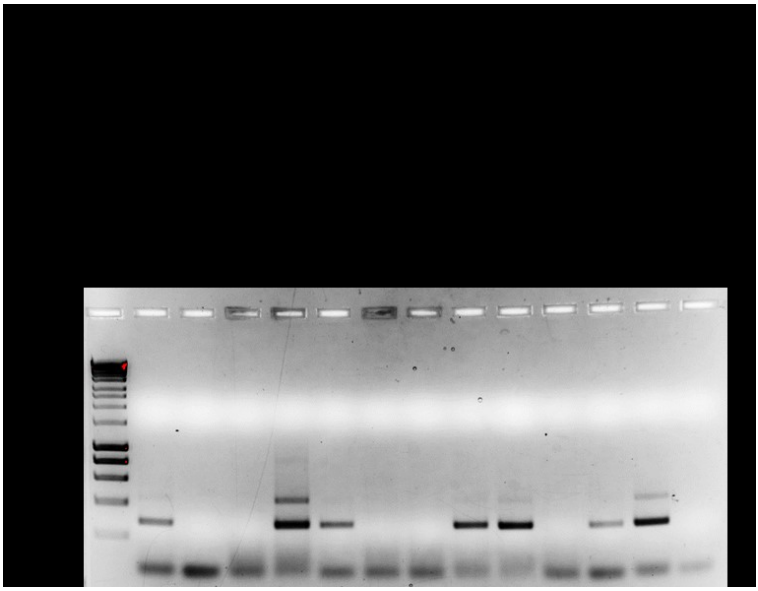

Figure 6.5 *Gel electrophoresis of RT-PCR products from 8013 cas9 mutant strains*

RT-PCR on *cas9* with primer pair 1227 x 1228. Estimated size of the PCR product: 268 bp. Bacteria were grown in GCBL^{++}. RNA samples were isolated in late logarithmic growth phase and transcribed. An unpredicted product of approximately 400 bp is traceable in almost every positive PCR, which may be due to unspecific primer binding. Genomic DNA of 8013 WT was used as a positive control (PC). DNA HyperLadder™ 1kb was used as a marker (M). Abbreviations: NC, negative control.

Since the WUE2594 CRISPR knockout strain did not show the expected fragment size, further PCR analyses were required. The binding sites of the primers used in PCRs for mutant verification are shown in Figure 5.2 and Figure 5.3.

The PCRs performed to verify knockout strains are given in Table 6.1. The PCR conditions in particular are given in Table 5.5. Figure 6.6 shows the stained PCR products after gel electrophoresis.

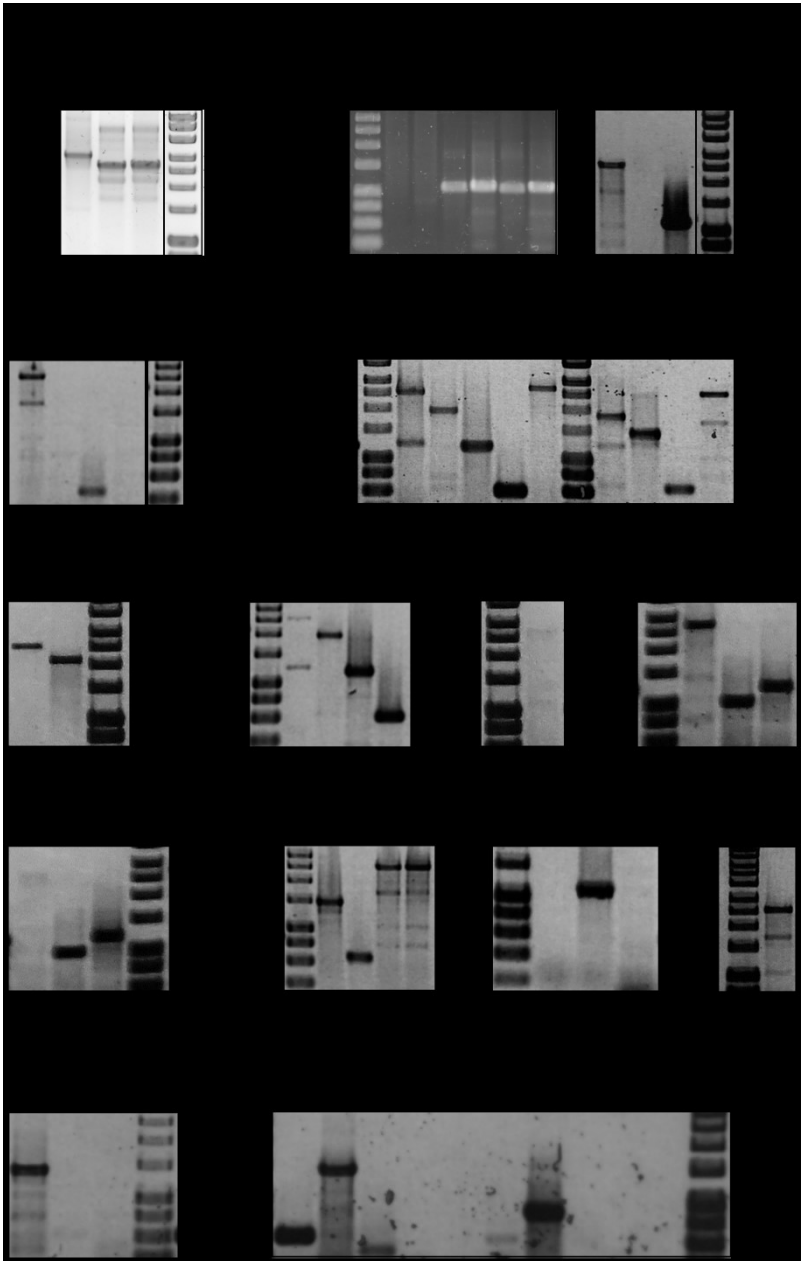

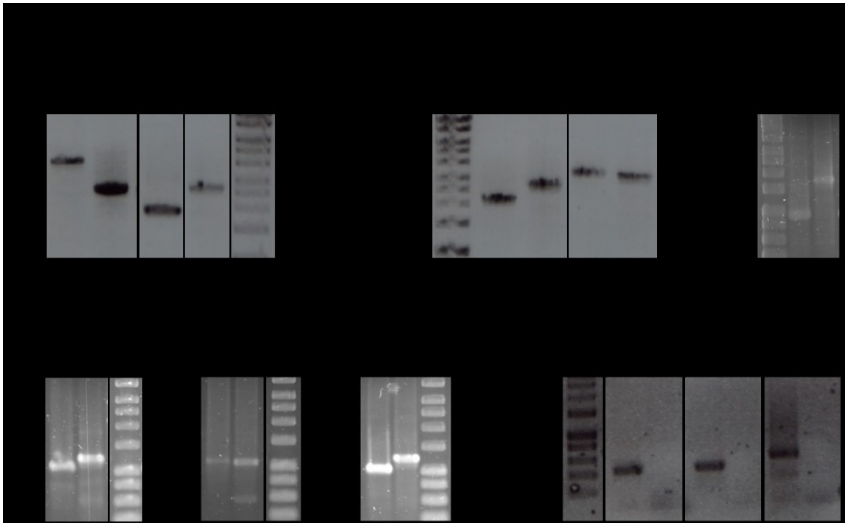

Figure 6.6 *PCR verification of mutant strains*

Products of PCRs performed to verify mutants in 8013 (A) and WUE2594 (B). Each lane is labelled with a unique PCR identifier shown in Table 6.1. PCRs were performed as described in Table 5.5 using bacterial lysates as template. Depicted are the stained PCR products after gel electrophoresis. PCR products of unexpected size are marked by asterisks (*), PCRs that repeatedly failed are marked by crosses ($^{+}$). The stained DNA HyperLadder™ 1kb is depicted next to the products and partially lettered in bp.

Table 6.1 *Explanation of the PCR identifier*

PCR identifier	strain	primer	expected product size (bp)
A-1-1	8013 ΔCRISPR [AH-1]	1031 x 1032	2574
A-1-2		1031 x 328	1069
A-1-3		1032 x 329	1088
A-5-1	8013 ΔCRISPR [AH-5]	1031 x 1032	2574
A-5-2		1031 x 328	1069
A-5-3		1032 x 329	1088
A-9-1	8013 ΔtracrRNA [AH-9]	903 x 739	2517
A-9-2		903 x 328	958
A-9-3		739 x 329	1082
A-15-1	8013 Δ*rmc* C*rmc* [AH-15]	988 x 989	2541
A-15-2		988 x 971	1966
A-15-3		989 x 970	1117
A-15-4		970 x 971	665
A-15-5		617 x 618	2653

PCR identifier	strain	primer	expected product size (bp)
A-18-1	8013 ΔtracrRNA CtracrRNA [AH-18]	988 x 989	1868
A-18-2		988 x 1047	1466
A-18-3		989 x 1048	618
A-18-4		903 x 739	2517
A-30-1	8013 Δ*rnc* [AH-30]	617 x 618	2653
A-30-2		617 x 329	1220
A-30-3		618 x 328	1016
A-34-1	8013 ΔtracrRNA C*cas9* [AH-34]	903 x 739	2517
A-34-2		903 x 328	958
A-34-3		739 x 329	1082
A-34-4		1122 x 1123	4056
A-34-5		976 x 1122	2514
A-34-6		977 x 1123	2234
A-38-1	8013 Δ*rnc* C*rnc* [AH-38]	988 x 989	2541
A-38-2		988 x 970	1966
A-38-3		989 x 971	1117
A-38-4		970 x 971	665

PCR identifier	strain	primer	expected product size (bp)
A-38-5		617 x 618	2653
A-41-1	8013 ΔtracrRNA CtracrRNA [AH-41]	988 x 989	1868
A-41-2		988 x 1047	1466
A-41-3		989 x 1048	618
A-41-4		903 x 739	2517
A-47-1	8013 ΔtracrRNA [AH-47]	903 x 739	2517
A-47-2		903 x 328	958
A-47-3		739 x 329	1082
A-56-1	8013 Δ*rnc* [AH-56/ BJ-49]	617 x 618	2653
A-56-2		617 x 329	1220
A-56-3		618 x 328	1016
A-65-1	8013 ΔtracrRNA [AH-65]	903 x 739	2517
A-WT-1	8013 WT	1031 x 1032	3059
A-WT-2	8013 WT	1031 x 328	-
A-WT-3	8013 WT	1032 x 329	-
A-WT-4	8013 WT	617 x 618	2172

PCR identifier	strain	primer	expected product size (bp)
A-WT-5	8013 WT	988 x 971	-
A-WT-6	8013 WT	989 x970	-
A-WT-7	8013 WT	970 x 971	665
A-WT-8	8013 WT	903 x 739	1423
A-WT-9	8013 WT	1047 x 1048	202
A-WT-10	8013 WT	988 x 1047	-
A-WT-11	8013 WT	989 x 1048	-
A-WT-12	8013 WT	977 x 1123	-
A-WT-13	8013 WT	988 x 989	866
A-WT-14	8013 WT	977 x 1123	-
A-WT-15	8013 WT	1122 x 1123	-
A-WT-16	8013 WT	617 x 329	
B-9-1	WUE2594 Δ*cas9* [BJ-9]	905 x 906	2736
B-9-2		905 x 329	1200
B-9-3		906 x 328	1064
B-9-4		976 x 977	-

PCR identifier	strain	primer	expected product size (bp)
B-11-1	WUE2594 ΔtracrRNA [BJ-11]	739 x 740	2651
B-11-2		740 x 328	1105
B-11-3		739 x 329	1082
B-57-1	WUE2594 *Δrnc* [BJ-57]	617 x 618	2699
B-57-2		618 x 328	1015
B-57-3		617 x 329	1220
B-57-4		970 x 971	-
B-70-1	WUE2594 ΔCRISPR [BJ-70]	11604 x 11605	3160
B-70-2		11605 x 328	1734
B-70-3		11604 x 329	962
B-70-4		972 x 973	-
B-WT-1	WUE2594 WT	905 x 906	4729
B-WT-2	WUE2594 WT	739 x 740	1570
B-WT-3	WUE2594 WT	617 x 618	2171
B-WT-4	WUE2594 WT	11604 x 11605	3399

PCR identifier	strain	primer	expected product size (bp)
B-WT-5	WUE2594 WT	976 x 977	546
B-WT-5	WUE2594 WT	970 x 971	665
B-WT-6	WUE2594 WT	972 x 973	661

The 8013 and the WUE2594 mutant strains were successfully verified by PCR analysis and showed the computationally predicted product sizes. Only the PCRs using the primer combination 903x328 failed repeatedly, possibly due to bad primer compatibility. The PCR A-34-4 amplifies a product larger than 4000 bp and was not performable using *Taq* polymerase.

Overall, the generated mutant strains were in line with the expectations.

6.2 Influence of the genetic alterations on the phenotype of 8013 and WUE2594 mutant strains

6.2.1 Macroscopic aspect of WUE2594 and 8013 mutant strains on COS agar plates

On many occasions during the experiments, the strains were cultivated on COS agar plates. It was continuously observable that the colonies of the *N. meningitidis* WUE2594 *rnc* knockout strain were smaller than other WUE2594 strains plated at the same time (Figure 6.7). This effect was not observable in *N. meningitidis* 8013.

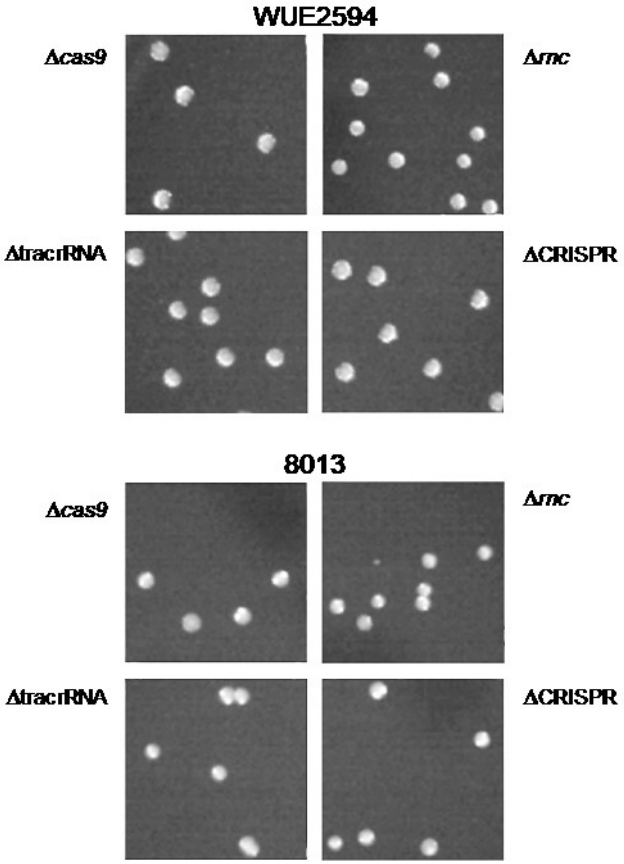

Figure 6.7 *Macroscopic aspect of the WUE2594 and 8013 mutant strains as colonies on COS plates*

Liquid cultures of the strains were adjusted to OD_{600} = 1.0, plated on COS plates, and incubated overnight at 37 °C and 5% CO_2. The photographs were taken using the *ProtoCOL* colony counter (Table 4.1). Depicted are equally scaled, representative parts of an entire agar plate.

6.2.2 Bacterial growth of WUE2594 mutant strains in liquid culture

The macroscopic aspect of the WUE2594 *rnc* knockout strain might indicate a growth deficiency of this strain. To exclude the presence of global phenotypic effects influencing further experiments, the *in vitro* growth of the strains in RPMI^{+} (Table 4.25) was examined. The results are depicted in Figure 6.8. Since the adhesion and invasion assays with WUE2594 strains were only performed in RPMI^{+}, the growth of WUE2594 strains in EMEM^{+++} was not assessed.

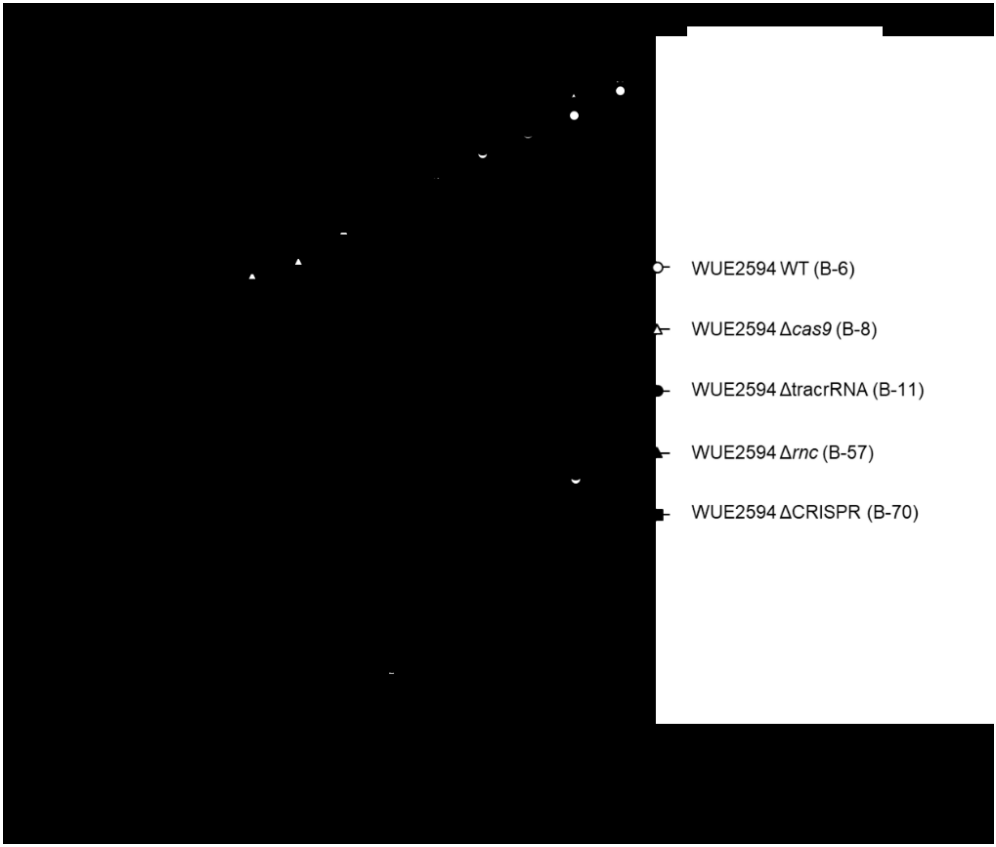

Figure 6.8 *Growth of WUE2594 strains in RPMI⁺*

WUE2594 wild type and mutant strains were grown in RPMI⁺ for 10 h at 37 °C, and the optical density (OD_{600}) was determined every hour (A). After 0 h, 5 h, and 9 h of incubation, the suspensions were serially diluted, and three dilution steps were plated twice on COS agar plates. After overnight incubation, the CFU was measured using the ProtoCol colony counter. Depicted are the weighted mean values and the standard deviations of six measurements (B).

Even though hourly measuring of the OD_{600} did not reveal differences in growth between WUE2594 mutant strains, the counted CFU of the *rnc* knockout were reduced compared to the wild type strain after 9 h of growth.

6.2.3 Bacterial growth of 8013 mutant strains in liquid culture

6.2.3.1 8013 mutant strains are able to survive in EMEM^{+++}

To preserve vital host cells, the cell adhesion and invasion assays had to be performed using EMEM^{+++} as culture medium. While EMEM^{+++} is a nutrient-rich medium (Table 4.23), the capability of *N. meningitidis* 8013 and the mutant strains to survive and grow in EMEM^{+++} had to be assessed.

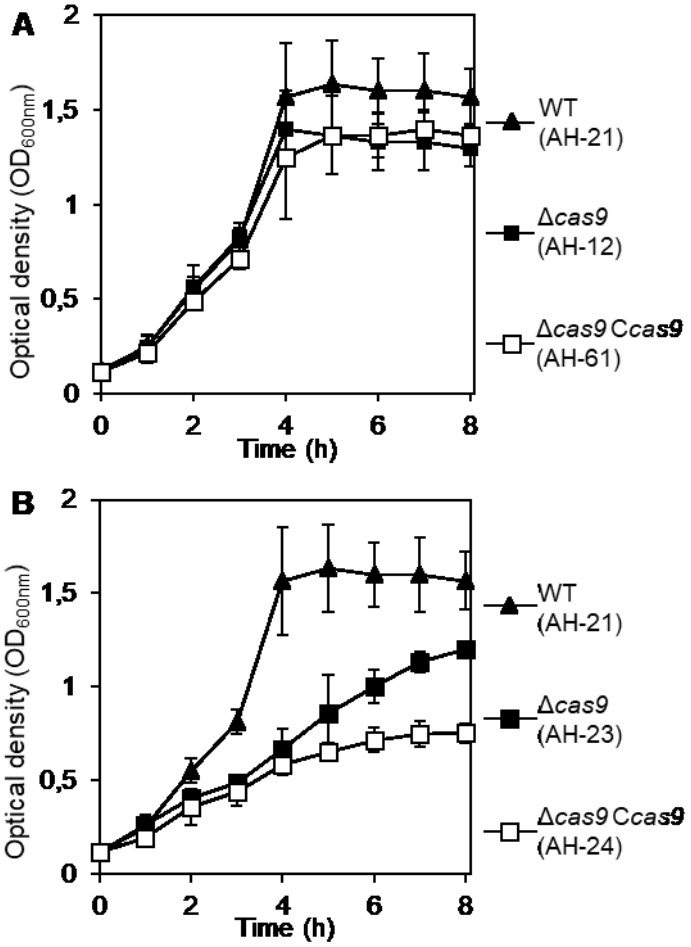
A
Optical density (OD600nm)
2
1,5
1
0,5
0
0
2
4
6
8
Time (h)
WT
(AH-21)
Δcas9
(AH-12)
Δcas9 Ccas9
(AH-61)
B
Optical density (OD600nm)
2
1,5
1
0,5
0
0
2
4
6
8
Time (h)
WT
(AH-21)
Δcas9
(AH-23)
Δcas9 Ccas9
(AH-24)

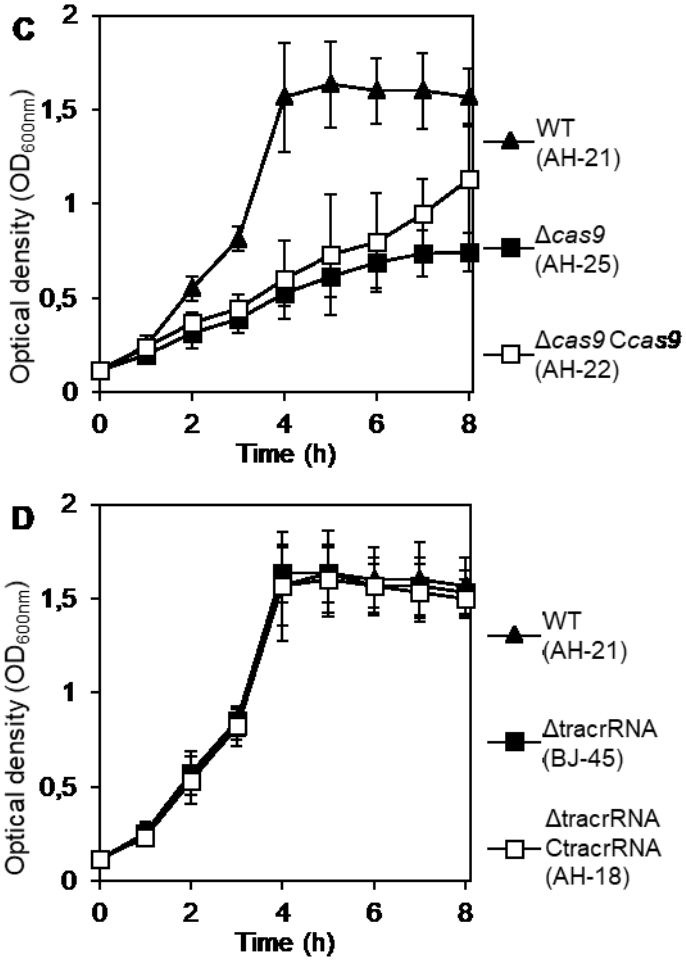
C
Optical density (OD600nm)
2
1,5
1
0,5
0
0
2
4
6
8
Time (h)
WT
(AH-21)
Δcas9
(AH-25)
Δcas9 Ccas9
(AH-22)
D
Optical density (OD600nm)
2
1,5
1
0,5
0
0
2
4
6
8
Time (h)
WT
(AH-21)
ΔtracrRNA
(BJ-45)
ΔtracrRNA
CtracrRNA
(AH-18)

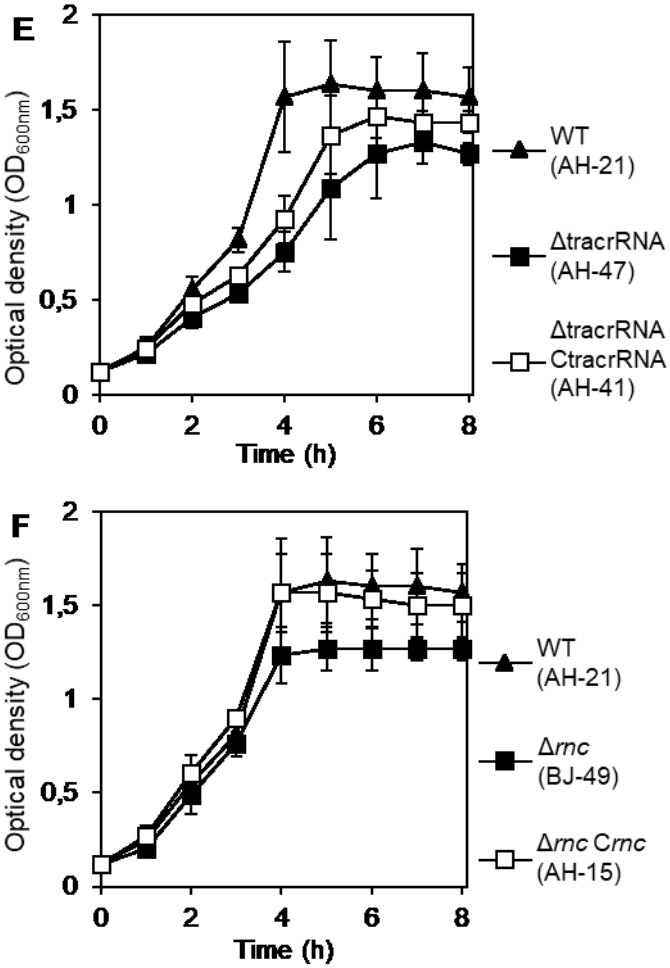
E
Optical density (OD600nm)
2
1,5
1
0,5
0
0
2
4
6
8
Time (h)
WT
(AH-21)
ΔtracrRNA
(AH-47)
ΔtracrRNA
CtracrRNA
(AH-41)
F
Optical density (OD600nm)
2
1,5
1
0,5
0
0
2
4
6
8
Time (h)
WT
(AH-21)
Δrnc
(BJ-49)
Δrnc Crnc
(AH-15)

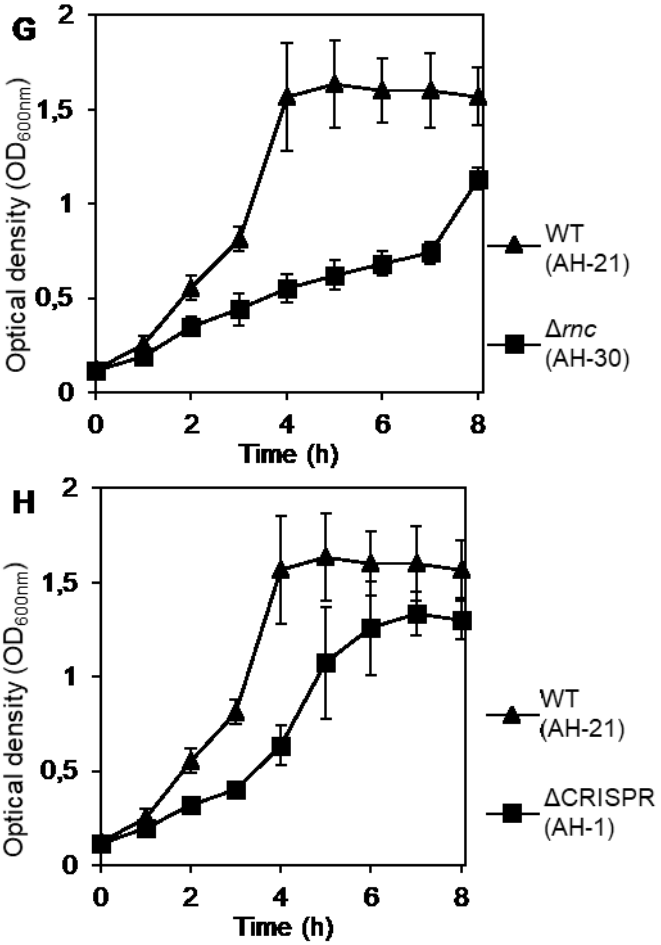

Figure 6.9 *Growth of 8013 strains in EMEM^{+++}*

8013 wild type (WT) with corresponding mutant strains and respective complementant strains were grown in EMEM^{+++} for 8 h at 37 °C, and the optical density (OD_{600}) was determined every hour. Depicted are the mean values of three individual measurements.

While every mutant strain was able to survive in EMEM^{+++}, two out of three *cas9* knockouts, AH-23 and AH-25 (Figure 6.9 B and C), and both *rnc* knockouts, AH-30 and BJ-49 (Figure 6.9 F and G), demonstrated decreased growth capacity. The growth defect was diminished by *rnc* complementation (Figure 6.9 F) but only partially by *cas9* complementation (Figure 6.9 B and C) in the respective mutant strain.

Since it has been shown that RNase III is a global regulator of gene expression in *E. coli* [94], it is conceivable that the knockout of *rnc* in a *N. meningitidis* strain leads to a growth deficiency, and this assumption is strengthened since the effect was absent in the complemented strain AH-15. An influence of Cas9 on the bacterial growth has not been described yet. Furthermore, since the effect was absent in strain AH-12 (Figure 6.9 A) and only partially restored in the complemented strains AH-22 and AH-24 (Figure 6.9 B and C), it is possible that a second genetic event occurred during the knockout of *cas9* in AH-23 and AH-25 that influences the growth capacity in EMEM^{+++}.

6.2.3.2 The knockout of *cas9* does not lead to a general growth deficiency

To examine whether the growth capacity of the *cas9* knockout strains is medium dependent, the growth experiments were also performed in GCBL^{++} (Table 4.16). GCBL^{++} is also a nutrient-rich medium and known to be suitable for meningococcal growth [95].

Under these conditions, all mutant strains demonstrated growth similar to the wild type (Figure 6.10).

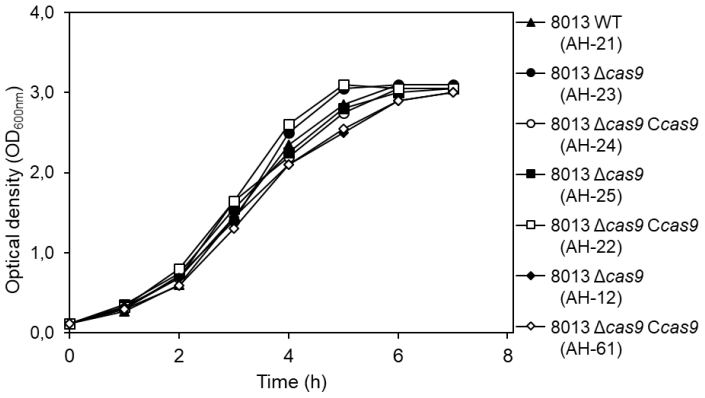

Figure 6.10 *Growth of 8013 cas9 mutant strains in GCBL^{++}*

8013 wild type, mutant, and respective complementant strains were grown in GCBL^{++} for 7 h at 37 °C, and the optical density (OD_{600}) was determined every hour. Depicted are the mean values of two individual measurements.

6.2.4 *N. meningitidis* 8013 does not form static biofilm in EMEM^{+++}

It has been shown that N. meningitidis forms biofilms on abiotic and biotic surfaces [96, 97], and biofilm formation might influence the adhesion of meningococci to host cells [15]. To examine whether the knockout of CRISPR/Cas related genes influences biofilm formation under static conditions, biofilm formation was assessed in a polystyrene microtiter plate as described in Chapter 5.26.

To ensure conditions comparable to the cell adhesion and invasion assay (Chapter 5.25), the static biofilm assay was performed in EMEM^{+++} cell culture medium (Table 4.22). Neither the wild type nor one of the tested knockouts formed a significant biofilm layer in EMEM^{+++} (Figure 6.11).

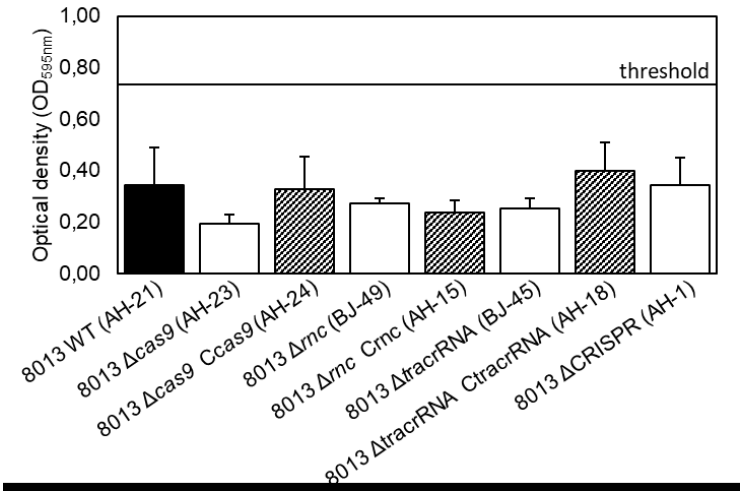

Figure 6.11 *Biofilm formation of 8013 mutant strains*

8013 wild type, mutant, and respective complementant strains were cultured in EMEM^{+++}, and the static biofilm formation was determined after 16 h of incubation. The assay was performed on a 96-well microtiter plate as described in Chapter 5.26. To quantify the biofilm formation, the biofilms were stained using crystal violet and the OD_{595} was measured. The threshold of significant biofilm formation was determined by staining and measuring uninoculated wells and multiplying the measured value by three. Depicted is one out of three similar experiments representing mean values of six technical replicates.

6.3 The CRISPR/Cas system influences the adhesion to host cells in a strain specific manner

The ability of meningococci to adhere to human host cells and to invade the cells is a crucial step in the development of IMD [6, 7].

To examine the influence of the CRISPR/Cas system on the interaction with human host cells, cell adhesion and invasion assays (Chapter 5.25) were performed on a nasopharyngeal cell line called Detroit562. Detroit562 cells are derived from pleural effusion caused by the metastasis of a nasopharyngeal carcinoma in a female Caucasian [85, 86]. They were cultivated in EMEM^{+++} and infected with the meningococcal strains. After 4 hours of infection, the number of adherent bacteria were determined as described in Chapter 5.25. Subsequently, the cells were treated with gentamicin, a bactericidal aminoglycoside antibiotic that irreversibly binds to the 30S subunit of the bacterial ribosome and inhibits protein synthesis [98]. Gentamicin cannot invade Detroit562 cells and is therefore unable to kill intracellularly and thus invasive meningococci. After 1 h of gentamicin treatment, the Detroit562 cells were lysed using saponin

and the gentamicin-protected invasive bacteria were determined as described in Chapter 5.25.

6.3.1 The adhesion and invasion to host cells is CRISPR/Cas independent in WUE2594

Ten individual adhesion and invasion assays were performed with WUE2594 strains and examined the wild type and two knockout strains simultaneously. The order of the strains in the experimental setup was appointed randomly to prevent bias. As shown in Table 6.2, the knockouts did not differ in their mean adhesion or in their mean invasion rate compared to the wild type.

Four out of six experiments performed with the WUE2594 *cas9* knockout strain (BJ-3) showed an adhesion and invasion rate similar to the wild type. In one experiment, the adhesion and invasion rate were reduced ($\alpha < 0.05$) and in one experiment the adhesion and invasion rate were significantly ($\alpha < 0.01$) increased.

The WUE2594 tracrRNA knockout BJ-11 was tested four times: three times with results similar to the wild type and one time with an increased adhesion rate ($\alpha < 0.05$).

The adhesion rate of the WUE2594 *rnc* knockout strain (BJ-57) was reduced in two out of six experiments, both

times with a moderate significance ($\alpha < 0.05$). In one experiment the invasion rate was reduced while in the other it was increased (both $\alpha < 0.05$). The other four experiments showed results similar to the wild type.

The knockout of the CRISPR array in WUE2594 (BJ-70) led to inconsistent results in the adhesion and invasion assay. The adhesion rate was significantly ($\alpha < 0.01$) decreased twice, and the invasion rate increased. One experiment showed an opposite result, an increased adhesion rate, and a decreased invasion rate, and one experiment produced results similar to the wild type.

Therefore, no consistent effect of the CRISPR/Cas system on host cells interaction was observed in strain WUE2594.

A

exp.no.[a]	WUE2594 Δ*cas9* (BJ-8) rel. adh. rate[b]	st. dev.[c]	*p*-value[d]	WUE2594 ΔtracrRNA (BJ-11) rel. adh. rate[b]	st. dev.[c]	*p*-value[d]	WUE2594 Δ*rnc* (BJ-57) rel. adh. rate[b]	st. dev.[c]	*p*-value[d]	WUE2594 ΔCRISPR (BJ-70) rel. adh. rate[b]	st. dev.[c]	*p*-value[d]
n=1	**1,08E+00** [2594_9_2014_05_15]	4,07E-01	n.s.	**8,38E-01** [2594_10_2014_05_14]	1,10E-01	n.s.	**1,49E+00** [2594_9_2014_05_15]	3,02E-01	n.s.	**5,22E-01** [2594_10_2014_05_14]	9,32E-02	< 0.01
n=2	**1,54E+00** [2594_4_2014_05_07]	5,17E-01	n.s.	**1,61E+00** [2594_8_2014_05_13]	1,38E-01	<0.05	**7,86E-01** [2594_4_2014_05_07]	2,35E-02	n.s.	**5,50E-01** [2594_8_2014_05_13]	8,19E-02	< 0.01
n=3	**3,03E-01** [2594_4_2014_05_07]	1,27E-01	<0.05	**9,05E-01** [2594_7_2014_05_09]	3,65E-01	n.s.	**2,32E-01** [2594_5_2014_05_07]	1,70E-02	<0.05	**1,41E+00** [2594_8_2014_05_13]	1,14E-01	<0.05
n=4	**8,93E-01** [2594_11_2014_04_29]	2,92E-02	n.s.	**1,14E+00** [2594_6_2014_05_08]	2,00E-01	n.s.	**1,06E+00** [2594_11_2014_04_29]	1,05E-01	n.s.	**1,08E+00** [2594_6_2014_05_08]	2,06E-01	n.s.
n=5	**9,06E-01** [2594_3_2014_04_08]	1,86E-01	n.s.	**n.d.**	n.d.	-	**5,33E-01** [2594_3_2014_04_08]	5,27E-02	<0.05	**n.d.**	n.d.	-
n=6	**1,86E+00** [2594_3_2014_04_08]	1,16E-01	< 0.01	**n.d.**	n.d.	-	**1,31E+00** [2594_1_2014_04_03]	1,64E-01	n.s.	**n.d.**	n.d.	-

B

exp.no.[a]	WUE2594 Δ*cas9* (BJ-8) rel. adh. rate[b]	SEM[e]	WUE2594 ΔtracrRNA (BJ-11) rel. adh. rate[b]	SEM[e]	WUE2594 Δ*rnc* (BJ-57) rel. adh. rate[b]	SEM[e]	WUE2594 ΔCRISPR (BJ-70) rel. adh. rate[b]	SEM[e]
mean (n=1-6)	**1,10E+00**	2,23E-01	**1,12E+00**	1,74E-01	**9,03E-01**	1,95E-01	**8,91E-01**	2,16E-01

[a] experiment number
[b] relative adhesion rate
[c] standard deviation
[d] *p*-value, comparing the adhesion rate of the mutant strain to the adhesion rate of the wildtype strain
[e] standard error of the mean

C

exp.no.[e]	WUE2594 Δ*cas9* (BJ-8) rel. inv. rate[f]	st. dev.[g]	*p*-value[h]	WUE2594 ΔtracrRNA (BJ-11) rel. inv. rate[f]	st. dev.[g]	*p*-value[h]	WUE2594 Δ*rnc* (BJ-57) rel. inv. rate[f]	st. dev.[g]	*p*-value[h]	WUE2594 ΔCRISPR (BJ-70) rel. inv. rate[f]	st. dev.[g]	*p*-value[h]
n=1	**8,08E-01** [2594_9_2014_05_15]	2,54E-01	n.s.	**9,97E-01** [2594_10_2014_05_14]	2,19E-01	n.s.	**3,36E-01** [2594_9_2014_05_15]	7,15E-02	n.s.	**1,50E+00** [2594_10_2014_05_14]	3,40E-01	< 0.01
n=2	**1,66E+00** [2594_4_2014_05_07]	4,37E-01	n.s.	**1,09E+00** [2594_8_2014_05_13]	2,49E-01	<0.05	**1,66E+00** [2594_4_2014_05_07]	7,74E-01	n.s.	**2,08E+00** [2594_8_2014_05_13]	4,28E-01	< 0.01
n=3	**1,93E+00** [2594_4_2014_05_07]	3,85E-01	<0.05	**5,39E-01** [2594_7_2014_05_09]	2,50E-01	n.s.	**1,74E+00** [2594_5_2014_05_07]	1,17E+00	<0.05	**4,61E-01** [2594_8_2014_05_13]	1,14E-01	<0.05
n=4	**9,44E-01** [2594_11_2014_04_29]	1,01E-01	n.s.	**1,27E+00** [2594_6_2014_05_08]	2,66E-01	n.s.	**7,52E-01** [2594_11_2014_04_29]	8,13E-02	n.s.	**9,30E-01** [2594_6_2014_05_08]	2,14E-01	n.s.
n=5	**9,22E-01** [2594_3_2014_04_08]	3,28E-01	n.s.	**n.d.**	n.d.	-	**6,69E-01** [2594_3_2014_04_08]	2,71E-01	<0.05	**n.d.**	n.d.	-
n=6	**1,61E+00** [2594_3_2014_04_08]	1,64E-01	< 0.01	**n.d.**	n.d.	-	**1,80E+00** [2594_1_2014_04_03]	9,56E-01	n.s.	**n.d.**	n.d.	-

D

exp.no.[e]	WUE2594 Δ*cas9* (BJ-8) rel. inv. rate[f]	SEM[i]	WUE2594 ΔtracrRNA (BJ-11) rel. inv. rate[f]	SEM[i]	WUE2594 Δ*rnc* (BJ-57) rel. inv. rate[f]	SEM[i]	WUE2594 ΔCRISPR (BJ-70) rel. inv. rate[f]	SEM[i]
mean (n=1-6)	**1,31E+00**	1,95E-01	**9,75E-01**	1,56E-01	**1,16E+00**	2,63E-01	**1,24E+00**	3,50E-01

[e] experiment number

[f] relative invasion rate

[g] standard deviation

[h] *p*-value, comparing the invasion rate of the mutant strain to the invasion rate of the wildtype strain

[i] standard error of the mean

Table 6.2 *Adhesion and invasion rates of WUE2594 knockout strains*

Listed are the observed adhesion rates relative to the wild type (rel. adh. rate, in bold) (A) and (B) and invasion rates relative to the wild type (rel. inv. rate, in bold) (C) and (D) on Detroit562 cells and the respective standard deviation (st. dev.) of the WUE2594 knockout strains as well as the *p*-value comparing the mutant adhesion or invasion rate relative to the wild type. The mean adhesion rate of the wild type over the depicted 10 experiments was 0.747 (SEM $1.95*10^{-1}$), and the mean invasion rate was $7.55*10^{-4}$ (SEM $1.40*10^{-4}$). The ID-number of each experiment (n) is given in square brackets below the values. The experiments were performed with two knockout strains and the wild type strain simultaneously. The mean relative adhesion rates (B) and invasion rates (D) of the knockout strains and the respective standard error of the mean are given below each column of individual results. Abbreviations: n.d., no data; n.s., not significant ($\alpha > 0.05$)

6.3.2 The knockout of *cas9*, tracrRNA and *rnc* leads to a reduced adhesion rate in 8013

In contrast to WUE2594, 8013 showed almost no invasive behaviour in Detroit562 cells. The COS plates with the gentamicin protected bacteria were grown with less than thirty colonies in the lowest dilution stage. Therefore, only the adhesion rate of 8013 was examined (Table 6.3).

Three biological replicates of the 8013 *cas9* knockout were tested, AH-12, AH-25 and BJ-3 (named AH-23 after transformation of an empty plasmid). AH-12 was tested two times, BJ-3, three times. All five experiments showed a significantly ($\alpha < 0.01$) reduced adhesion rate of the *cas9* knockout strain. Strain AH-23 and AH-25 were examined together with the corresponding complementant strain (see Chapter 6.3.3).

The 8013 tracrRNA knockout strain (AH-9) was used in three experiments and its adhesion rate was significantly ($\alpha < 0.01$) reduced every time compared to the wild type.

The knockout of *rnc* in 8013 leads to a reduced adhesion rate ($\alpha < 0.01$) in the five experiments, performed with two biological replicates, BJ-49 and AH-30.

However, the adhesion rate of the 8013 CRISPR knockouts adhesion rate was increased in four out of five experiments performed with two biological replicates (AH-1 and AH-5). In one experiment, the 8013 CRISPR knockout strain AH-5 showed an increased adhesion rate but with a high standard deviation and thus without statistical significance.

Overall, the mean adhesion rates of the *cas9*, the tracrRNA and the *rnc* knockout in 8013 were decreased and notably they were reduced to a similar level. The mean adhesion rates of the CRISPR knockout strains were increased with large fluctuations between the individual experiments and biological replicates.

strain	experiment n=1			experiment n=2			experiment n=3			mean (n=1-3)	
	rel. adh. rate[a]	st. dev.[b]	*p*-value[c]	**rel. adh. rate**[a]	st. dev.[b]	*p*-value[c]	**rel. adh. rate**[a]	st. dev.[b]	*p*-value[c]	**rel. adh. rate**[a]	SEM[d]
8013 Δ*cas9* (AH-12)	**5,36E-01** [8013_11_2014_9_19]	6,02E-02	< 0.01	**2,51E-01** [8013_10_2014_9_18]	8,54E-02	< 0.01	**n.d.**	n.d.	-	**3,94E-01**	1,42E-01
8013 Δ*cas9* (BJ-3)	**5,53E-02** [8013_3_2014_6_6]	2,24E-02	< 0.01	**2,01E-02** [8013_2_2014_6_5]	1,35E-03	< 0.01	**1,74E-01** [8013_1_2014_5_30]	4,39E-02	< 0.01	**8,32E-02**	4,66E-02
8013 ΔtracrRNA (AH-9)	**1,30E-01** [8013_20_2014_11_27]	2,10E-02	< 0.01	**4,62E-01** [8013_11_2014_9_19]	9,82E-02	< 0.01	**2,71E-01** [8013_10_2014_9_18]	7,44E-02	< 0.01	**2,88E-01**	9,61E-02
8013 Δ*rnc* (BJ-49)	**4,83E-02** [8013_2_2014_6_5]	6,51E-03	< 0.01	**1,79E-01** [8013_1_2014_5_30]	4,05E-02	< 0.01	**n.d.**	n.d.	-	**1,14E-01**	6,55E-02
8013 Δ*rnc* (AH-30)	**2,66E-01** [8013_19_2014_11_20]	3,58E-02	< 0.01	**3,36E-01** [8013_12_2014_9_24]	1,43E-02	< 0.01	**1,40E-01** [8013_7_2014_9_12]	2,41E-02	< 0.01	**2,47E-01**	5,74E-02
8013 ΔCRISPR (AH-1)	**1,96E+00** [8013_4_2014_6_11]	3,03E-01	< 0.05	**1,58E+00** [8013_20_2014_11_27]	1,23E-01	< 0.05	**n.d.**	n.d.	-	**1,77E+00**	1,89E-01
8013 ΔCRISPR (AH-5)	**3,60E+00** [8013_7_2014_9_12]	2,05E-01	< 0.01	**2,92E-02** [8013_12_2014_9_24]	2,79E-03	< 0.01	**2,20E+00** [8013_19_2014_11_20]	7,41E-01	n.s.	**1,95E+00**	1,04E+00

[a] relative adhesion rate

[b] standard deviation

[c] *p*-value, comparing the adhesion rate of the mutant strain to the adhesion rate of the wildtype strain

[d] standard error of the mean

Table 6.3 *Adhesion rates of 8013 knockout strains*

Listed are the observed adhesion rates relative to the wild type (rel. adh. rate, in bold) on Detroit562 cells and the respective standard deviation (st. dev.) of the 8013 knockout strains as well as the *p*-value comparing the adhesion rate of the mutant strain to the wild type. The mean adhesion rate of the wild type over the depicted 10 experiments was 1.05 (SEM $3.3*10^{-1}$). The ID-number of each experiment (n) is given in square brackets below the values. The experiments were performed with two knockout strains and the wild type strain simultaneously. The mean relative adhesion rates of the knockout strains and the respective standard error of the mean are given next to each row of individual results. Abbreviations: n.d., no data; n.s., not significant ($\alpha > 0.05$)

6.3.3 The effect of the *cas9* and *rnc* knockout on the adhesion to host cells is complementable

To determine whether the observed effect of the *cas9*, the tracrRNA and the *rnc* knockout on the adhesion to human host cells (Chapter 6.3.2) is complementable, the 8013 mutant strains were examined with the corresponding complementant strains simultaneously (Table 6.4).

strain	experiment n=1				experiment n=2				experiment n=3				mean (n=1-3)	
	rel. adh. rate[a]	st. dev.[b]	*p*-value[c]	*p*-value[d]	**rel. adh. rate**[a]	st. dev.[b]	*p*-value[c]	*p*-value[d]	**rel. adh. rate**[a]	st. dev.[b]	*p*-value[c]	*p*-value[d]	**rel. adh. rate**[a]	SEM[e]
8013 Δ*cas9* (AH-12)	**2,40E-01**	1,16E-02	< 0.01	< 0.01	**3,34E-01**	2,70E-02	< 0.01	< 0.01	**8,61E-02**	4,97E-03	< 0.01	< 0.01	**2,20E-01**	7,23E-02
8013 Δ*cas9* C*cas9* (AH-61)	**7,53E-01**	5,98E-02	< 0.05	-	**1,04E+00**	1,25E-01	n.s.	-	**1,24E+00**	1,28E-01	n.s.	-	**1,01E+00**	1,42E-01
	[8013_26_2015_2_19]				[8013_28_2015_2_24]				[8013_29_2015_4_8]					
8013 Δ*cas9* (AH-23)	**9,26E-02**	1,20E-02	< 0.01	< 0.01	**1,21E-01**	1,53E-02	< 0.01	< 0.01	**4,87E-02**	6,99E-03	< 0.01	< 0.01	**8,75E-02**	2,11E-02
8013 Δ*cas9* C*cas9* (AH-24)	**2,48E+00**	2,65E-01	< 0.01	-	**1,09E+00**	1,32E-01	n.s.	-	**9,64E-01**	1,83E-01	n.s.	-	**1,51E+00**	4,86E-01
	[8013_15_2014_10_14]				[8013_16_2014_10_15]				[8013_23_2014_11_28]					
8013 Δ*cas9* (AH-25)	**4,78E-02**	4,81E-03	< 0.01	< 0.01	**9,34E-02**	4,22E-02	< 0.01	< 0.01	**n.d.**	n.d.	-	-	**7,06E-02**	2,28E-02
8013 Δ*cas9* C*cas9* (AH-22)	**1,03E+00**	5,92E-02	n.s.	-	**4,33E-01**	6,01E-02	< 0.05	-	**n.d.**	n.d.	-	-	**7,29E-01**	2,96E-01
	[8013_17_2014_10_22]				[8013_22_2014_11_26]									
8013 ΔtracrRNA (BJ-45)	**1,94E-01**	2,47E-02	< 0.01	< 0.01	**2,43E-01**	7,59E-02	< 0.01	< 0.01	**9,59E-02**	9,17E-03	< 0.01	< 0.05	**1,77E-01**	4,31E-02
8013 ΔtracrRNA CtracrRNA (AH-18)	**5,07E-01**	6,23E-02	< 0.01	-	**6,60E-01**	5,92E-02	< 0.05	-	**3,28E-01**	7,32E-02	< 0.01	-	**4,98E-01**	9,60E-02
	[8013_8_2014_9_16]				[8013_9_2014_9_17]				[8013_21_2014_11_25]					
8013 ΔtracrRNA (AH-65)	**5,41E-01**	6,25E-02	< 0.01	n.s.	**2,03E-02**	1,16E-03	< 0.01	< 0.01	**n.d.**	n.d.	-	-	**2,81E-01**	2,60E-01
8013 ΔtracrRNA C*cas9* (AH-34)	**3,89E-01**	3,72E-02	< 0.01	-	**5,16E-02**	6,70E-03	< 0.01	-	**n.d.**	n.d.	-	-	**2,20E-01**	1,68E-01
	[8013_31_2015_4_9]				[8013_32_2015_4_10]									
8013 ΔtracrRNA (BJ-45)	**4,71E-01**	4,34E-02	< 0.01	n.s.	**6,71E-01**	4,59E-02	< 0.01	n.s.	**n.d.**	n.d.	-	-	**5,71E-01**	1,00E-01
8013 ΔtracrRNA C*cas9* (AH-34)	**4,62E-01**	2,85E-02	< 0.01	-	**5,69E-01**	3,29E-02	< 0.01	-	**n.d.**	n.d.	-	-	**5,15E-01**	5,35E-02
	[8013_33_2015_8_10]				[8013_34_2015_8_11]									
8013 Δ*mc* (BJ-49)	**1,96E-01**	2,65E-02	< 0.01	< 0.01	**3,84E-01**	3,99E-02	< 0.01	< 0.01	**2,93E-01**	1,73E-02	< 0.05	< 0.01	**2,91E-01**	5,41E-02
8013 Δ*mc* C*rnc* (AH-15)	**5,30E-01**	1,08E-01	< 0.05	-	**1,13E+00**	1,13E-01	n.s.	-	**8,11E-01**	7,58E-02	n.s.	-	**8,25E-01**	1,74E-01
	[8013_5_2014_9_9]				[8013_6_2014_9_10]				[8013_13_2014_9_29]					
8013 Δ*mc* (AH-30)	**8,24E-01**	1,31E-01	n.s.	n.s.	**1,53E-01**	1,79E-02	< 0.01	< 0.01	**3,84E-01**	6,87E-02	< 0.01	n.s.	**4,54E-01**	1,97E-01
8013 Δ*mc* C*rnc* (AH-38)	**1,18E+00**	1,38E-01	n.s.	-	**1,15E+00**	1,39E-01	n.s.	-	**4,77E-01**	9,17E-02	< 0.01	-	**9,38E-01**	2,31E-01
	[8013_27_2015_2_23]				[8013_30_2015_4_8]				[8013_35_2015_8_12]					

[a] relative adhesion rate
[b] standard deviation
[c] *p*-value, comparing the adhesion of the mutant strain to the adhesion rate of the wildtype strain
[d] *p*-value, comparing the adhesion of the mutant strain to the adhesion rate of the respective complementant strain
[e] standard error of the mean

Table 6.4 *Adhesion rates of 8013 knockout strains and complementant strains*

Listed are the adhesion rates on Detroit562 cells and the respective standard deviation (st. dev.) of the 8013 knockout strains along with their respective complementant strain as well as the *p*-values comparing the mutant's adhesion rate to the wild type and the complementant strain. The mean adhesion rate of the wild type over the depicted 17 experiments was 0.947 (SEM $1.40*10^{-1}$). The experiments were performed with knockout, complementant, and wild type strain simultaneously. The mean relative adhesion rates of the knockout strains and the respective standard error of the mean are given next to each row of individual results. Abbreviations: n.d., no data; n.s., not significant ($\alpha > 0.05$)

The reduced adhesion rate of AH-12 was consistently observable in each experiment, whereas the complemented strain AH-61 showed adhesion rates similar to the wild type. The *cas9* knockout strains AH-23 and AH-25 were tested together with their complementant strains AH-24 and AH-22 with comparable results.

The adhesion rate of the 8013 tracrRNA knockout strain BJ-45 was significantly reduced in the experiments, but the effect was only partially complementable, since the complementant strain AH-18 showed adhesion rates

significantly higher than BJ-45 but significantly lower than the wild type strain. Because of its proximity in the genome, a polar effect of the tracrRNA knockout on *cas9* was conceivable. However, the complementation of *cas9* into the 8013 tracrRNA knockout strain BJ-45 had no effect on the adhesion rate. In four out of four experiments, the *cas9* complemented tracrRNA knockout strain AH-34 showed a decreased adhesion rate compared to the wild type. In three out of four experiments, the adhesion rate was similar to the knockout, and only once was the adhesion rate of AH-34 significantly higher than its knockout. Thus, the knockout of tracrRNA is not complementable with a second copy of *cas9*.

In every experiment performed with the 8013 *rnc* knockout strain BJ-49, the adhesion rate was decreased compared to the wild type and the adhesion rate of the complemented strain AH-15 was significantly higher. The complemented strain showed adhesion rates on wild type level in two out of three experiments. The *rnc* knockout strain AH-30 was tested together with the complementant strains AH-38 and AH-22, with similar results.

The 8013 CRISPR knockout were not complementable in the way the other knockouts were (Chapter 5.18), which may be due to the frequent repeats. Therefore, the 8013 CRISPR knockouts were not tested further (Table 6.3).

Overall, effects of the knockouts on the adhesion rate demonstrated in Chapter 6.3.2 were confirmed and shown to be complementable for *cas9* and *rnc* and partially complementable for tracrRNA (Figure 6.12, Table 6.4). Notably, the integration of an empty plasmid in BJ-3 and BJ-45 did not alter the effect of the knockout on the adhesion rate.

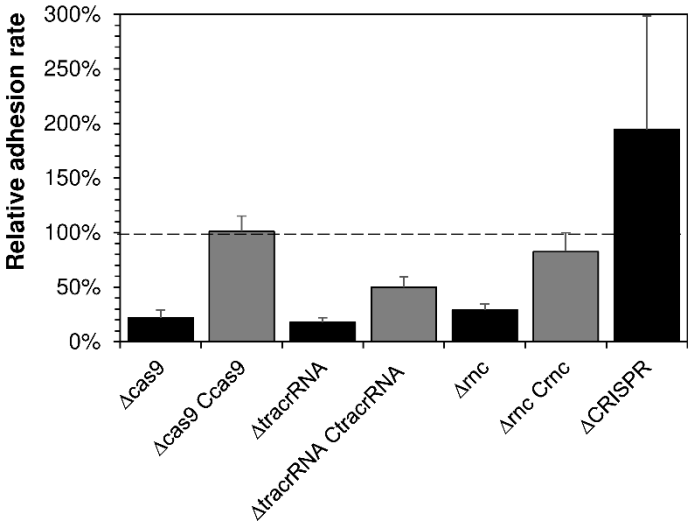

Figure 6.12 *Adhesion of 8013 CRISPR/Cas mutant strains to the human nasopharyngeal epithelial cell line Detroit562*

Depicted is the average adhesion rate of each mutant strain relative to the wild-type strain (set to 100%) from three independent experiments as shown in Table 6.4. The error bars indicate the standard error of the mean. For each strain, the adhesion rate was calculated as the number of colony-forming units (CFU) determined after 4 h of infection divided by the seeded CFU. The relative adhesion rate is the adhesion rate of the mutant divided by the adhesion rate of the wild-type strain.

6.4 The CRISPR/Cas loci of *Neisseria* strains differ in sequence

Since the knockout of genes of the CRISPR/Cas system in the two different strains WUE2594 and 8013 lead to different results in the performed experiments, computational analysis of the genes of interest were conducted to assess the genetic similarity of the strains.

Therefore, the nucleotide sequences of the respective genes in 8013 were compared to the *Neisseria* genomes published on NCBI using the NCBI blastn search (Chapter 5.27) and the megablast algorithm. As a result of the query, bitscores were obtained for each alignment. A higher bitscore corresponds to a higher similarity. To simplify the comparison between the examined strains, the bitscores were divided by the bitscore obtained for the 8013 self-hit to obtain a bit score normalized ratio (BSNR). Thus, the correct identity is given with BSNR = 1.0, whereas any result <1.0 refers to a lower grade of similarity. As an indicator for the overall similarity of the genome to 8013, highly conserved housekeeping genes were included in the query. In particular, *adk* which encodes for the adenylate kinase, *pip* encoding the proline iminopeptidase and *serC,* which

encodes for the phosphoserine aminotransferase, were used [99].

The nucleotide sequences of *cas1*, *cas2*, *cas9*, the CRISPR array, the tracrRNA, *rnc*, *adk*, *pip,* and *serC* from *N. meningitidis* 8013 were compared to 25 *Neisseria* genomes. Fourteen lacked a CRISPR/Cas system (data not shown). The other eleven were compared as described above and the results are listed in Table 6.5. To estimate the overall variance of a gene, the coefficient of variation (C_v) is given above the table.

The comparison revealed that none of the published strains has a Cas9 gene identical in sequence to 8013. However, the *cas9* sequence of the strains *N. meningitidis* WUE2594, *N. meningitidis* Z2491, *N. meningitidis* α14, *N. meningitidis* M01-240355, and *N. meningitidis* 51062 are very similar to *N. meningitidis* 8013. It is noteworthy that these strains belong to different serogroups. The strains *N. meningitidis* DE10444 and *N. meningitidis* α153 harbour a *cas9* sequence that is strikingly different to the *cas9* sequence of 8013.

The sequence of the tracrRNA was identical in every strain, whereas the CRISPR array had a great variance

(C_v = 0.96). Overall, the sequences of *cas1* and *cas2* are as highly conserved as those of *adk* and *pip,* and the sequence of *cas9* has a coefficient of variation as low as *serC*.

Table 6.5 *Similarity of genes in sequenced Neisseria genomes compared to N. meningitidis 8013*

		BSNR[b] $\frac{bitscore\ (gene\ 8013 \rightarrow genome\ requested\ strain)}{bitscore\ (gene\ 8013 \rightarrow genome\ 8013)}$									
Genome	**sg.**[a]	*cas1*	*cas2*	*cas9*	CRISPR	tracrRNA	*rnc*	*adk*	*pip*	*serC*	**Acc-No**[c]
N. meningitidis	C_V	0.05	0.02	0.11	0.96	0.00	0.05	0.03	0.06	0.11	
8013	B	1.00	1.00	1.00	1.00	1.00	1.00	1.00	1.00	1.00	FM999788.1
WUE2594	A	0.92	1.00	0.98	0.25	1.00	0.95	0.93	0.96	0.95	FR774048.1
Z2491	A	0.92	1.00	0.98	0.19	1.00	0.95	0.96	0.97	0.97	AL157959.1
053443	C	0.85	0.98	0.92	0.12	1.00	0.85	0.95	0.97	0.96	CP000381.1
α14	cnl	0.95	1.00	0.98	0.08	1.00	0.93	0.94	1.00	0.96	AM889136.1
M01-240355	B	0.89	0.97	0.98	0.26	1.00	0.88	0.97	0.95	0.97	CP002422.1
510612	A	0.92	1.00	0.98	0.27	1.00	0.95	0.93	0.96	0.95	CP007524.1

DE10444	n.d.	0.94	0.95	0.72	0.19	1.00	0.92	1.00	0.95	0.95	unpublished
α153	n.d.	0.84	0.98	0.79	0.15	1.00	0.93	0.98	0.95	0.93	unpublished
α275	n.d.	0.92	1.00	0.96	0.26	1.00	0.91	0.97	0.95	0.94	unpublished

[a] serogroup of the strain; abbreviations: cnl, capsule null locus; n.d., not determined; n.s., not suitable

[b] Bit Score Normalized Ratio

[c] Accession-Number

[d] coefficient of variation

6.5 Both strains express a highly similar Cas9 protein

Further comparison of the amino acid sequence of Cas9 in strain 8013 and strain WUE2594 revealed that the difference in nucleotide sequence leads to nine amino acid mismatches (Figure 6.13). Only one of those mismatches is located inside a functional domain, concerning the Arginine-rich motive (ARM). Those motives are known to mediate the protein-RNA interaction [100]. The C-terminal end of Cas9 is known to determine the recognized protospacer-adjacent motive (PAM) [101]. Since the mismatches between 8013 and WUE2594 accumulate in the N-terminal region of Cas9, the two orthologs will likely target identical PAM.

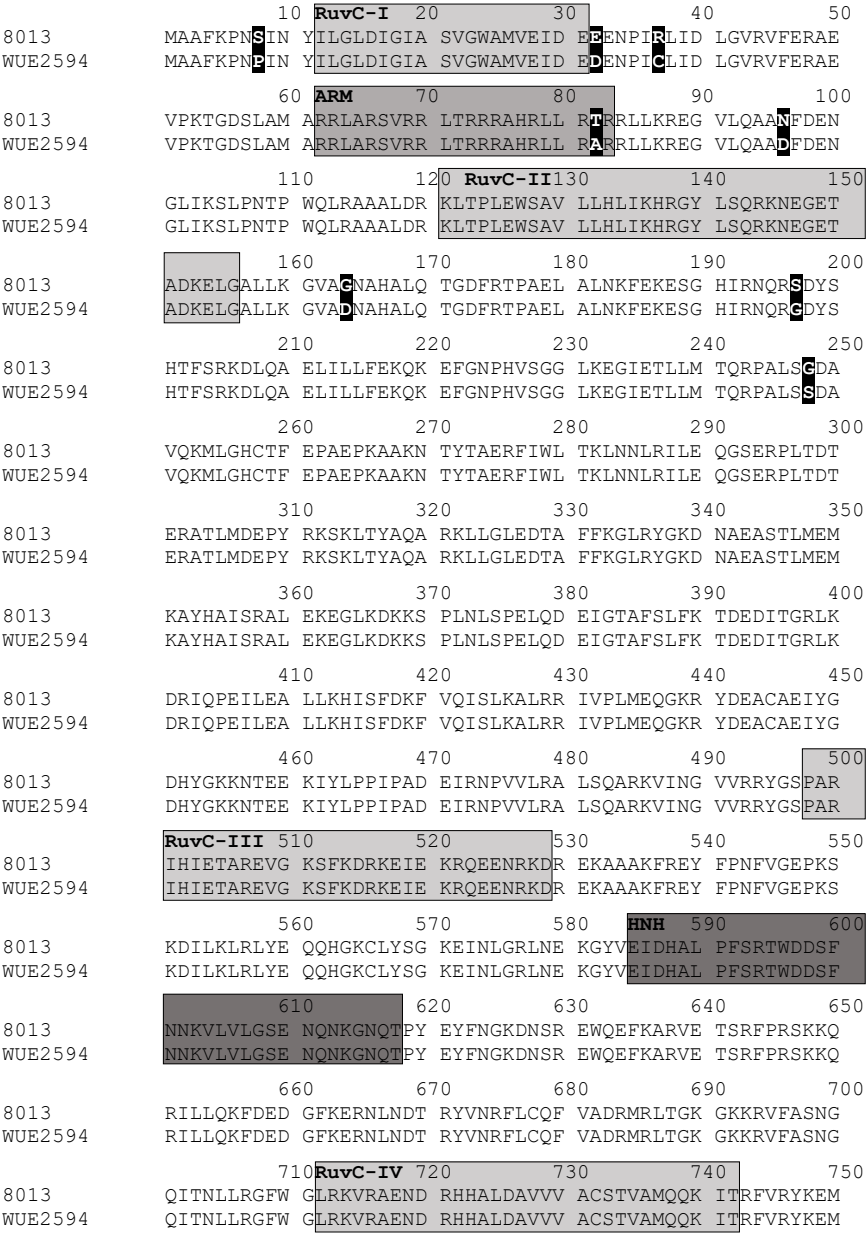
10 RuvC-I 20 30 40 50
8013 MAAFKPNSIN YILGLDIGIA SVGWAMVEID EBENPIRLID LGVRVFERAE
WUE2594 MAAFKPNPIN YILGLDIGIA SVGWAMVEID EDENPICLID LGVRVFERAE
60 ARM 70 80 90 100
8013 VPKTGDSLAM ARRLARSVRR LTRRRAHRLL RTRRLLKREG VLQAANFDEN
WUE2594 VPKTGDSLAM ARRLARSVRR LTRRRAHRLL RARRLLKREG VLQAADFDEN
110 120 RuvC-II130 140 150
8013 GLIKSLPNTP WQLRAAALDR KLTPLEWSAV LLHLIKHRGY LSQRKNEGET
WUE2594 GLIKSLPNTP WQLRAAALDR KLTPLEWSAV LLHLIKHRGY LSQRKNEGET
160 170 180 190 200
8013 ADKELGALLK GVAGNAHALQ TGDFRTPAEL ALNKFEKESG HIRNQRSDYS
WUE2594 ADKELGALLK GVADNAHALQ TGDFRTPAEL ALNKFEKESG HIRNQRGDYS
210 220 230 240 250
8013 HTFSRKDLQA ELILLFEKQK EFGNPHVSGG LKEGIETLLM TQRPALSGDA
WUE2594 HTFSRKDLQA ELILLFEKQK EFGNPHVSGG LKEGIETLLM TQRPALSSDA
260 270 280 290 300
8013 VQKMLGHCTF EPAEPKAAKN TYTAERFIWL TKLNNLRILE QGSERPLTDT
WUE2594 VQKMLGHCTF EPAEPKAAKN TYTAERFIWL TKLNNLRILE QGSERPLTDT
310 320 330 340 350
8013 ERATLMDEPY RKSKLTYAQA RKLLGLEDTA FFKGLRYGKD NAEASTLMEM
WUE2594 ERATLMDEPY RKSKLTYAQA RKLLGLEDTA FFKGLRYGKD NAEASTLMEM
360 370 380 390 400
8013 KAYHAISRAL EKEGLKDKKS PLNLSPELQD EIGTAFSLFK TDEDITGRLK
WUE2594 KAYHAISRAL EKEGLKDKKS PLNLSPELQD EIGTAFSLFK TDEDITGRLK
410 420 430 440 450
8013 DRIQPEILEA LLKHISFDKF VQISLKALRR IVPLMEQGKR YDEACAEIYG
WUE2594 DRIQPEILEA LLKHISFDKF VQISLKALRR IVPLMEQGKR YDEACAEIYG
460 470 480 490 500
8013 DHYGKKNTEE KIYLPPIPAD EIRNPVVLRA LSQARKVING VVRRYGSPAR
WUE2594 DHYGKKNTEE KIYLPPIPAD EIRNPVVLRA LSQARKVING VVRRYGSPAR
RuvC-III 510 520 530 540 550
8013 IHIETAREVG KSFKDRKEIE KRQEENRKDR EKAAAKFREY FPNFVGEPKS
WUE2594 IHIETAREVG KSFKDRKEIE KRQEENRKDR EKAAAKFREY FPNFVGEPKS
560 570 580 HNH 590 600
8013 KDILKLRLYE QQHGKCLYSG KEINLGRLNE KGYVEIDHAL PFSRTWDDSF
WUE2594 KDILKLRLYE QQHGKCLYSG KEINLGRLNE KGYVEIDHAL PFSRTWDDSF
610 620 630 640 650
8013 NNKVLVLGSE NQNKGNQTPY EYFNGKDNSR EWQEFKARVE TSRFPRSKKQ
WUE2594 NNKVLVLGSE NQNKGNQTPY EYFNGKDNSR EWQEFKARVE TSRFPRSKKQ
660 670 680 690 700
8013 RILLQKFDED GFKERNLNDT RYVNRFLCQF VADRMRLTGK GKKRVFASNG
WUE2594 RILLQKFDED GFKERNLNDT RYVNRFLCQF VADRMRLTGK GKKRVFASNG
710 RuvC-IV 720 730 740 750
8013 QITNLLRGFW GLRKVRAEND RHHALDAVVV ACSTVAMQQK ITRFVRYKEM
WUE2594 QITNLLRGFW GLRKVRAEND RHHALDAVVV ACSTVAMQQK ITRFVRYKEM

```
                760        770        780        790        800
8013        NAFDGKTIDK ETGEVLHQKT HFPQPWEFFA QEVMIRVFGK PDGKPEFEEA
WUE2594     NAFDGKTIDK ETGEVLHQKT HFPQPWEFFA QEVMIRVFGK PDGKPEFEEA

                810        820        830        840        850
8013        DTLEKLRTLL AEKLSSRPEA VHEYVTPLFV SRAPNRKMSG QGHMETVKSA
WUE2594     DTPEKLRTLL AEKLSSRPEA VHEYVTPLFV SRAPNRKMSG QGHMETVKSA

                860        870        880        890        900
8013        KRLDEGVSVL RVPLTQLKLK DLEKMVNRER EPKLYEALKA RLEAHKDDPA
WUE2594     KRLDEGVSVL RVPLTQLKLK DLEKMVNRER EPKLYEALKA RLEAHKDDPA

                910        920        930        940        950
8013        KAFAEPFYKY DKAGNRTQQV KAVRVEQVQK TGVWVRNHNG IADNATMVRV
WUE2594     KAFAEPFYKY DKAGNRTQQV KAVRVEQVQK TGVWVRNHNG IADNATMVRV

                960        970        980        990        1000
8013        DVFEKGDKYY LVPIYSWQVA KGILPDRAVV QGKDEEDWQL IDDSFNFKFS
WUE2594     DVFEKGDKYY LVPIYSWQVA KGILPDRAVV QGKDEEDWQL IDDSFNFKFS

                1010       1020       1030       1040       1050
8013        LHPNDLVEVI TKKARMFGYF ASCHRGTGNI NIRIHDLDHK IGKNGILEGI
WUE2594     LHPNDLVEVI TKKARMFGYF ASCHRGTGNI NIRIHDLDHK IGKNGILEGI

                1060       1070       1080
8013        GVKTALSFQK YQIDELGKEI RPCRLKKRPP VR
WUE2594     GVKTALSFQK YQIDELGKEI RPCRLKKRPP VR
```

Figure 6.13 *Sequence alignment of Cas9*

Amino acid sequence alignment of strain 8013 and strain WUE2594 Cas9 generated by CUSTALW [88]. Amino acids are annotated in one-letter code [102] and sorted in packages of ten amino acids. Mismatches are highlighted as white text on black background. Grey shaded boxes represent the functional domains of Cas9. Four RuvC endonuclease domains (RuvC-I through RuvC-IV), an HNH endonuclease domain, and an Arginine-Rich Motive (ARM) have been predicted for Cas9 [35]. The HNH nuclease domain cleaves the DNA strand complementary to the CRISPR RNA and the RuvC-like domain cleaves the non-complementary strand [38].

7 Discussion

Studies have demonstrated that genes located at the CRISPR/Cas locus are more frequent in carriage strains of meningococci than in strains from hyperinvasive lineages [19]. Furthermore, Cas9 has been shown to repress the endogenous transcript of a bacterial lipoprotein (blp) in *Francisella novicida*, thus affecting virulence, and it has been assumed that Cas9 also fulfils similar functions in *N. meningitidis* [35]. Studies regarding the *N. meningitidis* serogroup W135 strain 92045 investigated the interaction with A549 cells derived from a human lung adenocarcinoma. Since pneumonia is a rare end-organ manifestation of IMD, the medical relevance of these experiments seems questionable [43]. A crucial step in developing IMD is crossing the mucosal surface of the nasopharynx by penetrating the epithelial or endothelial cells [103]. Therefore, this study examined the influence of the CRISPR/Cas system on the adhesion to and invasion of a human nasopharyngeal cell line.

7.1 The impact of the CRISPR/Cas system on the adhesion to host cells depends on the genetic background

The adhesion assays performed using 8013 mutant strains revealed a significant reduction of the adhesion rates for strains carrying individual deletions of *cas9*, tracrRNA, or *rnc* (Chapter 6.3.2). The adhesion rates of the *cas9* knockout and the *rnc* knockout strain could be restored to the wild type level by complementing the respective genes *in trans* by integrating *rnc* into the *porA* and *cas9* into the *lctP* and *aspC* locus (see Chapter 5.18 and 6.3.3). Notably, this confirms the preceding experiments using *N. meningitidis* strain 92045, which demonstrate that Cas9 is required for meningococcal adhesion to human adenocarcinoma alveolar basal epithelial cells [35]. Neither the attempts to complement the ΔtracrRNA mutant by integrating a copy of tracrRNA *in trans* into the *porA* locus nor, assuming a polar effect of the tracrRNA knockout on *cas9* expression, the integration of a second copy of *cas9 in trans* into the *lctP* and *aspC* locus restored the adhesion rate to wild type level (Table 6.4). The knockout of the CRISPR array did not lead to consistent effects, but it increased the adhesion rate rather than diminish it, perhaps due to a

hyperactivity of Cas9 in the absence of crRNAs. Neither the wild type 8013 strain nor any mutant showed invasive behaviour on the epithelial cells.

In contrast to the results obtained for 8013, the deletion mutants in WUE2594 did not differ in their interaction with human host cells compared to the wild type, even though the CRISPR/Cas locus of 8013 and WUE2594 are, despite the CRISPR spacers, highly similar. The CRISPR spacers are acquired sequences derived from previously encountered invasive DNA [25]. Therefore, it is unsurprising that the CRISPR spacer of 8013 and WUE2594 differ in sequence and number [45].

The tracrRNA is identical in both strains (Table 6.5) but *cas9* and *rnc* are not. There are nine differences in the amino acid sequence of Cas9 in *N. meningitidis* 8013 and WUE2594, but those are mostly outside of functional domains (Figure 6.13). Only one mismatch concerns a functional domain called ARM, which is known to mediate protein-RNA interaction [35]. While strain 8013 has a polar threonine at position 82, WUE2594 has a nonpolar alanine instead (see Figure 6.13). Noteworthy, in *F. novicida* a single point mutation in the ARM completely abolished the ability of Cas9 to repress

blp [35]. Furthermore, it has been shown recently that the different Cas9 orthologs present in sequenced *N. meningitidis* strains recognize three different PAM depending on their C-terminal sequence [101]. The nucleotide sequence of the RNase III- encoding gene *rnc* is almost identical between 8013 and WUE2594 and thus is as highly conserved as housekeeping genes such as *adk*, *pip,* or *serC* (Table 6.5). Minor differences are unsurprising regarding the immense variations observed between strains, even of the same clonal complex [19]. Therefore, the alterations in the sequence of *rnc* are unlikely to be responsible for the observed differences in cas9 deletion strains.

It is more likely that the distinct results are due to the different genetic background of these strains. The target of the gene-regulating function of Cas9 in *N. meningitidis* is still unknown.

7.2 Limitations of the adhesion and invasion assay

The observed effects of the genetic alterations on the results of the adhesion and invasion assay are not necessarily caused by a diminished capacity to adhere to host cells. A global growth defect would probably also

reduce the measured number of bacteria after 4 h of incubation. To address this method problem, the growth capacity of the mutants was examined. However, the results of the growth experiments did not correlate with the results of the adhesion and invasion assay (Table 7.1). On the contrary, there were strains, for example AH-24, with a reduced growth capacity in EMEM^{+++} and a wild-type-like adhesion rate. Apparently, those traits are not necessarily linked. Additionally, there are differences in the growth conditions even though both experiments used EMEM^{+++} as culture medium. The growth experiments were performed in liquid culture under rigorous shaking in contrast to the adhesion and invasion assays (see Chapter 5.23). Furthermore, bacterial cells had to share the medium with eukaryotic cells in the adhesion and invasion assay. Thus, the pH and nutrient content of the medium shifted during the experiment. However, comparison of the growth of 8013 strains in EMEM^{+++} and GCBL^{++} demonstrates that the growth deficiency is medium specific (Chapter 6.2.3.2). Therefore, the results of the growth experiments are at best partially responsible for the observed differences in the adhesion and invasion assay.

Table 7.1 *Observed phenotypes of the 8013 mutant strains compared to the wild type strain*

8013 mutant strain	Growth in		Adhesion rate[c]
	EMEM^{+++a}	GCBL^{++b}	
Δ*cas9* (AH-12)	=	=	↓
Δ*cas9* C*cas9* (AH-61)	=	=	=
Δ*cas9* (AH-23)	↓	=	↓
Δ*cas9* C*cas9* (AH-24)	↓	=	=
Δ*cas9* (AH-25)	↓	=	↓
Δ*cas9* C*cas9* (AH-22)	↓	=	=
ΔtracrRNA (B-45/ AH-65)	=	-	↓
ΔtracrRNA CtracrRNA (AH-18)	=	-	= / ↓
ΔtracrRNA C*cas9* (AH-34)	-	-	↓
ΔtracrRNA (AH-47)	=	-	↓
ΔtracrRNA CtracrRNA (AH-41)	=	-	-
Δ*rnc* (B-49)	↓	-	↓
Δ*rnc* C*rnc* (AH-15)	=	-	=
Δ*rnc* (AH-30)	↓	-	↓
Δ*rnc* C*rnc* (AH-38)	-	-	=

8013 mutant strain	Growth in		Adhesion rate[c]
	EMEM^{+++}[a]	GCBL^{++}[b]	
ΔCRISPR (AH-1)	↓	-	=
ΔCRISPR (AH-5)	-	-	= / ↑

↓ decreased compared to the wild type; ↑ increased compared to the wild type; = similar to wild type; - no data
[a] see Figure 6.9
[b] see Figure 6.10
[c] see Table 6.3 and Table 6.4

Another possible confounder is the capacity to build biofilms, since biofilm formation enhances antibiotic resistance and increases the stability against mechanical stress [104, 105]. However, no biofilm formation was observed on abiotic surfaces in EMEM^{+++} for strain 8013. Thus, the obtained results in the adhesion and invasion assay are unlikely to be affected by biofilm formation.

7.3 Potential mode of action of Cas9 on cell adhesion

Since no experimental evidence indicates that Cas9 interacts directly with human host cells, it has to be assumed that Cas9 somehow modulates the activity of at least one bacterial adhesin and/or the integrity of the bacterial cell envelope. A hypothetical pathway is depicted in Figure 7.1.

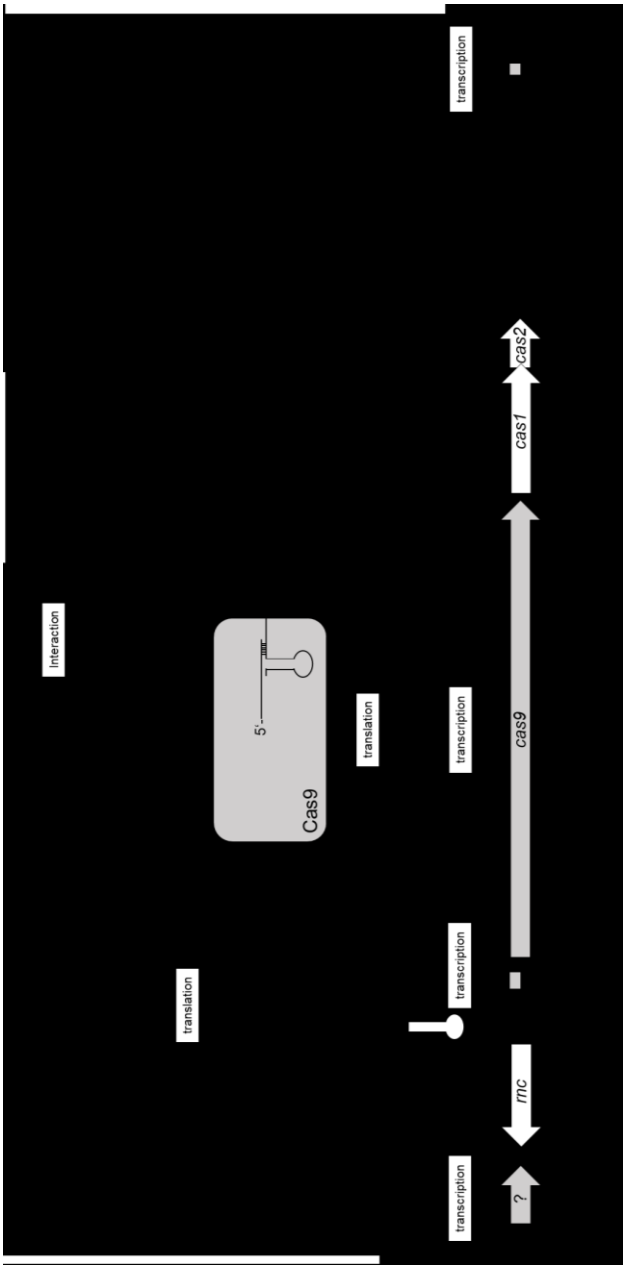
transcription
cas2
cas1
interaction
5'
Cas9
translation
transcription
cas9
translation
transcription
rnc
transcription
?

Figure 7.1 *Hypothetical gene regulation via CRISPR/Cas system in N. meningitidis 8013*

Depicted on the bottom are the CRISPR/Cas locus and the *rnc* locus in *N. meningitidis* 8013; the loci are drawn to scale. The position according to the published genome sequence is given in *bp* beneath the genes. Bold arrows indicate genes and their reading direction; loci of non-coding RNAs are indicated by boxes with angled arrows. Promotors were predicted by BPROM and are depicted as small angled arrows. Vertical lines indicate CRISPR spacer. Elements transcribed for putative gene regulation are highlighted in grey. Above the loci, a gene-regulating function of Cas9 is depicted as hypothesized for *F. novicida* [106]. The tracrRNA, scaRNA, and Cas9 build a complex that recognizes the mRNA of an unknown bacterial lipoprotein by its sequence and degrades it by cleavage. In this way, Cas9 may influence the interaction of *N. meningitidis* with human epithelial cells such as Detroit562 *in vitro*. It is shown that RNase III, encoded by *rnc*, interacts with tracrRNA, and thus may also play a role in the gene regulation (not depicted) [45]. Adapted from [107]

The most important adhesins are the tfp, Opa, and Opc, minor adhesins such as NhhA, App or NadA, and the polysaccharide capsule [14, 49, 50]. Each of those adhesins is a potential target of Cas9 and thus a potential link to the observed phenotype. Further experiments based on this study revealed that in strain 8013, the expression of *pilE* and the serogroup C

capsule did not differ between the mutant strains, the wild type, and the complemented strains [108]. Thus, the capsule and PilE are unlikely targets of Cas9's gene-regulating function. Nevertheless, the function or biogenesis of the meningococcal tfp as well as NhhA, App and NadA are reasonable candidates.

Assuming these possible pathways, it has to be explained why the knockouts in 8013 and WUE2594 led to different results in the adhesion and invasion assay, while the comparison of the CRISPR/Cas loci did not reveal major differences (Table 6.5).

As depicted in Figure 3.1, strain 8013 and WUE2594 obtain tfp of different classes [55]. In addition to that and the differing serogroup, the comparison of the adhesion associated genes listed in Table 7.2 reveals major differences in tfp glycosylation and biogenesis as well as notable sequence dissimilarities at the tfp associated proteins PilC1 and PilC2, whereas NhhA, App, and NadA are present and similar in strain 8013 and WUE2594.

Table 7.2 *Comparison of 8013 and WUE2594 adhesins*

adhesin	8013	WUE2594	annotation
Capsule (serogroup)	C	A	
Type IV pilus			
tfp class	I	II	
	BSNR[a]		
pilE	1.0	0.80	major pilin PilE
pglA	Ψ	complete	pilin glycosyl transferase A
pglB2	complete	truncated	pilin glycosyl transferase B2
pglC	1.0	0.81	pilin glycosyl transferase PglC
pglD	1.0	0.88	pilin glycosylation protein PglD
pglE	Ψ	complete	pilin glycosyl transferase E
pilC1	1.0	0.62	tfp-associated protein PilC1
pilC2	1.0	0.68	tfp-associated protein PilC2
pilD	1.0	0.95	type IV prepilin-like proteins leader peptide processing enzyme PilD (prepilin peptidase)
pilF	1.0	0.99	tfp biogenesis protein PilF

adhesin	8013	WUE2594	annotation
pilG	1.0	0.99	tfp biogenesis protein PilG
pilH	complete	truncated	tfp biogenesis protein PilH
pilI	1.0	0.75	tfp biogenesis protein PilI
pilJ	complete	Ψ	tfp biogenesis protein PilJ
pilK	1.0	0.90	tfp biogenesis protein PilK
pilM	1.0	0.99	tfp biogenesis protein PilM
pilN	1.0	1.0	tfp biogenesis protein PilN
pilO	1.0	0.98	tfp biogenesis protein PilO
pilP	1.0	0.98	tfp biogenesis lipoprotein PilP
pilQ	1.0	0.99	tfp secretin PilQ
pilS1	1.0	0.48	pilS1 cassette
pilS2	1.0	0.48	pilS2 cassette
pilS3	1.0	0.55	pilS3 cassette
pilS4	1.0	0.60	pilS4 cassette
pilS5	1.0	0.89	pilS5 cassette

adhesin	8013	WUE2594	annotation
pilT	1.0	0.98	tfp retraction ATPase PilT
pilT2	1.0	0.99	PilT-like protein PilT2
pilU	1.0	0.98	PilT-like protein PilU
pilV	1.0	0.91	minor pilin PilV
pilW	1.0	0.99	tfp biogenesis lipoprotein PilW
pilX	1.0	0.92	minor pilin PilX
pilZ	1.0	0.98	PilZ-like protein
Outer membrane proteins	status		
opc	missing	complete	outer-membrane protein Opc
opaA	Ψ	complete	opacity protein A
opaB	Ψ	complete	opacity protein B
opaC	Ψ	complete	opacity protein C
opaD	Ψ	complete	opacity protein D
Minor adhesins	BSNR[a]		
nhhA	1.0	0.73	autotransporter adhesin NhhA
app	1.0	0.64	autotransporter App

adhesin	8013	WUE2594	annotation
nadA	1.0	0.73	autotransporter adhesin NadA

Ψ pseudogene; missing: no similarities in sequence alignment, complete: complete sequence for a potentially functional protein
[a] Bit Score Normalized Ratio, Bitscore of sequence alignment relative to the Bitscores obtained for strain 8013 self-hit (see Table 6.5)

Since Opc and Opa are absent in 8013, they may be precluded as potential Cas9 targets. In addition to the findings in Table 7.2, the genes encoding the Opa proteins are known to be phase variable [109], and the polymeric tracts of all four genes in 8013 are in OFF-state [108]. Hypothetically, the adhesion and invasion assay performed with strain WUE2594 revealed no differences between the wild type and the knockout strains because the capacity to adhere was likely mediated by those outer-membrane proteins. In 8013, where those major adhesins are absent, the knockouts and the potentially associated alterations in the set of adhesin and/or the envelope integrity could have a greater influence on cell adhesion. Moreover, their absence in *N. meningitidis* strain 8013 might explain the deficiency of invasive behaviour (Chapter 6.3.2).

Potentially, the adhesion is influenced in the same way as in *F. novicida*, where blp was downregulated by Cas9 [35] and thereby the cell envelope's integrity was enhanced, which affects antibiotic resistance [106]. A similar mechanism has also been described for *C. jejuni,* where Cas9 was shown to affect virulence by controlling the topology and composition of the bacterial cell envelope [42].

Subsequent to this study, the transcriptomes of the 8013 wild type strain and the 8013 *cas9* knockout strains were compared by transcriptome sequencing [108]. While the classical adhesins were not differentially expressed, the mRNA of a hypothetical blp encoded by NMV_0031 was found to be strongly upregulated in the mutant strains. Additionally, RNAs bound to Cas9 were identified by Cas9 coimmunoprecipitation followed by deep-sequencing of the gathered RNA [108]. Adhesin-encoding RNAs were again not identified but the non-coding RNA NMnc0040 was significantly enriched. Therefore, these data somehow resemble the situation in *F. novicida*, although the meningococcal blp is about 100 AAs shorter and has only 27% similarity to its counterpart in *F. novicida* [108].

7.4 Outlook and Conclusion

The adhesion and invasion assays revealed that *cas9*, *rnc,* and tracrRNA are required for adhesion to human nasopharyngeal cells in *N. meningitidis* strain 8013 but not WUE2594. Since the crossing of the mucosal barrier is a crucial step in developing IMD, the CRISPR/Cas locus thus contributes to meningococcal virulence in a strain-dependant manner.

This study set the basis for ongoing research by revealing a gene regulation pathway using Cas9 that is novel in *N. meningitidis*. It has to be demonstrated how exactly Cas9 interacts with its targets. This will furthermore deepen the understanding of the function and versatility of the CRISPR/Cas system in meningococci, a system with wide-ranging applicability for research and medicine.

8 References

1. Rouphael NG, Stephens DS: **Neisseria meningitidis: biology, microbiology, and epidemiology**. *Methods in molecular biology (Clifton, NJ)* 2012, **799**:1-20.
2. Yazdankhah SP, Caugant DA: **Neisseria meningitidis: an overview of the carriage state**. *Journal of medical microbiology* 2004, **53**(Pt 9):821-832.
3. Stephens DS: **Conquering the meningococcus**. *FEMS microbiology reviews* 2007, **31**(1):3-14.
4. Bosis S, Mayer A, Esposito S: **Meningococcal disease in childhood: epidemiology, clinical features and prevention**. *Journal of preventive medicine and hygiene* 2015, **56**(3):E121-124.
5. Lipsitch M, Moxon ER: **Virulence and transmissibility of pathogens: what is the relationship?** *Trends in microbiology* 1997, **5**(1):31-37.
6. Stephens DS, Greenwood B, Brandtzaeg P: **Epidemic meningitis, meningococcaemia, and**

Neisseria meningitidis. *Lancet (London, England)* 2007, **369**(9580):2196-2210.

7. Rosenstein NE, Perkins BA, Stephens DS, Popovic T, Hughes JM: **Meningococcal disease**. *The New England journal of medicine* 2001, **344**(18):1378-1388.
8. Moxon ER, Jansen VA: **Phage variation: understanding the behaviour of an accidental pathogen**. *Trends in microbiology* 2005, **13**(12):563-565.
9. Coureuil M, Join-Lambert O, Lecuyer H, Bourdoulous S, Marullo S, Nassif X: **Pathogenesis of meningococcemia**. *Cold Spring Harbor perspectives in medicine* 2013, **3**(6):2157-1422.
10. Harrison OB, Schoen C, Retchless AC, Wang X, Jolley KA, Bray JE, Maiden MCJ: **Neisseria genomics: current status and future perspectives**. *Pathogens and disease* 2017, **75**(6):ftx060.
11. Pallen MJ, Wren BW: **Bacterial pathogenomics**. *Nature* 2007, **449**(7164):835-842.

12. Schoen C, Tettelin H, Parkhill J, Frosch M: **Genome flexibility in Neisseria meningitidis**. *Vaccine* 2009, **27 Suppl 2**:B103-111.
13. Tzeng YL, Thomas J, Stephens DS: **Regulation of capsule in Neisseria meningitidis**. *Critical reviews in microbiology* 2016, **42**(5):759-772.
14. Merz AJ, So M: **Interactions of pathogenic neisseriae with epithelial cell membranes**. *Annual review of cell and developmental biology* 2000, **16**:423-457.
15. Kim JJ, Mandrell RE, Griffiss JM: **Neisseria lactamica and Neisseria meningitidis share lipooligosaccharide epitopes but lack common capsular and class 1, 2, and 3 protein epitopes**. *Infection and immunity* 1989, **57**(2):602-608.
16. Hamilton HL, Dillard JP: **Natural transformation of Neisseria gonorrhoeae: from DNA donation to homologous recombination**. *Molecular microbiology* 2006, **59**(2):376-385.
17. Marri PR, Paniscus M, Weyand NJ, Rendon MA, Calton CM, Hernandez DR, Higashi DL, Sodergren E, Weinstock GM, Rounsley SD *et al*: **Genome sequencing reveals widespread**

virulence gene exchange among human Neisseria species. *PloS one* 2010, **5**(7):e11835.

18. Caugant DA, Maiden MC: **Meningococcal carriage and disease--population biology and evolution**. *Vaccine* 2009, **27 Suppl 2**:B64-70.
19. Joseph B, Schwarz RF, Linke B, Blom J, Becker A, Claus H, Goesmann A, Frosch M, Muller T, Vogel U *et al*: **Virulence evolution of the human pathogen Neisseria meningitidis by recombination in the core and accessory genome**. *PloS one* 2011, **6**(4):e18441.
20. Marraffini LA: **CRISPR-Cas immunity in prokaryotes**. *Nature* 2015, **526**(7571):55-61.
21. Jansen R, Embden JD, Gaastra W, Schouls LM: **Identification of genes that are associated with DNA repeats in prokaryotes**. *Molecular microbiology* 2002, **43**(6):1565-1575.
22. Makarova KS, Grishin NV, Shabalina SA, Wolf YI, Koonin EV: **A putative RNA-interference-based immune system in prokaryotes: computational analysis of the predicted enzymatic machinery, functional analogies with eukaryotic RNAi, and hypothetical mechanisms of action**. *Biology direct* 2006, **1**:7.

23. Mojica FJ, Diez-Villasenor C, Garcia-Martinez J, Soria E: **Intervening sequences of regularly spaced prokaryotic repeats derive from foreign genetic elements**. *Journal of molecular evolution* 2005, **60**(2):174-182.

24. Pourcel C, Salvignol G, Vergnaud G: **CRISPR elements in Yersinia pestis acquire new repeats by preferential uptake of bacteriophage DNA, and provide additional tools for evolutionary studies**. *Microbiology (Reading, England)* 2005, **151**(Pt 3):653-663.

25. Bolotin A, Quinquis B, Sorokin A, Ehrlich SD: **Clustered regularly interspaced short palindrome repeats (CRISPRs) have spacers of extrachromosomal origin**. *Microbiology (Reading, England)* 2005, **151**(Pt 8):2551-2561.

26. Lillestol RK, Redder P, Garrett RA, Brugger K: **A putative viral defence mechanism in archaeal cells**. *Archaea (Vancouver, BC)* 2006, **2**(1):59-72.

27. Haft DH, Selengut J, Mongodin EF, Nelson KE: **A guild of 45 CRISPR-associated (Cas) protein families and multiple CRISPR/Cas subtypes**

exist in prokaryotic genomes. *PLoS computational biology* 2005, **1**(6):e60.

28. Ebihara A, Yao M, Masui R, Tanaka I, Yokoyama S, Kuramitsu S: **Crystal structure of hypothetical protein TTHB192 from Thermus thermophilus HB8 reveals a new protein family with an RNA recognition motif-like domain**. *Protein science : a publication of the Protein Society* 2006, **15**(6):1494-1499.
29. Godde JS, Bickerton A: **The repetitive DNA elements called CRISPRs and their associated genes: evidence of horizontal transfer among prokaryotes**. *Journal of molecular evolution* 2006, **62**(6):718-729.
30. Grissa I, Vergnaud G, Pourcel C: **The CRISPRdb database and tools to display CRISPRs and to generate dictionaries of spacers and repeats**. *BMC bioinformatics* 2007, **8**:172.
31. Sorek R, Kunin V, Hugenholtz P: **CRISPR--a widespread system that provides acquired resistance against phages in bacteria and archaea**. *Nature reviews Microbiology* 2008, **6**(3):181-186.

32. Koonin EV, Makarova KS, Zhang F: **Diversity, classification and evolution of CRISPR-Cas systems**. *Current opinion in microbiology* 2017, **37**:67-78.

33. Makarova KS, Haft DH, Barrangou R, Brouns SJ, Charpentier E, Horvath P, Moineau S, Mojica FJ, Wolf YI, Yakunin AF *et al*: **Evolution and classification of the CRISPR-Cas systems**. *Nature reviews Microbiology* 2011, **9**(6):467-477.

34. Sorek R, Lawrence CM, Wiedenheft B: **CRISPR-mediated adaptive immune systems in bacteria and archaea**. *Annual review of biochemistry* 2013, **82**:237-266.

35. Sampson TR, Saroj SD, Llewellyn AC, Tzeng YL, Weiss DS: **A CRISPR/Cas system mediates bacterial innate immune evasion and virulence**. *Nature* 2013, **497**(7448):254-257.

36. Barrangou R, Fremaux C, Deveau H, Richards M, Boyaval P, Moineau S, Romero DA, Horvath P: **CRISPR provides acquired resistance against viruses in prokaryotes**. *Science (New York, NY)* 2007, **315**(5819):1709-1712.

37. Deltcheva E, Chylinski K, Sharma CM, Gonzales K, Chao Y, Pirzada ZA, Eckert MR, Vogel J,

Charpentier E: **CRISPR RNA maturation by trans-encoded small RNA and host factor RNase III**. *Nature* 2011, **471**(7340):602-607.

38. Jinek M, Chylinski K, Fonfara I, Hauer M, Doudna JA, Charpentier E: **A programmable dual-RNA-guided DNA endonuclease in adaptive bacterial immunity**. *Science (New York, NY)* 2012, **337**(6096):816-821.
39. Gasiunas G, Barrangou R, Horvath P, Siksnys V: **Cas9-crRNA ribonucleoprotein complex mediates specific DNA cleavage for adaptive immunity in bacteria**. *Proceedings of the National Academy of Sciences of the United States of America* 2012, **109**(39):E2579-2586.
40. Sampson TR, Weiss DS: **Alternative roles for CRISPR/Cas systems in bacterial pathogenesis**. *PLoS pathogens* 2013, **9**(10):e1003621.
41. Westra ER, Buckling A, Fineran PC: **CRISPR-Cas systems: beyond adaptive immunity**. *Nature reviews Microbiology* 2014, **12**(5):317-326.
42. Louwen R, Horst-Kreft D, de Boer AG, van der Graaf L, de Knegt G, Hamersma M, Heikema AP,

Timms AR, Jacobs BC, Wagenaar JA *et al*: **A novel link between Campylobacter jejuni bacteriophage defence, virulence and Guillain-Barre syndrome**. *European journal of clinical microbiology & infectious diseases : official publication of the European Society of Clinical Microbiology* 2013, **32**(2):207-226.

43. Vossen M, Mitteregger D, Steininger C: **Meningococcal pneumonia**. *Vaccine* 2016, **34**(37):4364-4370.

44. Mir A, Edraki A, Lee J, Sontheimer EJ: **Type II-C CRISPR-Cas9 Biology, Mechanism, and Application**. *ACS chemical biology* 2018, **13**(2):357-365.

45. Zhang Y, Heidrich N, Ampattu BJ, Gunderson CW, Seifert HS, Schoen C, Vogel J, Sontheimer EJ: **Processing-independent CRISPR RNAs limit natural transformation in Neisseria meningitidis**. *Molecular cell* 2013, **50**(4):488-503.

46. Bille E, Meyer J, Jamet A, Euphrasie D, Barnier JP, Brissac T, Larsen A, Pelissier P, Nassif X: **A virulence-associated filamentous bacteriophage of Neisseria meningitidis**

increases host-cell colonisation. *PLoS pathogens* 2017, **13**(7):e1006495.

47. Rusniok C, Vallenet D, Floquet S, Ewles H, Mouze-Soulama C, Brown D, Lajus A, Buchrieser C, Medigue C, Glaser P *et al*: **NeMeSys: a biological resource for narrowing the gap between sequence and function in the human pathogen Neisseria meningitidis**. *Genome biology* 2009, **10**(10):R110.
48. Schoen C, Weber-Lehmann J, Blom J, Joseph B, Goesmann A, Strittmatter A, Frosch M: **Whole-genome sequence of the transformable Neisseria meningitidis serogroup A strain WUE2594**. *Journal of bacteriology* 2011, **193**(8):2064-2065.
49. Joseph B, Schneiker-Bekel S, Schramm-Gluck A, Blom J, Claus H, Linke B, Schwarz RF, Becker A, Goesmann A, Frosch M *et al*: **Comparative genome biology of a serogroup B carriage and disease strain supports a polygenic nature of meningococcal virulence**. *Journal of bacteriology* 2010, **192**(20):5363-5377.
50. Carbonnelle E, Hill DJ, Morand P, Griffiths NJ, Bourdoulous S, Murillo I, Nassif X, Virji M:

Meningococcal interactions with the host. *Vaccine* 2009, **27 Suppl 2**:B78-89.

51. Imhaus AF, Dumenil G: **The number of Neisseria meningitidis type IV pili determines host cell interaction**. *The EMBO journal* 2014, **33**(16):1767-1783.
52. Carbonnelle E, Helaine S, Nassif X, Pelicic V: **A systematic genetic analysis in Neisseria meningitidis defines the Pil proteins required for assembly, functionality, stabilization and export of type IV pili**. *Molecular microbiology* 2006, **61**(6):1510-1522.
53. Virji M, Heckels JE: **Antigenic cross-reactivity of Neisseria pili: investigations with type- and species-specific monoclonal antibodies**. *Journal of general microbiology* 1983, **129**(9):2761-2768.
54. Virji M, Heckels JE, Potts WJ, Hart CA, Saunders JR: **Identification of epitopes recognized by monoclonal antibodies SM1 and SM2 which react with all pili of Neisseria gonorrhoeae but which differentiate between two structural classes of pili expressed by Neisseria meningitidis and the distribution of their**

encoding sequences in the genomes of Neisseria spp. *Journal of general microbiology* 1989, **135**(12):3239-3251.

55. Wormann ME, Horien CL, Bennett JS, Jolley KA, Maiden MC, Tang CM, Aho EL, Exley RM: **Sequence, distribution and chromosomal context of class I and class II pilin genes of Neisseria meningitidis identified in whole genome sequences**. *BMC genomics* 2014, **15**:253.
56. Cahoon LA, Seifert HS: **An alternative DNA structure is necessary for pilin antigenic variation in Neisseria gonorrhoeae**. *Science (New York, NY)* 2009, **325**(5941):764-767.
57. Wainwright LA, Frangipane JV, Seifert HS: **Analysis of protein binding to the Sma/Cla DNA repeat in pathogenic Neisseriae**. *Nucleic acids research* 1997, **25**(7):1362-1368.
58. Lory S, Strom MS: **Structure-function relationship of type-IV prepilin peptidase of Pseudomonas aeruginosa--a review**. *Gene* 1997, **192**(1):117-121.
59. Jennings MP, Virji M, Evans D, Foster V, Srikhanta YN, Steeghs L, van der Ley P, Moxon

ER: **Identification of a novel gene involved in pilin glycosylation in Neisseria meningitidis**. *Molecular microbiology* 1998, **29**(4):975-984.

60. Power PM, Roddam LF, Rutter K, Fitzpatrick SZ, Srikhanta YN, Jennings MP: **Genetic characterization of pilin glycosylation and phase variation in Neisseria meningitidis**. *Molecular microbiology* 2003, **49**(3):833-847.

61. Power PM, Roddam LF, Dieckelmann M, Srikhanta YN, Tan YC, Berrington AW, Jennings MP: **Genetic characterization of pilin glycosylation in Neisseria meningitidis**. *Microbiology (Reading, England)* 2000, **146 (Pt 4)**:967-979.

62. Warren MJ, Roddam LF, Power PM, Terry TD, Jennings MP: **Analysis of the role of pgll in pilin glycosylation of Neisseria meningitidis**. *FEMS immunology and medical microbiology* 2004, **41**(1):43-50.

63. Tonjum T, Freitag NE, Namork E, Koomey M: **Identification and characterization of pilG, a highly conserved pilus-assembly gene in pathogenic Neisseria**. *Molecular microbiology* 1995, **16**(3):451-464.

64. Freitag NE, Seifert HS, Koomey M: **Characterization of the pilF-pilD pilus-assembly locus of Neisseria gonorrhoeae**. *Molecular microbiology* 1995, **16**(3):575-586.

65. Merz AJ, So M, Sheetz MP: **Pilus retraction powers bacterial twitching motility**. *Nature* 2000, **407**(6800):98-102.

66. Wolfgang M, Lauer P, Park HS, Brossay L, Hebert J, Koomey M: **PilT mutations lead to simultaneous defects in competence for natural transformation and twitching motility in piliated Neisseria gonorrhoeae**. *Molecular microbiology* 1998, **29**(1):321-330.

67. Pujol C, Eugene E, Marceau M, Nassif X: **The meningococcal PilT protein is required for induction of intimate attachment to epithelial cells following pilus-mediated adhesion**. *Proceedings of the National Academy of Sciences of the United States of America* 1999, **96**(7):4017-4022.

68. Stimson E, Virji M, Makepeace K, Dell A, Morris HR, Payne G, Saunders JR, Jennings MP, Barker S, Panico M *et al*: **Meningococcal pilin: a glycoprotein substituted with digalactosyl**

2,4-diacetamido-2,4,6-trideoxyhexose. *Molecular microbiology* 1995, **17**(6):1201-1214.

69. Morand PC, Bille E, Morelle S, Eugene E, Beretti JL, Wolfgang M, Meyer TF, Koomey M, Nassif X: **Type IV pilus retraction in pathogenic Neisseria is regulated by the PilC proteins**. *The EMBO journal* 2004, **23**(9):2009-2017.

70. Morand PC, Tattevin P, Eugene E, Beretti JL, Nassif X: **The adhesive property of the type IV pilus-associated component PilC1 of pathogenic Neisseria is supported by the conformational structure of the N-terminal part of the molecule**. *Molecular microbiology* 2001, **40**(4):846-856.

71. Nassif X, Beretti JL, Lowy J, Stenberg P, O'Gaora P, Pfeifer J, Normark S, So M: **Roles of pilin and PilC in adhesion of Neisseria meningitidis to human epithelial and endothelial cells**. *Proceedings of the National Academy of Sciences of the United States of America* 1994, **91**(9):3769-3773.

72. Winther-Larsen HC, Hegge FT, Wolfgang M, Hayes SF, van Putten JP, Koomey M: **Neisseria gonorrhoeae PilV, a type IV pilus-associated**

protein essential to human epithelial cell adherence. *Proceedings of the National Academy of Sciences of the United States of America* 2001, **98**(26):15276-15281.

73. Helaine S, Carbonnelle E, Prouvensier L, Beretti JL, Nassif X, Pelicic V: **PilX, a pilus-associated protein essential for bacterial aggregation, is a key to pilus-facilitated attachment of Neisseria meningitidis to human cells**. *Molecular microbiology* 2005, **55**(1):65-77.

74. Sa ECC, Griffiths NJ, Murillo I, Virji M: **Neisseria meningitidis Opc invasin binds to the cytoskeletal protein alpha-actinin**. *Cellular microbiology* 2009, **11**(3):389-405.

75. Tettelin H, Saunders NJ, Heidelberg J, Jeffries AC, Nelson KE, Eisen JA, Ketchum KA, Hood DW, Peden JF, Dodson RJ *et al*: **Complete genome sequence of Neisseria meningitidis serogroup B strain MC58**. *Science (New York, NY)* 2000, **287**(5459):1809-1815.

76. Virji M, Makepeace K, Ferguson DJ, Achtman M, Moxon ER: **Meningococcal Opa and Opc proteins: their role in colonization and invasion of human epithelial and endothelial**

cells. *Molecular microbiology* 1993, **10**(3):499-510.

77. Gray-Owen SD: **Neisserial Opa proteins: impact on colonization, dissemination and immunity**. *Scandinavian journal of infectious diseases* 2003, **35**(9):614-618.

78. Peak IR, Srikhanta Y, Dieckelmann M, Moxon ER, Jennings MP: **Identification and characterisation of a novel conserved outer membrane protein from Neisseria meningitidis**. *FEMS immunology and medical microbiology* 2000, **28**(4):329-334.

79. Scarselli M, Serruto D, Montanari P, Capecchi B, Adu-Bobie J, Veggi D, Rappuoli R, Pizza M, Arico B: **Neisseria meningitidis NhhA is a multifunctional trimeric autotransporter adhesin**. *Molecular microbiology* 2006, **61**(3):631-644.

80. Serruto D, Adu-Bobie J, Scarselli M, Veggi D, Pizza M, Rappuoli R, Arico B: **Neisseria meningitidis App, a new adhesin with autocatalytic serine protease activity**. *Molecular microbiology* 2003, **48**(2):323-334.

81. Capecchi B, Adu-Bobie J, Di Marcello F, Ciucchi L, Masignani V, Taddei A, Rappuoli R, Pizza M, Arico B: **Neisseria meningitidis NadA is a new invasin which promotes bacterial adhesion to and penetration into human epithelial cells**. *Molecular microbiology* 2005, **55**(3):687-698.

82. Harrison OB, Claus H, Jiang Y, Bennett JS, Bratcher HB, Jolley KA, Corton C, Care R, Poolman JT, Zollinger WD *et al*: **Description and nomenclature of Neisseria meningitidis capsule locus**. *Emerging infectious diseases* 2013, **19**(4):566-573.

83. Tobiason DM, Seifert HS: **Genomic content of Neisseria species**. *Journal of bacteriology* 2010, **192**(8):2160-2168.

84. Ieva R, Alaimo C, Delany I, Spohn G, Rappuoli R, Scarlato V: **CrgA is an inducible LysR-type regulator of Neisseria meningitidis, acting both as a repressor and as an activator of gene transcription**. *Journal of bacteriology* 2005, **187**(10):3421-3430.

85. Peterson WD, Jr., Stulberg CS, Simpson WF: **A permanent heteroploid human cell line with type B glucose-6-phosphate dehydrogenase**.

Proceedings of the Society for Experimental Biology and Medicine Society for Experimental Biology and Medicine (New York, NY) 1971, **136**(4):1187-1191.

86. Peterson WD, Jr., Stulberg CS, Swanborg NK, Robinson AR: **Glucose-6-phosphate dehydrogenase isoenzymes in human cell cultures determined by sucrose-agar gel and cellulose acetate zymograms**. *Proceedings of the Society for Experimental Biology and Medicine Society for Experimental Biology and Medicine (New York, NY)* 1968, **128**(3):772-776.
87. Pelicic V, Morelle S, Lampe D, Nassif X: **Mutagenesis of Neisseria meningitidis by in vitro transposition of Himar1 mariner**. *Journal of bacteriology* 2000, **182**(19):5391-5398.
88. Hall TA: **BioEdit: a user-friendly biological alignment editor and analysis program for Windows 95/98/NT**. *Oxford University Press* 1999, **Nucleic Acids Symposium Series No. 41**:95-98.
89. Morgulis A, Coulouris G, Raytselis Y, Madden TL, Agarwala R, Schaffer AA: **Database indexing for production MegaBLAST**

searches. *Bioinformatics (Oxford, England)* 2008, **24**(16):1757-1764.

90. Zhang Z, Schwartz S, Wagner L, Miller W: **A greedy algorithm for aligning DNA sequences**. *Journal of computational biology : a journal of computational molecular cell biology* 2000, **7**(1-2):203-214.

91. Rutherford K, Parkhill J, Crook J, Horsnell T, Rice P, Rajandream MA, Barrell B: **Artemis: sequence visualization and annotation**. *Bioinformatics (Oxford, England)* 2000, **16**(10):944-945.

92. Solovyev V, Salamov A: **Automatic Annotation of Microbial Genomes and Metagenomic Sequences**. *Metagenomics and its Applications in Agriculture, Biomedicine and Enviromental Studies* 2011, **Nova Science Publishers**:61-78.

93. Carver TJ, Rutherford KM, Berriman M, Rajandream MA, Barrell BG, Parkhill J: **ACT: the Artemis Comparison Tool**. *Bioinformatics (Oxford, England)* 2005, **21**(16):3422-3423.

94. Court DL, Gan J, Liang YH, Shaw GX, Tropea JE, Costantino N, Waugh DS, Ji X: **RNase III: Genetics and function; structure and**

mechanism. *Annual review of genetics* 2013, **47**:405-431.

95. Pannekoek Y, Huis In 't Veld R, Schipper K, Bovenkerk S, Kramer G, Speijer D, van der Ende A: **Regulation of Neisseria meningitidis cytochrome bc1 components by NrrF, a Fur-controlled small noncoding RNA**. *FEBS open bio* 2017, **7**(9):1302-1315.

96. Lappann M, Haagensen JA, Claus H, Vogel U, Molin S: **Meningococcal biofilm formation: structure, development and phenotypes in a standardized continuous flow system**. *Molecular microbiology* 2006, **62**(5):1292-1309.

97. Lappann M, Vogel U: **Biofilm formation by the human pathogen Neisseria meningitidis**. *Medical microbiology and immunology* 2010, **199**(3):173-183.

98. Altucci P, Sapio U, Esposito E: **Gentamicin: Antibacterial activity in vitro and clinical studies**. *Chemotherapy* 1965, **10**(5):312-320.

99. Viscidi RP, Demma JC: **Genetic diversity of Neisseria gonorrhoeae housekeeping genes**. *Journal of clinical microbiology* 2003, **41**(1):197-204.

100. Bayer TS, Booth LN, Knudsen SM, Ellington AD: **Arginine-rich motifs present multiple interfaces for specific binding by RNA**. *RNA (New York, NY)* 2005, **11**(12):1848-1857.

101. Edraki A, Mir A, Ibraheim R, Gainetdinov I, Yoon Y, Song CQ, Cao Y, Gallant J, Xue W, Rivera-Perez JA *et al*: **A Compact, High-Accuracy Cas9 with a Dinucleotide PAM for In Vivo Genome Editing**. *Molecular cell* 2018, **73**(4):714-726.e714.

102. **IUPAC-IUB Joint Commission on Biochemical Nomenclature (JCBN). Nomenclature and symbolism for amino acids and peptides. Recommendations 1983**. *The Biochemical journal* 1984, **219**(2):345-373.

103. Stephens DS: **Biology and pathogenesis of the evolutionarily successful, obligate human bacterium Neisseria meningitidis**. *Vaccine* 2009, **27 Suppl 2**:B71-77.

104. Neil RB, Apicella MA: **Clinical and laboratory evidence for Neisseria meningitidis biofilms**. *Future microbiology* 2009, **4**(5):555-563.

105. Donlan RM, Costerton JW: **Biofilms: survival mechanisms of clinically relevant**

microorganisms. *Clinical microbiology reviews* 2002, **15**(2):167-193.

106. Sampson TR, Napier BA, Schroeder MR, Louwen R, Zhao J, Chin CY, Ratner HK, Llewellyn AC, Jones CL, Laroui H *et al*: **A CRISPR-Cas system enhances envelope integrity mediating antibiotic resistance and inflammasome evasion**. *Proceedings of the National Academy of Sciences of the United States of America* 2014, **111**(30):11163-11168.
107. Louwen R, Staals RH, Endtz HP, van Baarlen P, van der Oost J: **The role of CRISPR-Cas systems in virulence of pathogenic bacteria**. *Microbiology and molecular biology reviews : MMBR* 2014, **78**(1):74-88.
108. Heidrich N, Hagmann A, Bauriedl S, Vogel J, Schoen C: **The CRISPR/Cas system in Neisseria meningitidis affects bacterial adhesion to human nasopharyngeal epithelial cells**. *RNA biology* 2018:1-7.
109. Sadarangani M, Hoe CJ, Makepeace K, van der Ley P, Pollard AJ: **Phase variation of Opa proteins of Neisseria meningitidis and the**

effects of bacterial transformation. *Journal of biosciences* 2016, **41**(1):13-19.

9 Annex

9.1 Abbreviations

adk	adenylate kinase
Anti-DIG-ATP	Anti-Digoxidenin-AP Fab fragments
App	adhesion and penetration protein
APS	ammonium persulfate
ARM	arginine-rich motive
blp	bacterial lipoprotein
bp	base pairs
BSA	bovine serum albumin
BSNR	bit score normalized ratio
cas	CRISPR associated
CC	clonal complex
CFU	colony-forming units
cnl	capsule null locus
COS plates	columbia agar plates with 5% sheep blood

CRISPR	clustered, regularly interspaced short palindromic repeats
crRNA	CRISPR RNA
CSPD	chloro-5-substituted adamantly-1,2-dioxetane phosphate
CTP	carboxy-terminal domain
ddH_2O	double distilled water
DIG	digoxygenine
DNA	desoxyribonucleic acid
dNTPs	desoxynucleotide triphosphates
DTT	dithiothreitol
EDTA	ethylendiamin-tetra-acetic acid
FCS	fetal calf serum
fkbP	peptidyl-prolyl cis-trans isomerase
G4	guanine quartets
GCB	*N. gonorrhoea* medium base
GCBL	*N. gonorrhoea* liquid medium

gDNA	genomic DNA
HCl	hydrogen chloride
IMD	invasive meningococcal disease
katA	catalase
kb	kilo base pairs
KCl	potassium chloride
kD	kilo Dalton
LB	*Luria-Bertani* medium
LPS	lipopolysaccharides
lpxC	UDP-3-O-[3-hydroxymyristoyl] N-acetylglucosaminedeacetylase
M	molar (mol/litre)
Mb	mega base pairs
MDAΦ	meningococcal disease associated prophage
MLST	multilocus sequence typing
MOI	multiplicity of infection

MOPS	3-(N-morpholino)-propanesulfonic acid
n.d.	no data
n.s.	not significant
NaCl	sodium chloride
NadA	neisserial adhesin A
NaOH	sodium hydroxide
NCBI	National Center of Biotechnology Information
Nf	neisserial filamentous phage
NhhA	*Neisseria hia* homolog A
Nm	*N. meningitidis*
NTD	amino-terminal domain
Oca	oligomeric coiled-coil adhesin
OD_{595}	optical density measured at 595 nm
OD_{600}	optical density measured at 600 nm
Opa	Opacity associated proteins
Opc	Opacity proteins

PAA	polyacrylamide
PABA	4-Aminobenzoic acid
PAM	pattern adjacent motive
PBS	phosphate-buffered saline
PBS-T	PBS-Tween
PCR	polymerase chain reaction
pip	proline iminopeptidase
PorA	porine A
PPM	proteose peptone medium
PPM^{+}	proteose peptone medium with supplements (Table 4.13)
RNA	ribonucleic acid
rnc	RNase III
rpm	rounds per minute
RT	room temperature
scaRNA	small CRISPR/Cas associated RNA
SDS	sodium-dodecyl-sulfate

SDS-PAGE	SDS-polyacrylamide gel electrophoresis
SEM	standard error of the mean
serC	phosphoserine aminotransferase
SG	serogroup
SOB	super optimal broth
SOC	super optimal broth with glucose
SSC	saline-sodium-citrate buffer
SSPE	saline-sodium-phosphate-EDTA buffer
ST	sequence type
st. dev.	standard deviation
T_a	annealing temperature
TAE	TRIS-acetate-EDTA
TEMED	tetramethylethylenediamine
tfp	type IV pilus
T_m	melting temperature
tracrRNA	*trans* activating CRISPR RNA

TRIS	trishydroxymethylaminomethane
U	units
β-ME	beta-mercaptoethanol

9.2 Lists of Figures and Tables

9.2.1 Figures

9.2.2 Tables

9.3 Curriculum Vitae

name:

date of birth:

birthplace:

Education

Community service

Studies

Dissertation

Career

…… ……

Place, Date Signature

9.4 Publications and Presentations

Publications

Heidrich N, Hagmann A, Bauriedl S, Vogel J, Schoen C: *The CRISPR/Cas system in Neisseria meningitidis affects bacterial adhesion to human nasopharyngeal epithelial cells*. RNA biology 2018:1-7.

Presentations

Hagmann A, Schoen C *The impact of the CRISPR/Cas system on the interaction of Neisseria meningitidis with human host cells*. Poster Presentation 'EUREKA! 2017' International Symposium organized by the Graduate School of Life Sciences Würzburg, October 17th-18th, 2017

9.5 Acknowledgement

Ich möchte mich hiermit bei Herrn Prof. Dr. Matthias Frosch für die Möglichkeit bedanken, am Institut für Hygiene und Mikrobiologie promovieren zu können.

Ich danke Herrn Prof. Dr. Dr. Christoph Schoen für die Vergabe dieser Doktorarbeit und die stetige Unterstützung während ihrer Fertigstellung.

Herrn Prof. Dr. Jörg Vogel, Herrn Prof. Dr. Roy Gross und Herrn Prof. Dr. Johannes Liese danke ich für die Betreuung meiner Doktorarbeit und ihr Engagement in meinem Promotionskomitee.

Ein großes Dankeschön geht im Allgemeinen an die gesamte Arbeitsgruppe SCHOEN und im Besonderen an Barbara Conrad. Liebe Babsi, ohne deinen Rat und deine tatkräftige Unterstützung wäre ich oft nicht weitergekommen.

Meinen Schwiegereltern danke ich insbesondere für die Obhut und Versorgung während der langen, arbeitsreichen Wochenenden in der Rhön. Ich habe es sehr genossen.

Meinen Eltern danke ich für ihre unendliche Geduld, den sicheren Rückhalt, den sie mir gegeben haben, und den Zuspruch, mit dem sie mich bei der Anfertigung dieser Arbeit begleitet haben.

Von ganzem Herzen danke ich meiner Ehefrau und ehemaligen Mitdoktorandin Dr. Laura Hagmann, die von Anfang an an meiner Seite stand, die mit mir gelacht und auch mit mir gelitten hat und die diese Doktorarbeit zu einem Wendepunkt in meinem Leben gemacht hat.

Danke.

Hanns Antony Hagmann was supported by a grant of the German *Excellence Initiative* to the Graduate School of Life Sciences, University of Würzburg.